

## Chapter 8: Anthropogenic and Natural Radiative Forcing

**Coordinating Lead Authors:** Gunnar Myhre (Norway), Drew Shindell (USA)

**Lead Authors:** Francois-Marie Breon (France), William Collins (UK), Jan Fuglestedt (Norway), Jianping Huang (China), Dorothy Koch (USA), Jean-Francois Lamarque (USA), David Lee (UK), Blanca Mendoza (Mexico), Teruyuki Nakajima (Japan), Alan Robock (USA), Leon Rotstayn (Australia), Graeme Stephens (USA), Hua Zhang (China)

**Contributing Authors:** Joanna Haigh (UK), Brian O'Neill (USA)

**Review Editors:** Daniel Jacob (USA), A.R. Ravishankara (USA), Keith Shine (UK)

**Date of Draft:** 15 April 2011

**Notes:** TSU Compiled Version

---

### Table of Contents

<b>Executive Summary</b> .....	<b>2</b>
<b>8.1 Radiative Forcing and Other Climate Change Metrics, including Greenhouse Gas Equivalent, Global Warming Potential (GWP) and Global Temperature Change Potential (GTP)</b> .....	<b>2</b>
8.1.1 <i>The Radiative Forcing Concept</i> .....	2
8.1.2 <i>GWP, GTP and Other Metrics</i> .....	4
<b>Box 8.1: How Can Impacts of Emissions be Compared?</b> .....	<b>5</b>
<b>8.2 Natural Radiative Forcing Changes: Solar and Volcanic</b> .....	<b>12</b>
8.2.1 <i>Radiative Forcing of Solar Irradiance on Climate</i> .....	12
8.2.2 <i>Volcanic</i> .....	14
<b>8.3 Atmospheric Chemistry</b> .....	<b>16</b>
8.3.1 <i>Introduction (What Aspects of Chemistry are Relevant to Radiative Forcing?)</i> .....	16
8.3.2 <i>Chemistry, Troposphere and Stratosphere</i> .....	17
8.3.3 <i>Budgets for Key Species: Emissions, Deposition (Wet and Dry), Burden, Lifetimes, STE and Chemistry (includes Biogenics, Fires, etc., as well as Anthropogenic)</i> .....	18
8.3.4 <i>Evaluation of Chemistry Models</i> .....	18
8.3.5 <i>Concluding Remarks</i> .....	18
<b>8.4 Present-Day Anthropogenic Radiative Forcing</b> .....	<b>18</b>
8.4.1 <i>Changes in Our Understanding of the Spectral Properties of Radiative Transfer and Representation in Radiative Transfer Codes</i> .....	19
8.4.2 <i>Well-Mixed Greenhouse Gases</i> .....	19
8.4.3 <i>Short-Lived Gases</i> .....	21
8.4.4 <i>Land Surface Changes</i> .....	23
8.4.5 <i>Aerosol and Cloud Effects</i> .....	25
<b>8.5 Synthesis (Global Mean Temporal Evolution)</b> .....	<b>27</b>
8.5.1 <i>Summary of Radiative Forcing by Species and Uncertainties</i> .....	27
8.5.2 <i>Impacts by Emissions</i> .....	28
8.5.3 <i>Impacts by Activity</i> .....	30
8.5.4 <i>Future Radiative Forcing</i> .....	31
<b>8.6 Geographic Distribution of Radiative Forcing</b> .....	<b>32</b>
8.6.1 <i>Spatial Distribution of Current Radiative Forcing</i> .....	32
8.6.2 <i>Spatial Evolution of Radiative Forcing and Response over the Industrial Era</i> .....	33
8.6.3 <i>Spatial Evolution of Radiative Forcing and Response for the Future</i> .....	33
<b>FAQ 8.1: How Important is Water Vapour for Climate Change?</b> .....	<b>33</b>
<b>FAQ 8.2: Do Improvements in Air Quality have an Effect on Climate Change?</b> .....	<b>34</b>
<b>References</b> .....	<b>35</b>
<b>Figures</b> .....	<b>43</b>

## 1 **Executive Summary**

2  
3 [PLACEHOLDER FOR FIRST ORDER DRAFT]

### 4 5 **8.1 Radiative Forcing and Other Climate Change Metrics, including Greenhouse Gas Equivalent, 6 Global Warming Potential (GWP) and Global Temperature Change Potential (GTP)**

7  
8 [PLACEHOLDER FOR FIRST ORDER DRAFT]

#### 9 10 **8.1.1 The Radiative Forcing Concept**

11  
12 [PLACEHOLDER FOR FIRST ORDER DRAFT]

##### 13 14 *8.1.1.1 Uses and Limitations of Radiative Forcing*

15  
16 Radiative forcing is a metric of net change in the energy balance of the Earth system. It is expressed in watts  
17 per square meter and is a measure of the energy imbalance that occurs when the Earth system is exposed to  
18 some external change. Although heuristic and not readily observed, radiative forcing provides a simple  
19 quantitative basis for comparing some aspects of the possible eventual climate responses to different external  
20 agents.

21  
22 Two main types of forcing metrics have been widely adopted:

23 1) Instantaneous radiative forcing (IRF) is defined as the change in net (down minus up) irradiance (solar  
24 plus longwave; in  $\text{W m}^{-2}$ ) at the tropopause or top-of-the-atmosphere (TOA) in response to an instantaneous  
25 external perturbation. Climate change takes place when the system responds in order to counteract the flux  
26 changes, and all such responses to the changes in radiative fluxes are explicitly excluded from this definition  
27 of forcing.

28 2) Radiative forcing (RF) was defined in TAR and AR4 as the change in net irradiance at the tropopause  
29 after allowing for stratospheric temperatures to readjust to radiative equilibrium, but with surface and  
30 tropospheric temperatures and state held fixed at the unperturbed values. Hence this metric included  
31 adjustment of only stratospheric temperature. The rationale for including stratospheric temperature  
32 adjustment in the forcing is that it provides a more useful measure of that part of the forcing that is  
33 responsible for the surface and tropospheric temperature response to agents such as carbon dioxide or  
34 stratospheric ozone change.

35  
36 Although useful, the IRF or RF is not necessarily an accurate indicator of the eventual climate response it  
37 forces for all forcing agents. The efficacy – a measure of the global mean temperature response for a unit  
38 forcing relative to the response to a unit forcing from  $\text{CO}_2$  – can differ substantially from 1 (AR4) due to  
39 feedbacks that act over a variety of time scales and complicate the relationship between forcing and  
40 response. In recognition of this complication, a number of different measures of forcing have been  
41 introduced that attempt to include different types of responses. The stratospherically adjusted forcing  
42 described above is one example of an applied adjustment to remove effects of stratospheric responses to the  
43 IRF. More rapid feedbacks in the troposphere triggered by the IRF have also been incorporated into forcing  
44 estimates. One example is the notion of fast feedbacks that include effects on tropospheric temperature,  
45 water vapor and clouds induced by the IRF of  $\text{CO}_2$  (Gregory et al., 2004). A radiative forcing calculation  
46 allowing temperature throughout the atmosphere and on land to adjust has been shown to provide a better  
47 estimate of the eventual temperature change than either IRF or RF (Hansen et al., 2005).

48  
49 We introduce a new form of forcing to account for rapid responses in the climate system due to an imposed  
50 IRF. This adjusted radiative forcing (ARF) is defined as the change in net irradiance at the TOA after  
51 allowing for atmospheric temperatures, water vapor and clouds to adjust, but with either global mean or sea-  
52 surface temperatures unchanged. Note that since the atmospheric temperature has been allowed to adjust, the  
53 result would be almost identical if calculated at the tropopause instead of the TOA. Gregory et al. (2004)  
54 provide a method to calculate the ARF from the transient response in model simulations with a constant  
55 forcing, and the separation of rapid and slow responses is discussed further in Andrews et al. (2010).  
56 Lohmann et al. (2010) have also demonstrated the utility of including rapid adjustments in comparison of  
57 forcing agents, especially in allowing estimation of processes that affect climate but do not have an

1 instantaneous forcing such as aerosol indirect effects or so-called ‘semi-direct’ effects. As with the Gregory  
2 et al., technique, dedicated additional model simulations are required to diagnose the required radiative flux  
3 perturbations.  
4

5 Whereas the above concepts of radiative forcing typically provide useful metrics for assessing the global  
6 mean temperature response to forcings that are relatively evenly distributed over the Earth, evaluation of  
7 forcing from short-lived species poses substantial challenges in both calculation and interpretation. In the  
8 case of a well-mixed gas, emissions from any location and at any time within a year have comparable effects  
9 on atmospheric concentrations, so that the forcing can be related directly to the total change in emissions of  
10 that gas. In contrast, for short-lived gas or aerosol species, the forcing can depend strongly on the location of  
11 the emissions (both geographical and vertical) and on timing of the emission of that species or its precursors.  
12 Hence calculating forcing requires detailed knowledge of the spatio-temporal patterns of emissions, and the  
13 annual average global mean radiative forcing does not necessarily provide a useful guide to the forcing (and  
14 hence temperature change) resulting from any particular individual emission of those compounds.  
15

16 While TOA or tropopause adjusted radiative forcing provides a useful indication of the eventual change in  
17 global-mean surface temperature, it does not necessarily reflect regional climate changes. In the case of  
18 agents that strongly absorb incoming solar radiation (such as black carbon, and to a lesser extent OC and  
19 ozone) the TOA forcing fails to capture the change in radiation reaching the surface which can force local  
20 changes in evaporation (need references) and regional and general circulation patterns. Hence the forcing at  
21 the surface, or the atmospheric heating, defined as the difference between surface and tropopause/TOA  
22 forcing, can also be a useful metric for regional climate changes. Analysis has shown that global mean  
23 precipitation changes can be related separately to RF within the atmosphere and to a slower response to  
24 global mean temperature changes (Andrews et al., GRL, 2010). Relationships between surface forcing and  
25 more localized aspects of climate response have not yet been clearly quantified, however.  
26

27 In general, most types of widely-used radiative forcing metrics concentrate on indicating temperature  
28 response, and most analyses to date have explored the global mean temperature response only. These metrics  
29 clearly ignore impacts such as changes in precipitation, ocean acidity, air quality, surface sunlight available  
30 for photosynthesis, differential heating, etc, as well as regional temperatures. Hence although they are quite  
31 useful for understanding the factors driving global mean temperature change, they provide only an imperfect  
32 and limited perspective on the factors driving broader climate change.  
33

34 Use an updated version of this sort of Figure from AR4/Hansen et al. that reflects the AR5 terminology  
35 (Figure 8.1).  
36

### 37 [INSERT FIGURE 8.1 HERE]

38 **Figure 8.1:** Cartoon comparing (a)  $F_i$ , instantaneous forcing, (b)  $F_a$ , adjusted forcing, which allows  
39 stratospheric temperature to adjust, (c)  $F_g$ , fixed  $T_g$  forcing, which allows atmospheric temperature to adjust,  
40 (d)  $F_s$ , fixed SST forcing, which allows atmospheric temperature and land temperature to adjust, and (e)  $\Delta T_s$ ,  
41 global surface air temperature calculated by the climate model in response to the climate forcing agent. From  
42 Hansen et al. (2005).  
43

#### 44 8.1.1.2 *Historical and Forward Looking*

45

46 Analysis of the forcing change between preindustrial, defined here as 1750, and present provides an  
47 indication of the relative importance of different forcing agents to climate change during this period. Such  
48 analyses have been a mainstay of climate assessments. However, looking simply at two points in time does  
49 not take into account the varying time histories of the individual forcing components. One way to do this is  
50 to look at how much of the impact of the forcing has been realized already and how much has not been  
51 realized but is contributing to the Earth’s current energy imbalance with space (Murphy et al., JGR; Forster  
52 & Gregory ERBE; Hansen et al. imbalance Science, etc.) [though actual results are presented in 8.5 rather  
53 than here (for both historical and forward-looking)].  
54

55 Forward looking evaluations of radiative forcing include: (1) the forcing due to perpetual current  
56 atmospheric concentrations (equal to simply the present-day forcing), (2) the forcing due to current  
57 atmospheric emissions, again assuming that those stay constant in the future, or (3) the integrated forcing due

1 to a 1-year pulse of current emissions. AR4 referred to perpetual current concentrations as ‘committed’,  
2 though for carbon dioxide a substantial decrease in current emissions would be required to maintain current  
3 concentrations (as these are not in equilibrium). Constant current concentrations is equivalent to letting the  
4 temperature adjust to the current energy imbalance. Constant current emissions allows both current  
5 concentrations to adjust to emissions and temperature to adjust to the resulting energy imbalance. While all  
6 these methods allow forcing at a particular future time to be clearly presented, as with historical forcings the  
7 actual impact on temperature depends on both the time history of the forcings and the rate of response of  
8 various portions of the climate system. Metrics that attempt to account for these factors, and hence better  
9 indicate the eventual temperature response, by going beyond radiative forcing have been developed and are  
10 widely used in forward looking analyses (see Section 8.1.2, 8.5.2 and 8.5.3).

### 11 8.1.1.3 *Sensitivity of Forcing to Location (Vertical, Horizontal, Clouds, etc.; HTAP Results)*

12 The inhomogeneously distributed forcings have a different impact on climate from the quasi-homogeneous  
13 forcings due to well-mixed greenhouse gases or solar forcing because they activate climate feedbacks based  
14 on their regional distribution. For example, forcings over Northern Hemisphere middle and high latitudes  
15 induce snow and ice albedo feedbacks more than forcings at lower latitudes or in the Southern Hemisphere.  
16 The strong interaction of aerosols with incoming solar radiation makes their forcing sensitive to the local  
17 surface albedo and cloud cover. Reflective aerosols will have a much larger impact over relatively dark, open  
18 ocean than over bright deserts or snow, and vice-versa for absorbing aerosols, for example. Similarly,  
19 reflective aerosols will have less impact if located over bright clouds, whereas absorbing aerosols may have  
20 a greater impact. Ozone absorbs both incoming solar and outgoing terrestrial radiation, and hence it’s impact  
21 depends on location due to both the availability of sunlight and the difference between local temperature and  
22 the surface temperature. The result shows that ozone changes in the tropical upper troposphere tend to have  
23 the greatest radiative forcing. Even well-mixed greenhouse gases do not have a uniform forcing, due to both  
24 geographic variations in vertical temperature gradients and cloud cover. Forcing tends to be greatest in the  
25 relatively cloud-free subtropics.

## 26 8.1.2 *GWP, GTP and Other Metrics*

27 [PLACEHOLDER FOR FIRST ORDER DRAFT]

### 28 8.1.2.1 *Introduction*

29 In order to quantify and compare the climate impacts of various emissions – and place their impacts on a  
30 common scale – one has to choose a climate impact parameter by which to measure the effects. Various  
31 types of models are needed for the steps down the cause effect chain (Figure 8. 2). (See Box 8.1 on how  
32 comparisons can be done.)

33 [INSERT FIGURE 8.2 HERE]

34 **Figure 8.2:** Cause effect chain from emissions to climate change and impacts showing how metrics can be  
35 used to estimate responses to emissions. (Adapted from Fuglestvedt et al. (2003) and Plattner et al. (2009)).  
36 [The Figure will be improved.]

37 For assessments and evaluation one may apply simpler measures or *metrics* that are based on linearization of  
38 results from complex calculations – as an alternative to more complex models that explicitly include physical  
39 processes resulting in forcing and responses.

40 Metrics can be used to quantify and communicate the relative contributions to climate change of emissions  
41 of different substances, or of emissions from countries or sources/sectors. They can also serve in  
42 communicating the state of knowledge and uncertainties, as well as how effects depend on location of  
43 emissions. Furthermore, metrics can be used as exchange rates in multi-component mitigation policies, and  
44 in that case, metrics are not purely physical concepts since there are economic aspects involved in the  
45 formulation and application of the metrics.

46 It is common to use CO<sub>2</sub> as reference in metrics; i.e., the effect of an emission component is normalized to  
47 the effect of CO<sub>2</sub> for the same mass of emission. By multiplying the emission of component *i* with the metric

1 for this component ( $M_i$ ) the CO<sub>2</sub>-equivalent emission is obtained. Ideally, the climate effects should be the  
2 same regardless of composition of the equivalent CO<sub>2</sub> emissions, but in practice this is not possible. It has  
3 been emphasized that the metrics that are used for these purposes should be transparent and relatively easy to  
4 apply since the metrics are used by non-specialists (Shine 2009; Skodvin and Fuglestedt 1997). Metrics that  
5 have been proposed in the literature include purely physical metrics as well as more comprehensive metrics  
6 that account for both physical and economic dimensions (see Section 8.1.2.7).

7  
8 No single metric can accurately compare all consequences (i.e., responses in climate parameters over time)  
9 of different emissions, and therefore the most appropriate metric will depend on which aspects of climate  
10 change are most important to a particular application, and different climate policy goals may lead to different  
11 conclusions about what is the most suitable metric with which to implement that policy (Tol et al., 2009;  
12 Plattner et al., 2009).

13  
14 The metrics do not define the policy – they are tools that enable quantitative comparison of emissions and  
15 implementation of multi-component policies. A policy which defines the total future emission paths of  
16 climate gases may seek to avoid some future amount of warming. More sophisticated models are required to  
17 define these total emission paths while the metrics can be used by policymakers to decide which emissions to  
18 abate.

19  
20  
21 [START BOX 8.1 HERE]

### 22 23 **Box 8.1: How Can Impacts of Emissions be Compared?**

24  
25 Several approaches are possible for quantification and comparison of different emissions. Such  
26 quantifications may be based on a set of model calculations, with complex or simplified models.  
27 Alternatively, metrics may be used for approximations of climate impact (see Figure 8.2). In any case,  
28 whether complex or simplified approaches are used, many choices related to impact parameter, time, space,  
29 type of perturbation, etc. are needed (Fuglestedt et al., 2003; Tanaka et al., 2010).

30  
31 Typically the aim is to quantify and compare effects of emissions from different sources, sectors (e.g., Unger  
32 et al. (2010) and Fuglestedt et al. (2008)), regions, nations (den Elzen et al., 2005; Höhne et al., 2010;  
33 Prather et al., 2009) or various components (e.g., Forster et al., 2007)

34  
35 There is a set of choices that are related to *time frames*: One can apply a *backward looking* perspective and  
36 consider the effect of historical emissions and calculate the contributions to current effects. This is the  
37 perspective adopted in the RF bar charts in previous IPCC reports and in several studies of climate impacts  
38 of various sectors (Eyring et al., 2010a; Lee et al., 2010).

39  
40 Alternatively one may adopt a *forward looking* perspective. Emission *pulses* (e.g., representing the current  
41 annual emissions) may be used, and the future effects of these can be calculated (e.g., Fuglestedt et al.  
42 (2008) and Berntsen and Fuglestedt (2008a)). Alternatively, one may use *sustained* emissions; e.g., keep  
43 emissions constant at current levels (Unger et al., 2010) and calculate future effects.

44  
45 The most common approach for forward looking analyses is scenario studies. In this case start and end year  
46 of emissions must be decided as well as the evaluation year(s) (See Box 8.1, Figure 1).

47  
48 All choices of types of emission perturbation are somewhat artificial in construct and different choices serve  
49 different purposes.

50  
51 **[INSERT BOX 8.1, FIGURE 1 HERE]**

52 **Box 8.1, Figure 1:** Timeframes involved in calculations of impacts of emissions.

53  
54 The next set of choices is related to chosen parameter for evaluating the effects of the emissions. Impacts of  
55 climate may be measured as RF, integrated RF,  $\Delta T$ ,  $\Delta SL$  etc.; depending on what aspects of climate change  
56 one is most concerned about (Figure 8.2). For a chosen impact parameter one may use *level* of change or *rate*

1 of change. Furthermore, the impacts may also be integrated over time, or discounting of future effects may  
2 be introduced.

3  
4 There is also a spatial dimension involved, and this is related to both driver and response: It is important to  
5 distinguish between the fact that equal-mass emissions from different regions can vary in their global-mean  
6 climate response and that the climate response to emissions can also have a regional component irrespective  
7 of the regional variation in emissions.

8  
9 Ultimately, accurate evaluations of the impacts of emissions on climate require state-of-the-art Earth System  
10 Models that include detailed representations of, and interactions among, the atmosphere, its chemical  
11 composition, the oceans, biosphere, cryosphere, etc. These models encapsulate our understanding, at least on  
12 larger scales, of the important physical, chemical and biological processes.

13  
14 Results from these more sophisticated models form the basis for the parameter choices in the simpler models  
15 that are in widespread use. There is a hierarchy of simpler models available. For example, the Upwelling-  
16 Diffusion Energy Balance Models (UD-EBMs) have been widely used to explore the dependence on  
17 scenarios (e.g., Wigley and Raper (2001), Meinshausen et al. (2011b) and Meinshausen et al. (2009)). These  
18 models are tuned to reproduce the response of the much more sophisticated coupled ocean-atmosphere  
19 general circulation models (e.g., Olivie and Stuber (2010) and Meinshausen et al. (2011b)).

20  
21 A simpler modelling framework has commonly been adopted in studies of past and future climate change –  
22 the linear response (or impulse-response) model. This framework can be used to model both the response of  
23 concentrations to emissions, and the temperature response to the resulting forcings, and it has been widely  
24 applied in studies of the impact of the transport sector (e.g., Grewe and Stenke, (2008); Sausen and  
25 Schumann (2000)). Alternatively, for simple first order estimates of climate impacts of emissions, the  
26 amount of a given species emitted can be multiplied by its metric value (Figure 8.2).

27  
28 Some of the choices that are needed in the assessment of impacts of emissions are scientific (e.g., type of  
29 model, and how processes are included/parameterized in the models). Choices of time frames and impact  
30 parameter are policy related and cannot be based on science alone.

31  
32 [END BOX 8.1 HERE]

### 33 34 35 8.1.2.2 *The GWP concept*

36  
37 The Global Warming Potential (GWP) was used in The First IPCC Report (Houghton et al., 1990) and it was  
38 stated that “*It must be stressed that there is no universally accepted methodology for combining all the*  
39 *relevant factors into a single [metric] . . . A simple approach [i.e., the GWP] has been adopted here to*  
40 *illustrate the difficulties inherent in the concept.*” After this time the GWP was adopted as a metric to  
41 implement the multi-gas approach embedded in the UNFCCC and made operational in the Kyoto Protocol. It  
42 has become the default metric for transferring emissions of different gases to a common scale.

43  
44 The GWP is defined as the time-integrated radiative forcing due to a pulse emission of a given gas, relative  
45 to a pulse emission of an equal mass of CO<sub>2</sub> (Figure 8.3a); usually integrated over 20, 100 or 500 years. For  
46 gases with adjustment times shorter than the adjustment time for CO<sub>2</sub>, the GWP values will decrease with  
47 increasing time horizon. This is due to the increasing value of the integrated RF of CO<sub>2</sub> in the denominator;  
48 i.e., the AGWP<sub>CO<sub>2</sub></sub>.

49  
50 A time horizon of 100 years was adopted by the Kyoto Protocol and is almost the only time horizon used in  
51 climate (policy) assessments. The choice of time horizon has a strong effect on the GWP values – and thus  
52 also on the calculated effects and contributions of emissions, sectors and nations. Shine (2009) writes “*There*  
53 *is certainly no conclusive scientific argument that can defend 100 years compared to other choices, and in*  
54 *the end the choice is a value-laden one.*”

55  
56 The GWP is an indicator of magnitude of the radiative forcing of the climate system over time and does not  
57 translate directly into any specific climatic response parameter. Several studies have evaluated the concept

1 and its application (Fuglestedt et al., 2000; Fuglestedt et al., 2003; Godal, 2003; Manne and Richels, 2001;  
2 Manning and Reisinger, 2011; O'Neill, 2000; Smith and Wigley, 2000a; Smith and Wigley, 2000b) and these  
3 studies have served to clarify the interpretation and limitations of the concept; e.g., that emissions that are  
4 equal in terms of CO<sub>2</sub> equivalents will not result in the same climate response over time. As shown by Fisher  
5 et al. (1990), O'Neill (2000) and Shine et al. (2005b) the ratio of integrated forcing pulse emissions of two  
6 gases is similar to the ratio of the temperature response of these gases for sustained emissions changes,  
7 which offers one interpretation of the GWP concept. Furthermore, O'Neill (2000) and Peters et al. (2011)  
8 show that GWP can also be interpreted as integrated temperature change up to the chosen time horizon (see  
9 Section 8.1.2.7).

### 10 8.1.2.3 The GTP Concept

11 The Global Temperature change Potential (GTP) (Shine et al., 2005b) goes one step further down the cause-  
12 effect chain (Figure 8.1) and uses the change in global mean temperature for a chosen point in time as impact  
13 parameter. While GWP is an integrative metric (2a), the GTP is based on the temperature change for selected  
14 years (Figure. 8.3b). Like for the GWP, the impact from CO<sub>2</sub> is used as reference.

15 By accounting for the climate sensitivity and the exchange of heat between the atmosphere and the ocean,  
16 the GTP includes more physical processes than do the GWP. The GTP accounts for the response and lag due  
17 to the ocean which give a temperature response time larger than the decay time of the atmospheric  
18 concentration (Fuglestedt et al., 2010b; Sausen and Schumann 2000; Shine et al., 2005b; Solomon et al.,  
19 2010a). Shine et al. (2005b) presented the GTP for both pulse and sustained emissions, and used a simple  
20 model to account for the uptake of heat by the ocean. This has later been developed by accounting for the  
21 longer timescales of the ocean (Berntsen and Fuglestedt, 2008b; Boucher and Reddy, 2008; Collins et al.,  
22 2010; Fuglestedt et al., 2010a; Fuglestedt et al., 2010b). Thus, there are two important timescales included  
23 in the GTP; the atmospheric adjustment time of the component under consideration and the response time of  
24 the climate system.

### 25 [INSERT FIGURE 8.3 HERE]

26 **Figure 8.3:** The GWP is calculated by integrating the RF due to pulses over chosen time horizons (a), while  
27 the GTP is based on the temperature response for selected years after emission (b). [The Figure will be  
28 improved.]

29 The GWP and GTP are fundamentally different by construction and different numerical values can be  
30 expected. In particular, the short-lived components get higher values with GWP due to the integrative nature  
31 of the metric. No climate response is included in the GWP concept (except rapid adjustments captured by the  
32 RF concept.)

33 A further key difference between the GTP and the GWP is that, because the GTP requires additional  
34 assumptions about the climate sensitivity and the uptake of heat by the ocean, its values can be significantly  
35 affected by these assumptions. Thus, the uncertainty ranges are wider for the GTP concept compared to  
36 GWP. But the additional uncertainty is not necessarily a weakness of the GTP concept itself and is a  
37 consequence of moving down the cause effect chain and closer to responses of higher relevance (Figure 8.2).  
38 Since the formulation of the ocean response in the GTP has a significant impact on the values this also  
39 represents a trade-off between simplicity and accuracy.

40 A modification of the GTP concept was introduced by Shine et al., (2007) in which the time horizon is  
41 determined by the proximity to a target year; see Sections 8.1.2.6 and 8.1.2.7.

### 42 8.1.2.4 Uncertainties and Limitations

43 Uncertainties in the values of emission metrics in general can be classified as *structural* or *scientific* (Plattner  
44 et al., 2009; Shine et al., 2005a). Structural uncertainties refer to the consequences of using different types of  
45 metrics for a given application, or to choices about key aspects of a metric such as impact parameter, time  
46 horizon and whether discounting is applied. Scientific uncertainties refer to the range of values that can be  
47 calculated for a given metric due to incomplete knowledge of processes from emissions to climate change  
48 and impacts.

1  
2 For the GWP, uncertainties in adjustment times and radiative efficiency determine the scientific uncertainty.  
3 Inclusion of indirect effects in metrics (e.g., through atmospheric chemistry or via interactions with clouds)  
4 will strongly increase the uncertainty in the metric values (see Section 8.1.2.5). For the reference gas CO<sub>2</sub>,  
5 the scientific uncertainty includes the uncertainties in the impulse response function that describes the  
6 development in atmospheric concentration. This impulse response function is sensitive to several factors;  
7 e.g., background levels of CO<sub>2</sub> and uncertainties in the impulse response function will impact on values of  
8 all metrics that use CO<sub>2</sub> as reference (Reisinger et al., 2011; Solomon et al., 2009).  
9

10 Usually a constant background is assumed, but this is strictly not a part of the definition of GWP. The  
11 background concentrations influence both the gas cycles and the concentration-forcing relationships.  
12 Reisinger et al. (2010) have shown that the uncertainties in GWPs are larger than previously reported. This  
13 arises primarily because of significant uncertainties in the global carbon cycle, which controls the rate at  
14 which CO<sub>2</sub> from a pulse emission will decline, and because consistency with the full range of carbon cycle  
15 and coupled ocean–atmosphere climate models used in AR4 leads to significantly larger uncertainties in the  
16 GWP values than was estimated in that assessment. Reisinger et al. (2010) also show that these uncertainties  
17 increase with the time horizon because of fundamental questions involved in determining the details of long-  
18 term carbon cycle responses to both the additional atmospheric CO<sub>2</sub> and the resulting climate change.  
19 Reisinger et al. (2011) studied the sensitivities of GWPs to changes in future atmospheric concentrations and  
20 found that GWP(100) for CH<sub>4</sub> would increase up to 20% under the lowest RCP by 2100 but would decrease  
21 by up to 10% by mid-century under the highest RCP. For N<sub>2</sub>O the GWP(100) would increase by more than  
22 30% by 2100 under the highest RCP but would vary by less than 10% under other scenarios.  
23

24 The same factors as for GWP will contribute to uncertainties in GTP, with a significant additional  
25 contribution from the parameters describing the ocean heat uptake and climate sensitivity. In the first  
26 presentation of an analytical formulation of the GTP concept, Shine et al. (2005b) used one time-constant for  
27 the ocean response to a forcing perturbation. A somewhat more sophisticated approach was used in Collins  
28 et al. (2010), Berntsen and Fuglestedt (2008a) and Fuglestedt et al. (2010a) that includes a representation  
29 of the deep ocean which increases the climate system’s long-term memory to a pulse forcing. This was based  
30 on a temperature response function with two time-constants derived from GCM results. Use of a function  
31 that represents both the fast response of the land and upper ocean as well as the slower response of the deep  
32 ocean substantially changes the GTP values of the shorter-lived compounds,(Boucher and Reddy, (2008);  
33 Shine et al. (2007) and Shine et al. (2005b)) and provides more realistic results.  
34

35 The GTP is generally presented as a ratio of the AGTP for a given species to that of CO<sub>2</sub>; this means that  $\lambda$   
36 appears in both the numerator and denominator of the GTP expression and the GTP is less sensitive to  
37 variations in  $\lambda$  than the AGTP. However, over the range of uncertainty of  $\lambda$ , the GTP is still sensitive to the  
38 value of  $\lambda$  for short-lived species. Using a 2-box model (Berntsen and Fuglestedt 2008b) across the range of  
39 ‘‘likely’’ climate sensitivities, the GTP(50) for BC was found to vary by a factor of 2, the methane GTP(50)  
40 varied by about 50%, while for the long-lived gas N<sub>2</sub>O there was essentially no dependence (Fuglestedt et  
41 al., 2010a). A study by Reisinger et al. (2010) indicates that the relative uncertainties for GTP are almost  
42 twice as high as for GWP for a time horizon of 100 years. These examples illustrate that increasing relevance  
43 of the end-point is associated with increasing uncertainty (see Figure. 8.2)  
44

#### 45 8.1.2.5 Short Lived Climate Forcers and Indirect Effects

46

47 Many short-lived climate forcers (SLCF) (such as ozone or secondary aerosols) are not directly emitted into  
48 the atmosphere, but are formed through the reactions of emitted precursors. Therefore it is not possible to  
49 assign emission-based metrics to the secondary SLCFs, rather this has to be done for the individual  
50 precursors (e.g., Collins et al., 2002; Derwent et al., 2001). Emitting reactive chemicals into the atmosphere  
51 perturbs the chemical system affecting many secondary SLCFs and ideally all these indirect effects have to  
52 be taken into account. Shindell et al. (2009a) quantified the impact of reactive species emissions on both  
53 gaseous and aerosol forcing species and found that a substantial climate impact of ozone precursors was  
54 manifested through perturbations to the sulphur cycle rather than to ozone itself. Studies with different  
55 formulations of sulphur oxidation chemistry have found lower sensitivity (Collins et al., 2010).  
56

1 Methane has a direct climate effect and indirect effects through its chemical reactions. The indirect effects on  
2 its own lifetime, tropospheric ozone and stratospheric water have been traditionally included in its GWP  
3 metric (Houghton et al., 1990). More recently Shindell et al. (2009a) have quantified an indirect effect of  
4 methane on sulphur oxidation, and Boucher et al. (2009) have quantified its indirect effect on CO<sub>2</sub> (for fossil  
5 fuel methane sources). Both these additional effects increase the warming effect of methane.  
6

7 SLCFs tend to be distributed inhomogeneously, so the resulting forcing (and consequently also the GWPs  
8 and GTPs) will depend on where the species are emitted. Factors that affect the forcing are the lifetime of the  
9 species, the albedo of the underlying surface, presence of clouds and the vertical distribution. For BC the  
10 indirect forcing through deposition on snow is very regionally sensitive. Reddy and Boucher (2007)  
11 considered only deposition to the Arctic and found that European emissions had the largest indirect effect.  
12 Rypdal et al. (2009) considered deposition to all snow covered regions in which case BC emissions from the  
13 middle east had the greatest indirect effect, but Shindell et al. (2011) also considered deposition to all regions  
14 and found that European emissions had the greatest impact, with emissions from North America and China  
15 also having large indirect impacts.  
16

17 For secondary SLCFs there is an additional dependence on the local chemical regime. Species affecting the  
18 oxidation of methane have larger effects towards the tropics. NO<sub>x</sub> has a larger impact on ozone when  
19 emitted into a clean environment, whereas VOCs and CO have large impacts on ozone in polluted  
20 environments (Berntsen et al., 2005; Naik et al., 2005; Stevenson et al., 2004; West et al., 2007).  
21

22 Bond et al. (2011) calculated RF from BC and organic matter and presented a new measure – Specific  
23 Forcing Pulse (SFP) – which gives the integrated forcing within a specific region. The global sum of SFP  
24 equates with AGWP.  
25

26 The GWP concept has been expanded by inclusion of efficacies (Berntsen et al., 2005; Fuglestvedt et al.,  
27 2003). Moving down the effects chain from forcing to temperature change, both the global and regional  
28 temperature responses depend on the location of the forcing (analogous to “efficacy”) (Shindell and Faluvegi  
29 2009, 2010). This can be characterised as a regional temperature change potential (RTP) which has the form  
30 of a matrix relating the emission in one region to the temperature change in another.  
31

32 In order to illustrate ranges of metric values in the literature we may use an illustration similar to a figure  
33 from Shindell et al.; see Figure 8.4  
34

#### 35 **[INSERT FIGURE 8.4 HERE]**

36 **Figure 8.4:** Metric values (or ranges) to give overview for NO<sub>x</sub>, CO, VOC, BC, OC, sulphate from the  
37 literature could be used here; e.g., something similar to this Figure from Shindell et al. (2009) for various  
38 studies and for GWP100 and GTP50.  
39

#### 40 *8.1.2.6 Applications of Metrics*

41  
42 In order to transform the effects of different emission to a common scale – CO<sub>2</sub> equivalents – the emissions  
43 can be multiplied with the adopted metric for a chosen time horizon:  
44

$$45 M_i(H) \times E_i = \text{CO}_2 \text{ eq,}$$

46  
47 where M is the chosen metric, H is the chosen time horizon and *i* is component.  
48

49 The numerical values obtained for CO<sub>2</sub> equivalents are very sensitive to choices being made. The GWP for  
50 methane changes to approx. 1/3 from H = 20 to 100, and for GTP it drops to less than 1/10 over the same  
51 time horizons. Thus the calculated contributions will be very sensitive to choice of metric and time horizon.  
52 This will strongly affect the calculated contributions from components, sources and sectors. For instance,  
53 aviation much higher values for calculated contributions with GWP than with GTP, while the cooling from  
54 shipping gets higher weight and appears to be more long-lived than with a GTP based evaluation (Berntsen  
55 and Fuglestvedt, 2008b; Eyring et al., 2010a; Fuglestvedt et al., 2010a). In general, emission profiles with  
56 large contributions from components that are removed on timescales different from that of CO<sub>2</sub> will be most  
57 sensitive to these choices, e.g., sources/sectors with emissions of CH<sub>4</sub> and BC.

The pulse approach has usually been adopted in calculations of metrics, partly on the grounds that the choice of sustained emission metrics implies a commitment for future policymakers, and partly because pulse emissions possess a greater generality; they can be combined to produce metrics for the sustained case or any emissions scenario. The pulse based AGTPs can be used to calculate the temperature change due to sustained emissions: This can be calculated as the integral over pulse emissions multiplied by the absolute temperature change potential (AGTP):

$$\Delta T(t_H) = \sum_i \int_{t_e=0}^{t_H} em_i(t_e) \cdot AGTP_i(t_H - t_e) dt_e$$

where  $i$  is component, and  $t_e$  is time of emission (Berntsen and Fuglestvedt, 2008b). The AGTP values need to be known for all times up to  $t_H$ .

In an analysis of the climate impact of economic sectors (Unger et al., 2010) RF at chosen points in time (20 and 50 years) for *sustained* emissions was used as the metric for comparison. This is approximately equal to using integrated RF up to the chosen times for *pulse* emissions.

#### 8.1.2.7 New Metric Concepts and the Relationship to Economics

A number of new metric concepts have been introduced recently, often in an attempt to better account for economic aspects of metric applications. The use of purely physical metrics, in particular GWPs, in policy contexts has been criticized for many years by economists (Bradford, 2001; De Cara et al., 2008; Reilly, 1992). A prominent use of metrics is to set relative prices of greenhouse gases when implementing a multi-gas emissions reduction policy (Figure 8.2). In these applications, metrics play a fundamentally economic role, and theoretically appropriate metrics include economic dimensions such as mitigation costs, damage costs, and discount rates.

For example, if mitigation policy is set within a *cost-effectiveness* framework with the aim of making the least cost mix of emissions reductions across gases to meet a global average temperature target, the appropriate emissions metric is the “price ratio” (Manne and Richels, 2001). The price ratio, also called the Global Cost Potential (GCP (Tol et al., 2009)), is defined as the ratio of the marginal abatement cost of a gas to the marginal abatement cost of CO<sub>2</sub>, as determined within an integrated climate-economy model. Similarly, if policy is set within a *cost-benefit* framework, the appropriate index is the ratio of the marginal damages from the emission of a gas relative to the marginal damages of an emission of CO<sub>2</sub>, known as the Global Damage Potential (Kandlikar, 1995).

Using physical metrics such as the GWP, instead of economic metrics, within these settings will lead to higher mitigation costs, typically due to favouring reductions of short-lived gases more than would be economically optimal (van Vuuren et al., 2006). While the increase in costs at the global level may be relatively small (Aaheim et al., 2006; Johansson et al., 2006; Johansson, 2008, 2010; O'Neill, 2003) the implications at the project or country level could be significant (Shine, 2009).

Nonetheless, physical metrics remain attractive due to the added uncertainties in mitigation and damage costs introduced by economic metrics. Efforts have been made to view purely physical metrics such as GWPs and GTPs as approximations of more comprehensive economic indexes. GTPs, for example, can be interpreted as an approximation of a Global Cost Potential designed for use in a cost effectiveness setting (Shine et al., 2007; Tol et al., 2009). Quantitative values for GTPs reproduce in broad terms several features of price ratios such as the initially low value of metrics for short-lived gases until a climate policy target is approached, see Figure 8.5 (Shine et al., 2007). Similarly, GWPs can be interpreted as approximations of the Global Damage Potential designed for use in a cost-benefit framework.

In both cases, a number of simplifying assumptions must be made for these approximations to hold. In the case of the GTP, one such assumption is that the influence of emissions on temperature change beyond the time at which a temperature target is reached does not affect the value of the metric. A new metric, the Cost Effective Temperature Potential (CETP (Johansson, 2010)) has been explicitly derived as an approximation to the GCP and is similar to the GTP but accounts for longer-term temperature effects. Like the GTP, it is

1 based on the response of temperature to emissions and includes an assumption about the date at which a  
2 target is achieved. It also requires an assumption about one economic quantity, the discount rate, in order to  
3 account for longer-term temperature effects. Quantitative values for the CETP reproduce values of the GCP  
4 more closely than does the GTP (Johansson, 2010).

5  
6 **[INSERT FIGURE 8.5 HERE]**

7 **Figure 8.5:** Global temperature change potential (GTP(t)) for methane and nitrous oxide for each year from  
8 2010 to the time at which the temperature change target ( $T_{tar}$ ) is reached. The 100-year GWP is also shown  
9 for the two gases. (From Shine et al. (2007)).

10  
11 Other metrics have also been proposed that take into account temperature effects over a broader time horizon  
12 than does the GTP. For example, the Temperature Proxy (TEMP) index (Tanaka et al., 2009) is the index  
13 that, if used to convert an emission pathway of a non-CO<sub>2</sub> gas into an equivalent pathway of CO<sub>2</sub>, would best  
14 reproduce the original pathway of temperature change over a specified time period. TEMP values derived for  
15 the historical period have been shown to differ significantly from 100-year GWP values for CH<sub>4</sub> and CO<sub>2</sub>,  
16 and to behave in a way that is qualitatively similar to GCP and GTP. An integrated version of the GTP could  
17 be a similar measure (Fuglestedt et al., 2003; Shine, 2009). Such an approach was investigated  
18 quantitatively in the derivation of a time-averaged GTP called the Mean Global Temperature Change  
19 Potential (MGTP (Gillett and Matthews, 2010)), which was shown to be quantitatively similar to GWPs if  
20 the time horizon is 100 years. O'Neill (2000) and Peters et al. (2011) present and discuss integrated Global  
21 Temperature change Potentials (iGTP) and show that the values are very close to the GWP values – which  
22 gives an interpretation of the GWP.

23  
24 *8.1.2.8 Summary of Status*

25  
26 In addition to progress in understanding of GWP, new concepts have been introduced since AR4; both  
27 purely physical and some that combine perspectives from various disciplines. Among the alternatives, the  
28 GTP concept has reached the broadest application. The time variant version of GTP (Shine et al., 2007)  
29 introduces a more dynamical view of the contributions of the various species (in contrast to the static GWP).

30  
31 As metrics use parameters further down the cause effect chain (Figure 8.2) the metrics become in general  
32 more relevant, but at the same the uncertainties increase due to more degrees of freedom. For example, there  
33 is less numerical uncertainty related to the transparent and comparatively simple GWP than the uncertainty  
34 related to the more relevant and more complex GTP.

35  
36 The chosen type of metric and the adopted time horizon have strong effects on perceived impacts, costs and  
37 abatement strategies. While scientific choices of input data have to be made, there are value based choices  
38 (such as time horizon or discount rate) needed and this will strongly impact on the metric values and the  
39 calculated contributions of components, sources and sectors. In some economic metrics the value based  
40 choices are not always explicit and transparent, which may be desirable in a policy context.

41  
42 All metrics discussed here (except the SFP (Bond et al., 2011) and RTP (Shindell and Faluvegi, 2009), 2010)  
43 apply global mean values of RF or dT as impact parameter. Consequently, they give no information about  
44 the spatial variability of the response. Many perturbations of atmospheric species, especially the short-lived,  
45 produce a distinctly heterogeneous radiative forcing. Shine et al. (2005a) discuss approaches to account for  
46 regional response patterns in global aggregated metrics.

47  
48 In the application and evaluation of metrics, it is important to distinguish between two main types of  
49 uncertainty; *structural* and *scientific*. In order to improve the accuracy of metrics (and the calculated effects  
50 of emissions) the scientific uncertainty (such as lifetime, impulse response functions, RF, climate sensitivity,  
51 etc.) needs to be reduced. But one also needs to acknowledge the structural uncertainty which is linked to the  
52 application; e.g., using GWP or GTP will for many components have a much larger effect on calculated  
53 contributions of emissions than improved estimates of input parameters such as radiative efficiency and  
54 lifetimes. Furthermore, metrics that account for regional variations in sensitivity to emissions or regional  
55 variation in response, could give a very different emphasis to various emissions.

As new metrics have continued to be developed and explored, a clear conclusion has been that there is no single best metric that is appropriate in all circumstances (Manning and Reisinger, 2011; Plattner et al., 2009; Shine, 2009; Tol et al., 2009). Rather, the most appropriate metric depends on the particular use to which it will be put and which aspect of climate change is considered relevant in a given context. As pointed out in several studies (Manne and Richels, 2001; Manning and Reisinger, 2011; Plattner et al., 2009; Reisinger et al., 2011; Shine et al., 2007; Tol et al., 2009), the time invariant GWP is not well suited for a policy context with a global concentration, forcing or temperature target.

## 8.2 Natural Radiative Forcing Changes: Solar and Volcanic

[PLACEHOLDER FOR FIRST ORDER DRAFT]

### 8.2.1 Radiative Forcing of Solar Irradiance on Climate

The RF is the solar irradiance change divided by 4 and multiplied by  $\sim 0.7$ : The Earth absorbs solar radiation as  $(1-A)I/4$ , where  $A$  is the albedo ( $\sim 0.3$ ) and  $I$  is the Total Solar Irradiance (TSI). The factor of 4 arises since the Earth intercepts  $\pi R^2 I$  energy per unit time ( $R$  is the mean Earth radius), but this is averaged over the surface area of the Earth  $4\pi R^2$ . In AR4 a best IRF estimate of  $0.12 \text{ W m}^{-2}$  was given between 1750 and the present. Similar to previous IPCC estimates this RF was estimated as the instantaneous RF at TOA.

However, due to solar activity-wavelength dependence, the wavelength-albedo dependence, and absorption within the stratosphere and the resulting stratospheric adjustment, the RF is reduced to 78% of the TOA IRF (Gray et al., 2009). Here we use this RF.

#### 8.2.1.1 Observed Variations of TSI

[PLACEHOLDER FOR FIRST ORDER DRAFT]

##### 8.2.1.1.1 Satellite measurements

Since 1978, several independent space-based instruments have directly measured the TSI. Three main composite series were constructed referred to as the ACRIM (Willson and Mordinov, 2003), the IRMB (Dewitte et al., 2004) and the PMOD (Fröhlich, 2006). Analysis of instrument degradation and pointing issues (Fröhlich, 2006) and an independent modeling based on solar magnetograms (Wenzler et al., 2006) indicates that the PMOD composite (see Figure 8.6) is the most realistic.

##### 8.2.1.1.2 Variability inferred from the PMOD Composite series

Variations of  $\sim 0.1\%$  were observed between the sunspot maximum and sunspot minimum of the 11-years solar activity cycle (SC) (Fröhlich, 2006). This modulation is mainly due to a compensation between relatively dark sunspots, bright faculae and bright network elements (e.g., Foukal et al., 2006). The PMOD shows a TSI decline trend since 1985 (Lockwood and Fröhlich, 2007), this is reflected in the lower peak seen during SC 23 minimum compared to the previous two minima: the mean for September 2008 is  $1365.26 \pm 0.16 \text{ W m}^{-2}$ , while in the minimum of 1996 it was  $1365.45 \text{ W m}^{-2}$  and in the minimum of 1986 it was  $1365.57 \text{ W m}^{-2}$  (Fröhlich, 2009). Between the minima of 1986 and 2008 there is a RF of  $-0.04 \text{ W m}^{-2}$ .

[INSERT FIGURE 8.6 HERE]

**Figure 8.6:** The Physikalisch-Meteorologisches Observatorium Davos (PMOD) composite of Total Solar Irradiance (<http://www.pmodwrc.ch/pmod.php?topic=tsi/composite/SolarConstant>).

#### 8.2.1.2 TSI Variations Since Preindustrial Time.

The year of 1750 is used as the nominal representation of the preindustrial atmosphere. Considering reconstructions of TSI, from 1750 to 2005, the AR4 indicate that the RF was  $0.09 \text{ W m}^{-2}$  ( $0.12 \text{ W m}^{-2}$  for instantaneous forcing at TOA) with a range of estimates of  $0.05\text{--}0.23 \text{ W m}^{-2}$ , involving a factor of  $\sim 5$ . A recent analysis reconstruction assembled in support of the paleoclimate modeling intercomparison project (PMIP) and based on various proxy data shows a RF range of about  $0.02$  to  $0.11 \text{ W m}^{-2}$  for 1750 to 2000 (Schmidt et al., 2011), also involving a factor of  $\sim 5$  (see Figure 8.7). However, the upper and lower limits of this range are reduced to nearly a half of those estimated in AR4.

1 Gray et al. (2010) point out that choosing the years of 1700 or 1800 would substantially increase the RF  
2 while leaving the anthropogenic forcings essentially unchanged. These years are within the Maunder (Mm)  
3 and Dalton (Dm) solar minima correspondingly. The AR4 RF (see Table 2.10) shows a range of ~0.08 to  
4 0.22 W m<sup>-2</sup>, involving a factor of ~3, the estimates based on irradiance changes at cycle minima derived  
5 from brightness fluctuations in Sun-like stars are not included in this range because they are no longer  
6 considered valid (e.g., Krivova and Solanki, 2007). The reconstructions in Schmidt et al. (2011) indicate a  
7 Mm-to-present RF range of 0.08 to 0.18 W m<sup>-2</sup>, involving a factor of ~2 (compared to the factor of 5  
8 mentioned above) (see Figure 8.7). The range given by Schmidt et al. (2011) is within the AR4 range  
9 although narrower. Notice that the AR4 ranges for Mm-to-present and 1750-to-present are very close. But  
10 for the Schmidt et al. (2011) ranges, the Mm-to-present upper (lower) limit is ~1.6 (4) times the upper  
11 (lower) limit of 1750-to-present. Choosing the year 1850 we find solar activity conditions similar to those in  
12 1750.

#### 14 [INSERT FIGURE 8.7 HERE]

15 **Figure 8.7:** Some reconstructions of past Total Solar Irradiance time series. PMOD composite time series.  
16 WLS, physically-based model for the open flux with (back) and without (noback) independent change in the  
17 background level of irradiance (Wang et al., 2005). Taking past geomagnetic field variations into account,  
18 the solar activity record can be obtained from the isotope records: MEA (Muscheler et al., 2007) and DB  
19 (Delaygue and Bard, 2010) using a linear relation derived from WLS modern-to-Mm differences (back and  
20 noback cases). SBF, model using <sup>10</sup>Be data and observationally derived relationships between TSI and open  
21 solar magnetic field (Fröhlich 2009; Steinhilber et al., 2009). VSK, physical modeling of surface magnetic  
22 flux and its relationship with the isotopes (Vieira et al., 2010).

#### 24 8.2.1.3 Attempts to Estimate Future Centennial Trends of TSI

25  
26 Proxy records of solar activity such as the <sup>10</sup>Be and <sup>14</sup>C cosmogenic radioisotopes of the last 10,000 years  
27 (Horiuchi et al., 2008; Stuiver et al., 1998; Vonmoos and Muscheler, 2006) show grand minima and maxima  
28 times. Frequency analysis of these series (Tobias et al., 2004) present several significant long-term  
29 periodicities such as the ~80–90 years (Gleissberg), ~200 years (de Vries or Suess) or the ~2300 years  
30 (Hallstatt), motivating attempts to predict trends in solar activity.

31  
32 Cosmogenic isotope and sunspot data (Rigozo et al., 2001; Usoskin et al., 2003) reveal that we are within a  
33 grand activity maximum that began ~1920. However, SC 23 showed a previously unseen activity decline  
34 (McComas et al., 2008; Russell et al., 2010; Smith and Balogh, 2008). Although several studies predict the  
35 occurrence of a Dalton-type minimum in the forthcoming solar cycles, there is no consensus yet on this  
36 matter (Abreu et al., 2008; Lockwood et al., 2009; Rigozo et al., 2010; Russell et al., 2010; Velasco-Herrera,  
37 2011).

#### 39 8.2.1.4 Variations in Spectral Irradiance.

40  
41 [PLACEHOLDER FOR FIRST ORDER DRAFT]

##### 43 8.2.1.4.1 Satellite measurements

44 Solar spectral irradiance (SSI) in the far (120–200 nm) and middle UV (200–300 nm) is the primary driver  
45 for heating, composition, and dynamic changes of the middle atmosphere. Measurements of the UV  
46 spectrum made by UARS go back to 1991 (Brueckner et al., 1993; Rottman et al., 1993). These indicate SC  
47 variations of ~50% at wavelengths ~120 nm, ~10% near 200 nm and ~3% near 300 nm. The UV variations  
48 account for ~30% of the SC TSI variations, while ~70% are produced by visible and infrared wavelengths  
49 (Rottman 2006). Recent measurements by SORCE (Harder et al., 2009) suggest that over the SC 23  
50 declining phase, 200–400 nm UV flux decreased far more than in prior observations, in phase with the TSI  
51 trend (the visible presents an opposite trend).

##### 53 8.2.1.4.2 Reconstructions of preindustrial UV variations

54 Krivova et al. (2011) reconstructed spectra from what is known about spectral properties of sunspots, and the  
55 relationship between TSI and magnetic fields, then they interpolated backwards based on sunspots and  
56 magnetic information. Their results show smoothed 11-years UV SSI changes between the Mm-to-present of

1 ~50% at ~120 nm, ~13% at 130 to 175 nm, ~6% at 175 to 200 nm, and ~0.7% at 200 to 350 nm. Thus, the  
2 UV SSI appears to have increased over the past 2-3 centuries with larger trends at shorter wavelengths.  
3

#### 4 *8.2.1.4.3 Impacts of UV variations on the stratosphere*

5 Ozone is the main gas involved in stratospheric radiative heating. Variations in ozone production rate are  
6 largely due to solar UV irradiance changes (Haigh, 1994), with observations showing statistically significant  
7 variations in the upper stratosphere of 2–4% along the SC (Soukharev and Hood, 2006). UV variations may  
8 also produce transport-induced ozone changes due to indirect effects on circulation (Shindell et al., 2006c).  
9 Additionally, statistically significant evidence for an 11-year variation in stratospheric temperature and zonal  
10 winds is attributed to UV radiation (Frame and Gray, 2010).  
11

12 The radiative forcing due to solar-induced ozone changes is  $0.004 \text{ W m}^{-2}$  which is a small enhancement of  
13 the solar irradiance forcing ( $0.14 \text{ W m}^{-2}$ ) from maximum to minimum (Gray et al., 2009). Incorporating the  
14 ozone response to UV variations and taking the SORCE results (Harder et al., 2009), Haigh et al. (2010)  
15 found a solar radiative forcing of the surface climate which is out of phase with solar activity. Additional  
16 analyses are needed to determine if the difference between the few years of SORCE measurements and  
17 previous observations results from instrument biases or represents a real difference in the Sun's behaviour,  
18 and if the latter, how representative such behaviour is for longer-term changes in the Sun's output.  
19

#### 20 *8.2.1.5 Summary of Other Radiative Solar-Related Forcings*

21  
22 [PLACEHOLDER FOR FIRST ORDER DRAFT: The effects of energetic particles on clouds to be taken  
23 from Chapter 7.]  
24

#### 25 *8.2.1.6 Limitations of the Solar Forcing Metric*

26  
27 The overall global mean RF from 1750–2010 is very small. During the last three decades with direct satellite  
28 observations, forcing has been negative. As the efficacy of solar forcing is near 1, these RFs provide a good  
29 indication of the impact of solar forcing on global mean annual average temperature change. Though the  
30 ozone responses to solar irradiance variations have a minimal impact on the efficacy of solar forcing, studies  
31 have shown that they can play a significant role in driving circulation anomalies that lead to regional  
32 temperature and precipitation changes (Frame and Gray, 2010; Gray et al., 2010; Haigh, 1999; Shindell et  
33 al., 2006c). These effects are primarily due to differential heating driven by both the SSI changes and the  
34 resulting ozone changes. Solar forcing can also interact with natural modes of circulation such as the  
35 Northern Annular Mode. Additionally, changes in solar irradiance will lead to a surface forcing in clear sky  
36 areas such as the subtropics that is substantially larger than the surface forcing in cloudy regions such as the  
37 tropics, and this differential may also induce ocean-atmosphere response (e.g., Meehl et al., 200x). The RF  
38 metric is unable to capture these aspects of the climate response to solar forcing. [Section to be expanded  
39 somewhat.]  
40

## 41 **8.2.2 Volcanic**

42  
43 [PLACEHOLDER FOR FIRST ORDER DRAFT: (Meehl et al., 2007)]  
44

### 45 *8.2.2.1 Introduction*

46  
47 Explosive volcanic eruptions that inject substantial amounts of  $\text{SO}_2$  into the stratosphere are the dominant  
48 natural cause of climate change on the annual, decadal, and century time scales, and can explain much of the  
49 preindustrial climate change of the last millennium. While volcanic eruptions inject both mineral particles  
50 (called ash or tephra) and sulphate aerosol precursors into the atmosphere, it is the sulphate aerosols, because  
51 of their small size and long lifetimes, that are responsible for radiative forcing important for climate. Only  
52 eruptions that are powerful enough to inject sulphur into the stratosphere are important for climate change, as  
53 the e-folding lifetime of aerosols in the troposphere is only about one week, while sulphate aerosols in the  
54 stratosphere from tropical eruptions have a lifetime of about one year, while those from high-latitude  
55 eruptions last several months. (Robock, 2000) and AR4 (Forster et al., 2007) provide summaries of this  
56 relatively well understood climate forcing.  
57

1 There have been no large volcanic eruptions with a detectable climatic response since the 1991 Mt. Pinatubo  
2 eruption, but several moderate high latitude eruptions have led to a better understanding of their effects. New  
3 work has also produced a better understanding of the hydrological response to volcanic eruptions  
4 (Anchukaitis et al., 2010; Trenberth and Dai, 2007), better long-term records of past volcanism, and better  
5 understanding of the effects of very large eruptions.

6  
7 There are several ways to measure both the SO<sub>2</sub> precursor and sulphate aerosols in the stratosphere. While  
8 both the ultraviolet signal measured by satellite instruments can measure SO<sub>2</sub>, the resulting aerosols are  
9 harder to observe. The only limb scanner now in orbit is OSIRIS (Bourassa et al., 2008; Bourassa et al.,  
10 2010; Llewellyn et al., 2004). The Cloud-Aerosol Lidar with Orthogonal Polarization (CALIOP) on  
11 CALIPSO can measure the vertical profile in thin slices of aerosol clouds and several ground-based lidars  
12 are ready to look up at stratospheric clouds, but there are few in the tropics. In situ balloon and airplane  
13 sampling is possible, but there is no organized system to be ready for the next big eruption.

14  
15 As clearly described by (Forster et al., 2007), there are four types of volcanic forcing: direct radiative  
16 forcing; differential (vertical or horizontal) heating, producing gradients and circulation; interactions with  
17 other modes of circulation, such as El Niño/Southern Oscillation (ENSO); and ozone depletion, which  
18 depends on anthropogenic chlorine with its effects on stratospheric heating.

#### 19 20 8.2.2.2 *Recent Eruptions*

21  
22 Although the background stratospheric aerosol concentration has had an upward trend for the past decade  
23 (Hofmann et al., 2009), there have been no climatically significant eruptions since the 1991 Mt. Pinatubo  
24 eruption. Two recent high-latitude eruptions, of Kasatochi Volcano (52.1°N, 175.3°W) on August 8, 2008  
25 and of Sarychev Volcano (48.1°N, 153.2°E) on June 12–16, 2009, each injected ~1.5 Tg SO<sub>2</sub> into the  
26 stratosphere, but did not produce detectable climate response. Their eruptions, however, led to better  
27 understanding of the dependence of the amount of material and time of year of high-latitude injections to  
28 produce climate impacts (Haywood et al., 2010; Kravitz and Robock, 2011; Kravitz et al., 2010) (Kravitz et  
29 al., 2011; Sarychev, submitted). The radiative forcing from high-latitude eruptions is a function of the  
30 amount of sunlight available to block and the 3-4 month e-folding lifetime of high-latitude volcanic aerosols.  
31 (Kravitz and Robock 2011) showed that eruptions must inject at least 5 Tg SO<sub>2</sub> into the lower stratosphere in  
32 the spring or summer, and much more in fall or winter, to have a detectible climatic response.

33  
34 On April 14, 2010 the Eyjafjallajökull volcano in Iceland (63.6°N, 19.6°W) began an explosive eruption  
35 phase that shut down air traffic in Europe for 6 days and continued to disrupt it for another month. While the  
36 1991 Mt. Pinatubo eruption injected about 20 Tg SO<sub>2</sub> into the lower stratosphere, Eyjafjallajökull emitted a  
37 few kilotons of SO<sub>2</sub> per day into the troposphere for several weeks. Thus, because of the difference in total  
38 emissions by a factor of 1000 and difference in lifetime by a factor of 50, the climatic impact of  
39 Eyjafjallajökull was 50,000 times less than that of Pinatubo and was therefore undetectable amidst the  
40 chaotic weather noise in the atmosphere (Robock, 2010).

41  
42 Figure 8.8 shows a reconstruction of volcanic aerosol optical depth.

#### 43 44 **[INSERT FIGURE 8.8 HERE]**

45 **Figure 8.8:** Two volcanic reconstructions of aerosol optical depth (at 550 μm) as developed for the  
46 Paleoclimate Model Intercomparison Project (top), with a comparison to the modern estimates of Sato et al.  
47 (1993) (bottom) (note the different vertical scales in the two panels). Figure from Schmidt et al., 2011.

#### 48 49 8.2.2.3 *Long-Term Effects*

50  
51 While lunar brightness and color during eclipses (Stothers, 2007) and tree ring records (Salzer and Hughes,  
52 2007) are useful for producing records of past volcanism, because ice cores actually preserve the very  
53 material that was in the stratosphere they are the most useful way of producing such records. New work  
54 using ice core records of sulphur deposition has produced better records of volcanic forcing for use in  
55 climate models and analyses of past climate change. (Gao et al., 2006) showed that the 1452 or 1453 Kuwae  
56 eruption of was even larger in terms of radiative forcing than the 1815 Tambora eruption. Accounting for the  
57 dependence of the spatial distribution of sulphate on precipitation (Gao et al., 2007) and using more than 40

1 ice core records from Greenland and Antarctica, (Gao et al., 2008) and (Gao et al., 2009) produced a record  
2 of volcanic forcing of climate for the past 1500 years (Figure 8.9) that is a function of latitude, month, and  
3 altitude that is being used for new climate model simulations for this period (see Section x).

4  
5 New work on the mechanisms by which a supereruption (Self and Blake 2008) could force climate has  
6 focused on the 74,000 B.P. eruption of the Toba volcano (2.5°N, 99.0°E). (Robock et al., 2009) used  
7 simulations of up to 900 times the 1991 Pinatubo sulphate injection to show that the forcing is not linear as a  
8 function of the injection after a substantial part of the solar radiation is blocked. They also showed that  
9 chemical interactions with ozone had small impacts on the forcing and that the idea of (Bekki et al., 1996)  
10 that water vapour would limit and prolong the growth of aerosols was not supported. (Timmreck et al., 2010)  
11 however, incorporating the idea of (Pinto et al., 1989) that aerosols would grow and therefore both have less  
12 radiative forcing per unit mass and fall out of the atmosphere more quickly, found much less of a radiative  
13 impact from such a large stratospheric input.

#### 14 [INSERT FIGURE 8.9 HERE]

15 **Figure 8.9:** Annual stratospheric volcanic sulfate aerosol injection for the past 1500 years in the (top)  
16 NH, (middle) SH, and (bottom) global. Figure from (Gao et al., 2008).

#### 17 8.2.2.4 Future Effects

18  
19 How well can we predict the next climatically-important eruption? (Ammann and Naveau, 2003) and  
20 (Stothers, 2007) suggested an 80-year periodicity in past eruptions, but the data record is quite short and  
21 imperfect. While the period 1912–1963 C.E. was unusual for the past 500 years in having no large volcanic  
22 eruptions, and the period 1250–1300 C.E. had the most climatically-significant eruptions in the past 1500  
23 years (Gao et al., 2008), current knowledge only allows us to predict such periods on a statistical basis,  
24 assuming that the recent past distributions are stationary. (Ammann and Naveau, 2003; Deligne et al., 2010;  
25 Gusev, 2008) studied these statistical properties and (Ammann and Naveau, 2010) showed how they could  
26 be used to produce a statistical distribution for future simulations.

27  
28 While the future forcing from volcanic eruptions will only depend on the stratospheric aerosol loading for  
29 most forcing mechanisms, the future effects on ozone will diminish as ozone depleting substances diminish  
30 in the future (Eyring et al., 2010b).

### 31 8.3 Atmospheric Chemistry

32 [PLACEHOLDER FOR FIRST ORDER DRAFT: Section to coordinate with Chapter 7 on aerosol  
33 chemistry, with Chapter 2 and Chapter 6 on ozone chemistry and observations and nitrogen deposition, and  
34 Chapter 6 and Chapter 7 for biogenic emissions.]

#### 35 8.3.1 Introduction (What Aspects of Chemistry are Relevant to Radiative Forcing?)

36 Atmospheric chemistry converts precursor emissions into concentrations of chemical species (both gas-phase  
37 and aerosols) that are relevant to climate. It also influences the removal rate of many of these species.  
38 Chemical species can interact with climate with 4 different pathways: 1) direct radiative impact 2) cloud-  
39 aerosols interaction 3) deposition of aerosols (mostly black carbon or soot and dust) on snow and ice and 4)  
40 interaction with the biosphere (land and ocean).

41  
42 Chemistry in the atmosphere determines the location and rate at which a specific compound is produced or  
43 destroyed by interaction with light or other reactive compounds. In particular, integrated chemical losses  
44 define the chemical lifetime of the affected compound. Species can also be affected by physical removal  
45 processes (usually referred to as dry and wet deposition), for which an equivalent lifetime can be estimated.  
46 At steady-state, lifetime is simply the ratio of the atmospheric burden to the total loss rate of the compound  
47 of interest. For short-lived species, this concept is of limited application as this lifetime can strongly depend  
48 on time and location.

49 Because of the interactive nature of chemistry, any chemically reactive gas, whether itself a greenhouse gas  
50 or not, will produce some level of indirect greenhouse effect through its impact on atmospheric chemistry. In

1 particular, indirect changes in emissions of short-lived gases can lead to long-lived perturbations (Prather  
2 papers; Fulestvedt et al., 1996; Collins et al., 2002; Collins et al., 2010; Derwent et al., 2001).

3  
4 [PLACEHOLDER FOR FIRST ORDER DRAFT: Schematic?]

### 6 **8.3.2 Chemistry, Troposphere and Stratosphere**

7  
8 Chemical rates of reaction are strongly affected by temperature, radiation, density and availability of surface  
9 area and water (existence of cloud...). As a consequence, chemistry in the troposphere and stratosphere  
10 behave quite differently. In addition, many compounds emitted at the surface are relatively short lived (few  
11 weeks or less) and can therefore be present in significant amounts only in the troposphere. Finally, water  
12 vapour in the troposphere is several orders of magnitude larger than in the stratosphere. All these combined  
13 provide a strong vertical structure in atmospheric chemistry.

14  
15 Tropospheric chemistry is characterized by the presence of aerosols, VOCs and smog-like conditions. In this  
16 region, the lifetime of many chemical species is related to their interaction with the hydroxyl radical (OH);  
17 this is of particular importance for methane as the levels of OH are varying in time (Montzka et al., 2011).  
18 Nonlinearities in the net chemical production of ozone are associated with the presence of NO<sub>x</sub>, leading to  
19 ozone loss with too little or too much NO<sub>x</sub>. The actual levels at which these transitions occur are dependent  
20 on VOC levels. The troposphere is also where most of the formation of aerosols (sulphate, nitrate, SOA)  
21 occur from gas-phase and aerosol (including liquid-phase) reactions. Recent results in chemistry have  
22 highlighted shortcomings in our understanding of the oxidation of hydrocarbons, especially isoprene, with  
23 significant influence on surface OH conditions (Taraborelli, Paulot). Furthermore, this field of research is  
24 complementing the overall research field on the formation of secondary-organic aerosols. Organic material  
25 contributes 20–50% of the total fine aerosol mass at continental mid-latitudes (Saxena and Hildemann, 1996;  
26 Putaud et al., 2004) and as much as 90% in the tropical forested areas (Andreae and Crutzen, 1997; Talbot  
27 et al., 1988; 1990; Artaxo et al., 1988; 1990; Roberts et al., 2001; Kanakidou et al., 2005). However, Heald et  
28 al. has indicated that the present modelling of secondary-organic aerosols is significantly lower than the  
29 observations. Additional field studies (Kleinman/Volkamer in MILAGRO, Johnson in TORCH...) have  
30 shown that this is a widespread problem. Numerous approaches are being studied to resolve this deficiency  
31 (Seinfeld 2-product, Griffin mechanism, Donahue volatility) with limited results at present; Inhomogeneous  
32 nucleation is important in this process (Liao and Seinfeld, 2005; Pozzoli et al., 2008) OC is still  
33 underestimated even with SEinfeld 2-product. Furthermore, recent studies (EPA paper) are emphasizing the  
34 coupling between biogenic and anthropogenic emissions; in particular, these highlight the importance of pre-  
35 existing particles in enhancing the contribution of biogenic compounds to the aerosol composition (Jimenez  
36 paper).

37  
38 Recent papers have highlighted the role of short-lived halogen species (Saiz-Lopez, Read) in defining the  
39 boundary-layer composition, especially for its role on ozone. This additional chemistry was shown to help  
40 representing the observed low-ozone levels at the turn of the 20th century (Harvard reference to be added).

41  
42 In summary, much remains to be learned about the chemistry and composition of the atmosphere, especially  
43 in the remote regions; this may have very strong influence on our ability to fully define the pre-industrial  
44 conditions and therefore the impact of man-made emissions, especially with respect to aerosols and their  
45 impact

46  
47 Stratospheric chemistry is characterized by the ozone-layer (with the recent perturbation from man-made  
48 CFCs; due to the Montreal protocol, the observed levels of chlorine in the stratosphere has likely reached its  
49 peak) and the occasional volcanic eruptions. While water vapour entering the stratosphere through the  
50 tropical tropopause region is limited by the existence of a minimum in temperature, stratospheric water  
51 formation occur from methane oxidation and photolysis. This is strongly influenced by the presence of CO<sub>2</sub>  
52 in the stratosphere, leading to increased cooling.

53  
54 Both are coupled through stratosphere-troposphere exchange. Extra-tropical STE is mostly of importance to  
55 tropospheric ozone budget (Collins et al., 2003; Hegglin and Shepherd; CCMval papers), while tropical TSE  
56 (and to some extent transport through the monsoon regions; HCN paper by Randel) defines the rate and  
57 composition of air entering the stratosphere, especially water vapour. There is indication that, owing to

1 climate change, the overall stratospheric circulation (aka Brewer-Dobson) has been accelerating in the recent  
2 past (WMO, 2011; Lamarque and Solomon, 2010).

### 3 4 **8.3.3 Budgets for Key Species: Emissions, Deposition (Wet and Dry), Burden, Lifetimes, STE and** 5 **Chemistry (includes Biogenics, Fires, etc., as well as Anthropogenic)** 6

7 [PLACEHOLDER FOR FIRST ORDER DRAFT: Discuss global budgets of (use ACC-MIP results to refine  
8 previous publications); Ozone (Stevenson et al., in AR4); Nitrogen species (discuss role of deposition);  
9 Methane (and stratospheric water); main loss is  $\text{CH}_4 + \text{OH}$ ;  $\text{N}_2\text{O}$ ; and Aerosols (coordination with Chapter  
10 7).]

### 11 12 **8.3.4 Evaluation of Chemistry Models** 13

14 [PLACEHOLDER FOR FIRST ORDER DRAFT: Section to coordinate with Chapter 9 on  $\text{O}_3$ , OH,  
15 stratospheric  $\text{H}_2\text{O}$ , TES ozone RF; perhaps  $\text{NO}_2$  and CO; and coordinate with Chapter 7 on aerosols.]

#### 16 17 **8.3.4.1 Modeling of Atmospheric Chemistry (Constituents, Reaction, Processes)** 18

19 Models provide a representation of the four-dimensional structure (space and time) of all the processes  
20 influencing the distribution of chemical species. These include emissions, deposition, transport and chemical  
21 reactions. Each model includes those processes with varying degrees of complexity and it is the interplay of  
22 these processes that defines the ability of a model to simulate atmospheric chemistry.

23  
24 Because of the limited availability of observations and the strong variations in the distributions of short-lived  
25 species of importance to climate, models are necessary to define the overall increase between pre-industrial  
26 and present-day conditions (include Table). The simulation of the latter period (or recent decades since few  
27 reliable observations are available before 1980; coordination with Chapter 2 needed) can be used to evaluate  
28 models.

29  
30 Model evaluation can be performed at the process level (looking for example at the ratio of two VOCs to  
31 define the amount of OH that was encountered by a specific air parcel) or at the concentration level  
32 (comparing modelled ozone with ozone sondes). Also, comparison with more extensive models (for example  
33 compare chemistry solver with Master Mechanism).

34  
35 Limitations in models arise from:

- 36 1. Limitation in representation of chemistry (limited mechanisms; especially for VOC)
- 37 2. Limitation in resolution (chemistry is nonlinear; Wild and Prather for convergence)
- 38 3. Limitation in representation of physical processes (uptake by aerosol, water droplets/ vegetation, STE)

39  
40 Careful comparison and validation of simplified processes in the coarse-gridded global climate models is  
41 needed with detailed regional chemical transport models with full chemical processes.

#### 42 43 **8.3.4.2 Comparison with Observations** 44

45 [PLACEHOLDER FOR FIRST ORDER DRAFT: Section to include climatology, trends to the extent results  
46 are available. Present-day climatology, including from satellites CO,  $\text{NO}_2$ ,  $\text{NH}_3$ , ozone (including  
47 tropospheric). Observed trends in surface and mid-troposphere ozone and observed trends in nitrogen  
48 deposition (coordination with Chapter 2 needed). Observed trends of aerosol direct effects, optical and  
49 chemical properties. Include CO/ $\text{O}_3$  correlation from satellites (Voulgarakis et al., ACPD, 2011).]

### 50 51 **8.3.5 Concluding Remarks** 52

53 [PLACEHOLDER FOR FIRST ORDER DRAFT]  
54

## 55 **8.4 Present-Day Anthropogenic Radiative Forcing** 56

57 [PLACEHOLDER FOR FIRST ORDER DRAFT]

#### 8.4.1 *Changes in Our Understanding of the Spectral Properties of Radiative Transfer and Representation in Radiative Transfer Codes*

Radiative forcing estimates are performed with a combination of radiative transfer codes typical for GCMs as well as more detailed radiative transfer codes. Physical properties are needed in the radiative transfer codes such as absorption data for gases. HITRAN (High Resolution Transmission) (Rothman, 2010) is widely used in radiative transfer models and satellite retrievals and the current edition is HITRAN 2008 (Rothman and Coauthors, 2009). Some researchers studied the difference among different editions of HITRAN databases for diverse uses (Feng et al., 2007; Kratz, 2008; Feng and Zhao, 2009; Fomin and Falaleeva, 2009). GEISA (Gestion et Etude des Informations Spectroscopiques Atmosphériques) (Jacquinet-Husson and Coauthors, 2008) and Ford Motor Company databases (Sihra et al., 2001; Sihra et al., 2001; Gohar et al., 2004; Bravo et al., 2010) are also used in radiative forcing estimates. Bravo et al. (2010) use both measured and theoretical determined absorption data.

Model calculations have shown that modifications of the spectroscopic characteristics tend to have a modest effect on the determination of spectrally integrated radiances, fluxes and radiative forcing estimates, with the largest differences being of order  $1 \text{ W m}^{-2}$  for the total thermal infrared fluxes, and of order 2–3% of the calculated radiative forcing at the tropopause attributed to the combined doubling of  $\text{CO}_2$ ,  $\text{N}_2\text{O}$  and  $\text{CH}_4$  (Kratz, 2008). These results show the updated edition is advised to be used. It is shown that cloud can greatly reduce the effects on the radiative forcing due to HFCs, the maximum decrease is –25% (Zhang et al., 2011). So, the parameterization of the optical properties of clouds is also an important part to be improved in radiative transfer models.

Line by line (LBL) model is the benchmark of radiative transfer models with using the HITRAN dataset as an input. The accuracy given by LBL is important to evaluate the calculated radiative forcing by diverse models. Some researchers compared different LBL models (Zhang et al., 2005; Collins et al., 2006) and line-wing cutoff, line-shape function and water vapor continuum treatment effect on LBL calculations (Zhang et al., 2008; Fomin and Falaleeva, 2009). Prior experience indicates that LBL codes generally agree with each other very well (Collins et al., 2006).

Correlated-K method for gas absorption is widely used in GCM RT codes because of its high accuracy and fast speed. Many researchers improved their expressions in GCMs with using the updated spectral dataset (Fomin, 2000); Fomin and Correa, 2005; Zhang and Shi, 2005b; Zhang et al., 2006a; Zhang et al., 2006b; Shi and Zhang, 2007; Tarasova and Fomin, 2007; Moncet et al., 2008; Hasekamp and Butz, 2008; Shi et al., 2009; Hogan, 2010; Li et al., 2010). Zhang et al. (2003) has shown the accuracy of the radiative forcing for the double  $\text{CO}_2$  concentration is  $0.04 \text{ W m}^{-2}$ . Fomin (2004) has shown the error in simulation the radiative forcing at the tropopause is below 3%. Li et al. (2010) added the incoming solar energy in longwave and showed that more solar energy are absorbed in the atmosphere and less at the surface; they also added  $\text{CH}_4$  absorption in the shortwave for their RT code in GCM since none of GCM RT codes in the IPCC AR4 included the shortwave effect of  $\text{CH}_4$ . The shortwave radiative forcing at the surface due to  $\text{CH}_4$  since the preindustrial period is estimated to exceed that due to  $\text{CO}_2$ . The  $\text{CH}_4$  shortwave forcing of  $0.53 \text{ W m}^{-2}$  at the surface is 68% larger than that of  $\text{CO}_2$ ; however, the shortwave RF of  $\text{CH}_4$  at tropopause is weak. Li et al. (2010) show that the  $\text{CH}_4$  shortwave effect can be included in a correlated k-distribution model, with the additional flux being accurately simulated in comparison with LBL models.

#### 8.4.2 *Well-Mixed Greenhouse Gases*

[PLACEHOLDER FOR FIRST ORDER DRAFT]

##### 8.4.2.1 $\text{CO}_2$

As shown in Chapter 2. The atmospheric mixing ration of  $\text{CO}_2$  has increased globally by about 109ppm (x%) from  $278 \pm 1.2 \text{ ppm}$  (MacFarling Meure et al., 2006) in 1750 (before large scale industrialisation) to 386 in 2009. Most of this growth has occurred since 1970.

1 The increases in global atmospheric CO<sub>2</sub> since 1750 are mainly due to emissions from fossil fuel  
2 combustion, cement production, land use change and biomass burning. As described in Chapter 6 only a  
3 fraction (known as the “airborne fraction”) of the historical CO<sub>2</sub> emissions have remained in the atmosphere.  
4 Approximately half (or is it 40% AR4 p139?) have been taken up by the land and ocean.  
5

6 A contribution to the uncertainty in the anthropogenic forcing of the long-lived greenhouse gases (LLGHGs)  
7 comes from the choice of the baseline date (1750) representing the division between natural and  
8 anthropogenic driven changes. There may be a small contribution to the CO<sub>2</sub> increase from rising  
9 temperatures in the second half of the 18th Century (MacFarling Meure et al., 2006).  
10

11 Using the simple formula from Ramaswamy et al. (2001) the CO<sub>2</sub> radiative forcing (as defined in Section  
12 8.1) from 1750 to 2009 is 1.76 W m<sup>-2</sup>. The uncertainties in the total forcing are approximately 10%. The  
13 impact of land use change on CO<sub>2</sub> has contributed 0.17–0.51 W m<sup>-2</sup> (this is included in the RF for CO<sub>2</sub> rather  
14 than land-use).  
15

16 Table 8.1 shows the concentrations and RF in AR4 (2005) and 2009 for the most important LLGHGs. Figure  
17 8.10 shows the time evolution of RF (will be updated).  
18

### 19 [INSERT FIGURE 8.10 HERE]

20 **Figure 8.10:** Radiative forcing from long-lived greenhouse gases. This will be extended backwards and  
21 forwards in time. Speciation of the 15 minor gases will be added.  
22

23 Indirect effects: latent heat flux (Doutriaux-Boucher et al., 2009), clouds (Andrews and Forster, 2008).  
24

#### 25 8.4.2.2 CH<sub>4</sub>

26  
27 Global averaged (surface) methane concentrations have risen from 715 ± 4 ppb in 1750 to 1794 ppb by 2009.  
28 Over that timescale the rise has been predominantly due to changes in anthropogenic-related methane  
29 emissions including fossil fuel extraction and transport, waste management, and agriculture. Anthropogenic  
30 emissions of other compounds have also affected methane concentrations. As described in Section 8.3,  
31 emissions of oxidised nitrogen (NO<sub>x</sub>) increase the removal of methane from the atmosphere, whereas  
32 emissions of carbon monoxide and non-methane hydrocarbons tend to decrease the rate of methane removal.  
33

34 As with CO<sub>2</sub> the trend in methane concentrations before 1750 was not flat, but showed a gradual rise from  
35 AD 0 (MacFarling Meure et al., 2006). Part of this trend may be due to changes in climate (which affects  
36 both the emissions and removal), but anthropogenic emissions from agriculture, domestic waste, wood fuel,  
37 and biomass burning may also have contributed. If so, then the radiative forcing from 1750 to present day  
38 may underestimate the human contribution.  
39

40 Using the formula from Ramaswamy et al. (2001) the RF for methane from 1750 to 2009 is 0.49 W m<sup>-2</sup>, with  
41 an uncertainty of ±10% from the radiative transfer codes. This increase of 0.01 W m<sup>-2</sup> since AR4 is due to  
42 the 20 ppb increase in the methane mixing ratio driven by a combination of increase in natural and  
43 anthropogenic emissions.  
44

#### 45 8.4.2.3 Others

##### 46 N<sub>2</sub>O

47  
48 Concentrations have risen from 270 ppb in 1750 to 322.5 ppb in 2009, leading to a forcing of 0.17 W m<sup>-2</sup>  
49 (0.16 W m<sup>-2</sup>) in AR4. This is an increase of 3.3 ppb since 2005. N<sub>2</sub>O has now the third largest RF of the  
50 well-mixed greenhouse gases and has now larger RF than CFC-12.  
51

##### 52 Halocarbons

53 The Montreal Protocol gases contribute approximately 11% of the LLGHG forcing. Although emissions  
54 have been drastically reduced for CFCs, their long lifetimes means this takes time to affect their  
55 concentrations. The forcing from CFCs has declined since 2005 (mainly due to a reduction in the  
56 concentration of CFC-12), whereas the forcing from HCFCs is still rising (mainly due an increase in the  
57 concentrations of HCFC-22).

1  
2 *New species*

3 NF<sub>3</sub>: 0.45 ppt (Weiss et al., 2008) × 0.21 W m<sup>-2</sup> ppbv<sup>-1</sup> (Forster et al., 2007) gives 0.0001 W m<sup>-2</sup>. Sulfuryl  
4 Fluoride: 1.4 ppt (Muhle et al., 2009) × 0.2 W m<sup>-2</sup> ppbv<sup>-1</sup> (Andersen et al., 2009) gives 0.0003 W m<sup>-2</sup>.

5  
6  
7 **Table 8.1:** Present-day concentrations (in ppt except where specified) and RF (in W m<sup>-2</sup>) for the measured  
8 LLGHGs. The data for 2005 (the time of the AR4 estimates) are also shown.

<i>Species</i>	Concentrations (ppt)		Radiative forcing	
	2009	2005	2009	2005
CO <sub>2</sub> (ppm)	386.3	378.7	1.76	1.66
CH <sub>4</sub> (ppb)	1794.2	1774.5	0.49	0.48
N <sub>2</sub> O (ppb)	322.5	319.2	0.17	0.16
CFC-11	243.1	251.5	0.0608	0.0631
CFC-12	532.6	541.5	0.170	0.173
CFC-13	2.7		0.00068	
CFC-113	75.9	78.8	0.0228	0.0236
CFC-115	8.0		0.00144	
HCFC-22	198.4	168.3	0.0397	0.0337
HCFC-141b	19.8	17.6	0.00277	0.00246
HCFC-142b	19.4	15.2	0.00388	0.00304
HFC-23	22.6	19.0	0.00429	0.00361
HFC-32	3.0		0.00033	
HFC-125	7.3	3.9	0.00168	0.000897
HFC-134a	52.4	34.4	0.00838	0.00550
HFC-143a	9.0	5.1	0.00117	0.00663
HFC-152a	5.9	3.6	0.000531	0.000324
SF <sub>6</sub>	6.76	5.67	0.00352	0.00295
CF <sub>4</sub>				
C <sub>2</sub> F <sub>6</sub>				
CH <sub>3</sub> CCl <sub>3</sub>	9.1	18.4	0.000546	0.00110
CCl <sub>4</sub>	89.4	94.6	0.0116	0.0123
CFCs			0.263 <sup>a</sup>	0.269 <sup>b</sup>
HCFCs			0.0463	0.0392
Montreal Gases			0.322	0.322
Halocarbons			0.334	0.326
<b>Total</b>			<b>2.76</b>	<b>2.64</b>

9 Notes:

10 (a) Totals includes 0.007 W m<sup>-2</sup> to account for CFC-114, Halon-1211 and Halon-1301.

11 (b) Totals includes 0.009 W m<sup>-2</sup> forcing (as in AR4) to account for CFC-13, CHF-114, CFC-115, Halon-1211 and  
12 Halon-1301.

### 15 8.4.3 Short-Lived Gases

17 [PLACEHOLDER FOR FIRST ORDER DRAFT]

#### 19 8.4.3.1 Tropospheric Ozone (including by precursor)

21 Ozone is not emitted directly into the atmosphere; instead it is formed by photochemical reactions. In the  
22 troposphere these reactions involve precursor species such as oxides of nitrogen and organic compounds that  
23 are emitted into the atmosphere from a variety of natural and anthropogenic sources (Section 8.3).

1 Due to the limited spatial and temporal coverage of observations, models of tropospheric photochemistry are  
2 usually used to estimate both the pre-industrial and present day ozone distributions. Satellite instruments are  
3 able measure the total long-wave forcing from ozone (i.e., present day ozone compared to zero). Two using  
4 the TES instrument (Aghedo et al., 2011; Worden et al., 2008) have come up with similar values ( $0.37 \text{ W m}^{-2}$   
5 global using 1 month of observations,  $0.48 \text{ W m}^{-2}$  tropical oceans), where as one estimating the contribution  
6 of tropospheric ozone indirectly by examining the residual between the much larger total column from OMI  
7 and the stratospheric column from MLS (Joiner et al., 2009) calculates a total longwave ozone forcing of  
8  $1.53 \text{ W m}^{-2}$ .

9  
10 Anthropogenic emissions of precursor species have increased the concentration of tropospheric ozone.  
11 Changes in climate have also affected tropospheric ozone concentrations through changes in the chemistry,  
12 natural emissions and transport from the stratosphere (Isaksen et al., 2009).

13  
14 The most recent estimates of changes in anthropogenic emissions over the historical period come from  
15 Lamarque et al. (2010) although models using these emissions are still unable to reproduce recent trends in  
16 surface ozone or pre-industrial levels. Some text here on the radiative forcing estimates from ACCMIP. The  
17 forcing is sensitive to the assumed pre-industrial distribution (Mickley et al., 2001). This forcing can be  
18 attributed to anthropogenic emissions of the different precursors. Shindell et al. (2009a) calculate a  
19 tropospheric ozone forcing of  $0.37 \text{ W m}^{-2}$  of which  $0.28 \text{ W m}^{-2}$  is due to methane emissions since 1750,  $0.04$   
20  $\text{W m}^{-2}$  from  $\text{NO}_x$  emissions, and  $0.05 \text{ W m}^{-2}$  from CO and VOCs. These results were calculated by holding  
21 emissions of all precursors at present day levels and reducing one at a time to pre-industrial levels. Due to  
22 the non-linearity of the chemistry, starting from pre-industrial conditions and increasing precursor emissions  
23 singly may give a different result. Note that as well as inducing an ozone forcing, these ozone precursor  
24 species can also strongly effect the concentrations of methane and aerosols, adding extra terms (both positive  
25 and negative) to their total indirect forcings.

26  
27 [PLACEHOLDER FOR FIRST ORDER DRAFT: Ozone RFs since the AR4, (Shindell et al., 2006a),  $0.40$   
28  $\text{W m}^{-2}$  (instantaneous); ACCMIP data to be added.]

29  
30 Tropospheric ozone can also affect the radiation balance indirectly by reducing the natural uptake of carbon  
31 dioxide by terrestrial vegetation. Sitch et al. (2007) found that this indirect affect was approximately equal to  
32 the direct one, thus roughly doubling the overall climate impact of tropospheric ozone. Collins et al. included  
33 this in calculations of the GTP of ozone precursors.

#### 34 35 8.4.3.2 *Stratospheric Ozone*

36  
37 Stratospheric ozone concentrations have been reduced by emissions of ozone-depleting substance (ODSs),  
38 whereas emissions of tropospheric precursors increase ozone concentrations in the troposphere and lower  
39 stratosphere. Changes in stratospheric climate (temperature and circulation) caused by both increases in  $\text{CO}_2$   
40 and decreases in ozone also affect the ozone concentrations. Forster et al. (2007) quote a forcing due to  
41 observed changes in stratospheric ozone from 1979 to 1998 of  $-0.05 \pm 0.1 \text{ W m}^{-2}$ . A more recent  
42 observational dataset (Randel and Wu, 2007) leads to a positive forcing of  $+0.03$  between the 1970s and  
43 2005 (WMO Ozone Assessment, 2010, Section 4.4.1). The same assessment calculated a model-based  
44 forcing (from 17 CCMVal models (SPARC CCMVal 2010)) due to stratospheric ozone changes of  $-0.03 \pm$   
45  $0.2 \text{ W m}^{-2}$ . The wide spread between the models may be in part due to different treatments of tropospheric  
46 ozone chemistry. The observational based studies and the CCMVal experimental setup are unable to  
47 distinguish between these various contributing factors. Thus the quoted forcing should not be attributed solely  
48 to ozone depletion. In one study comparisons between a troposphere-only and a troposphere-stratosphere  
49 model suggest a contribution to stratospheric ozone forcing from tropospheric ozone precursors of  $0.03 \text{ W}$   
50  $\text{m}^{-2}$  (Shindell et al., 2006b)

51  
52 It should be noted that the direct radiative forcing from ODSs far outweighs their contribution to the ozone  
53 forcing.

#### 54 55 8.4.3.3 *Stratospheric Water*

Oxidation of methane is the main contributor to water vapour in the stratosphere. However stratospheric water vapour can also vary through changes in dynamics (Solomon et al., 2010b) and through volcanic emission (Joshi and Jones, 2009), neither of which can be considered an anthropogenic forcing.

Myhre et al. (2007) used observations of the vertical profile of methane to deduce a contribution from oxidation of anthropogenic methane of  $0.083 \text{ W m}^{-2}$  (no error bar) which compares with the value of  $0.07 \text{ W m}^{-2}$  from calculations in a 2D model in Hansen et al. (2005).

Water vapour is directly emitted into the stratosphere by aircraft. Contributions from the current subsonic aircraft fleet are very small. Lee et al. (2009) estimate an anthropogenic contribution in 2005 of  $0.0028 \text{ W m}^{-2}$ , based on scaling up calculations of Sausen et al. (2005) to 2005 emissions.

#### 8.4.4 Land Surface Changes

[PLACEHOLDER FOR FIRST ORDER DRAFT]

##### 8.4.4.1 Introduction

Anthropogenic land cover change has a direct impact on the Earth radiation budget through a change in the surface albedo. It also impacts the climate through modifications in the surface roughness, latent heat flux, and river runoff. In addition, human activity may change the water cycle through irrigation and power plant cooling, and also generate direct input of heat to the atmosphere by consuming energy.

AR4 referenced a large number of RF estimates resulting from a change in land cover Albedo. It discussed the uncertainties due to the reconstruction of historical vegetation, the characterization of present day vegetation and the surface radiation processes. On these basis, AR4 gave a best estimate of RF relative to 1750 due to land-use related surface albedo at  $-0.2 \pm 0.2 \text{ W m}^{-2}$  with a level of scientific understanding at medium-low.

##### 8.4.4.2 Land Cover Changes

Until the mid-20th century most land use change took place over the temperate regions of the Northern hemisphere. Since then, reforestation is observed in Western Europe and North America as a result of land abandonment, while deforestation is concentrated to the tropics. After a rapid increase of the rate of deforestation during the 80s and 90s, satellite data indicate a slowdown in the past decade (FAO, 2010).

Since AR4, (Pongratz et al., 2008) extended existing reconstructions on land use back in time to the past millennium, accounting for the progress of agriculture technique, historical events such as the black death or war invasions. Note that, as agriculture was already widespread over Europe and South-Asia by 1750, the land use radiative forcing with respect to this date is weaker than that defined with respect to natural vegetation cover. Deforestation in Europe and Asia during the last millennium led to a significant negative forcing. (Betts et al., 2007) and (Goosse et al., 2006) argue that it probably contributed together with natural solar and volcanic activity to the “Little Ice Age” before the increase in greenhouse gas concentration led to temperature similar to those experienced in the early part of the second millennium.

##### 8.4.4.3 Surface Albedo and Radiative Forcing

Surface albedo is the ratio between reflected and incident solar radiation at the surface. It varies with the surface cover. Most forests are darker (i.e., lower albedo) than grasses and croplands, which are darker than barren land and desert. As a consequence, deforestation tends to increase the Earth albedo (negative radiative forcing) while cultivation of some bright surfaces may have the opposite effect. Deforestation also leads to a large increase in surface albedo in case of snow cover as low vegetation is more easily covered by snow that reflects sunlight much more than vegetation does.

The pre-industrial radiative forcing due to land use change is estimated to be on the order of  $-0.05 \text{ W m}^{-2}$  (Pongratz et al., 2009). Since then, the increase in world population and agriculture development led to additional forcing. Based on reconstruction of land use since the beginning of the industrial era, (Betts et al., 2007) computed spatially and temporally distributed estimate of the land use radiative forcing. They estimate

1 that the present day forcing due to albedo change from potential vegetation is  $-0.2 \text{ W m}^{-2}$ . A similar value  
2 ( $-0.22 \text{ W m}^{-2}$ ) was found by (Davin et al., 2007) but for the period 1860 to 1992.

3  
4 In recent years, the availability of global scale MODIS data (Liang et al., 2005) improved the surface albedo  
5 estimates (Rechid et al., 2009). These data have been used by (Myhre et al., 2005a) and (Kvalevag et al.,  
6 2010). They argue that the observed albedo difference between natural vegetation and croplands is less than  
7 usually assumed, so that the radiative forcing due to land use change is weaker than in estimates that do not  
8 use the satellite data.

9  
10 On the other hand, (Nair et al., 2007) show observational evidence of an underestimate of the surface albedo  
11 change in land use analysis. Overall, there is still a wide range of radiative forcing estimates for the albedo  
12 component of land use forcing.

13  
14 Section 8.4.2.1 quantifies the impact of deforestation on the greenhouse radiative forcing. Some authors have  
15 compared the radiative impact of deforestation/aforestation that results from either the albedo change or the  
16 greenhouse effect of  $\text{CO}_2$  released/sequestered. (Pongratz et al., 2010) shows that the historic land use  
17 change has had a warming impact (i.e., greenhouse effect dominates) at the global scale and over most regions  
18 with the exception of Europe and India. (Bala et al., 2007) results show latitudinal contrast where the  
19 greenhouse effect dominates for low latitude deforestation while the combined effect of albedo and  
20 evapotranspiration impact does at high-latitude. These results are confirmed by (Bathiany et al., 2010).  
21 Similarly, (Lohila et al., 2010) shows that the aforestation of boreal peatlands results in a balanced radiative  
22 forcing between the albedo and greenhouse effect. (Rotenberg and Yakir, 2010) shows that for a semi-Arid  
23 forest in southern Israel, the greenhouse impact of deforestation is only partly counterbalanced by the albedo  
24 impact.

25  
26 The albedo component of land use change is a radiative forcing that can be compared to other forcing such  
27 as those of GHG. However, (Davin et al., 2007) argues that the climate sensitivity to land use forcing (i.e.,  
28 the climate efficacy as defined in AR4) is lower than that for other forcings, due to its spatial distribution but  
29 also the role of non-radiative processes. This is somewhat confirmed by (Findell et al., 2007) climate  
30 simulations that show a negligible impact of land use change on the global mean temperature, although there  
31 are some significant regional changes. There is increasing evidence that the impact of land use on  
32 evapotranspiration - a non radiative effect on climate - is comparable, but of opposite sign, than the albedo  
33 effect, so that RF is not as useful a metric as it is for gases and aerosols. This is discussed in Section 8.4.4.5.

#### 34 35 8.4.4.4 *Fire-Induced Changes in Albedo*

36  
37 Burn scars resulting from agriculture practices, uncontrolled fires or deforestation have a lower albedo than  
38 unperturbed vegetation (Jin and Roy, 2005). On the other hand, at high latitude, burnt areas are more easily  
39 covered by snow, which may result in an overall increase of the surface albedo. (Myhre et al., 2005b)  
40 estimates a global radiative effect due to African fires of  $0.015 \text{ W m}^{-2}$ .

41  
42 In addition, biomass burning may impact the Earth albedo as soot particles can be deposited on snow, which  
43 has a large impact on its absorption. This is discussed in Section xxx.

#### 44 45 8.4.4.5 *Other Impacts of Surface Change on Climate*

46  
47 Numerical climate experiments demonstrate that the impact of land use on climate is much more complex  
48 than just the radiative forcing. This is due in part to the very heterogeneous nature of land use change  
49 (Barnes and Roy, 2008), but mostly due to the impact on the hydrological cycle through evapotranspiration  
50 and root depth. As a consequence, the forcing on climate is not purely radiative and the net impact on the  
51 surface temperature may be either positive or negative depending on the latitude (Bala et al., 2007). Davin  
52 and de Noblet-Ducoudre (2010) analyzes the impact on climate of large scale deforestation; the albedo  
53 cooling effect dominates for high latitude whereas reduced evapotranspiration dominates in the tropics.

54  
55 Irrigated areas have continuously increased during the 20th century although a slowdown has been observed  
56 in recent decades (Bonfils and Lobell, 2007). There is clear evidence that irrigation leads to local cooling of  
57 several degrees (Kueppers et al., 2007). Irrigation also affects cloudiness and precipitation (Puma and Cook,

2010). In the United States, (DeAngelis et al., 2010) found that irrigation in the Great Plains in the summer produced enhanced precipitation in the Midwest 1000 km to the northeast.

Campra et al. (2008) reports very large (+0.09) change in albedo and  $-20 \text{ W m}^{-2}$  radiative forcing over the province of Almeria in Southeastern Spain, a consequence of greenhouse horticulture development, which led to significant cooling, in contrast with the temperature trend in nearby regions.

Urbanization also leads to significant local climate change referred to as Urban Heat Island. This is due partly to reduced evaporation, and also to the impact of wasted heat from anthropogenic activity. Although the global-average energy input is small ( $0.03 \text{ W m}^{-2}$ ) it may reach several hundred  $\text{W m}^{-2}$  in some cities and the local warming can be as large as that estimated for a doubling of  $\text{CO}_2$  (McCarthy et al., 2010).

#### 8.4.4.6 Conclusions

There is still a rather wide range of estimates of the albedo change due to anthropogenic land use change, and its impact on the Earth radiative forcing. Although most published studies provide an estimate close to  $-0.2 \text{ W m}^{-2}$ , there is convincing evidence that it may be weaker. In addition, non-radiative impact of land use have a similar magnitude, and may be of opposite sign, as the albedo effect. A comparison of the impact of land use change according to seven climate models showed a wide range of results (Pitman et al., 2009), partly due to difference in the implementation of land cover change, but mostly due to different assumptions. There is no agreement on the sign of the temperature change induced by anthropogenic land use change. As a consequence, the level of scientific understanding cannot be raised from the medium-low value stated in AR4.

#### 8.4.5 Aerosol and Cloud Effects

[PLACEHOLDER FOR FIRST ORDER DRAFT]

##### 8.4.5.1 Introduction and Summary of AR4

In TAR RF estimates were provided for three aerosol effects. These were the direct aerosol effect, the cloud albedo effect (indirect aerosol effect), and impact of black carbon on snow and ice surface albedo. The direct aerosol effect is scattering and absorption of shortwave and longwave radiation by atmospheric aerosols. Several different aerosol types from various sources are present in the atmosphere. Most of the aerosols mostly scatter solar radiation, but some components absorb solar radiation to various extents with black carbon as the most absorbing component. Scattering aerosols exert a negative RF, whereas strongly absorbing components give a positive RF, which also depends on the underlying surface albedo. A best estimate RF of  $-0.5 \pm 0.4 \text{ W m}^{-2}$  was given in AR4 for the direct aerosol effect and a medium to low level of scientific understanding (LOSU).

An increase in the hygroscopic aerosol abundance may enhance the concentration of cloud condensation nuclei (CCN). This may increase the cloud albedo and under the assumption of fixed cloud water content it is referred to as the 'cloud albedo effect'. For the cloud albedo effect a best estimate RF of  $-0.7 \text{ W m}^{-2}$  (range from  $-1.8$  to  $-0.3$ ) was given in AR4 and a low LOSU.

Black carbon in the snow or ice can lead to a decrease of the surface albedo. This leads to a positive RF. In AR4 this mechanism was given a best estimate of  $0.1 \pm 0.1 \text{ W m}^{-2}$  and a low LOSU.

Impacts on clouds from the cloud lifetime effect and the semi-direct effect were not in accordance with the radiative forcing concept, because they involve tropospheric changes in variables other than the forcing agent, so no best estimates were provided in AR4 (see Section 8.1). The mechanisms influenced by anthropogenic aerosol including the aerosol cloud interactions are discussed in detail in Chapter 7 and summarized in the subsections below.

##### 8.4.5.2 Direct Aerosol by Component

1 Several aerosol components contribute to the direct aerosol effect, most of them mainly scatter solar  
2 radiation whereas a few also absorb solar radiation of various extent. The local RF is dependent of the  
3 mixture of aerosols, aerosol vertical profile in relation to the cloud distribution, and the underlying surface  
4 albedo (Forster et al., 2007). Based on a combination of global aerosol models and observational based  
5 methods and best estimate of the direct aerosol effect is ? with an uncertainty ? (see further description in  
6 Chapter 7). [Information on the change from AR4 to be added.]  
7

8 The direct aerosol effect is separated in 6(?) components in this report; namely sulphate, BC from fossil fuel,  
9 OC from fossil fuel, BC and OC combined from biomass burning, nitrate, and secondary organic aerosol. BC  
10 and OC from biomass burning are combined due to the joint sources, whereas treated separately for fossil  
11 fuel since there is larger variability in the ratio of BC to OC in the fossil fuel emissions. This approach is  
12 consistent with TAR and AR4. A figure of the global mean RF of these components will be added.  
13 Secondary organic aerosol is a new component compared to AR4. [Information on the change from AR4,  
14 and anthropogenic mineral dust and sea-salt changes due to climate change to be added.]  
15

16 The time evolution of the RF of the direct aerosol effect is more uncertain than the current RF. The  
17 availability of detailed observations of atmospheric aerosols has improved with the development of the  
18 Aeronet network and the launch of the MODIS instruments starting in 2000 and the current RF is  
19 constrained by the aerosol observations. The aerosol observations are very limited backward in time and  
20 uncertainties in the emission of aerosols and their precursors used in the global aerosol modeling are larger  
21 previously than for current condition. Figure 8.11 shows an example (*this will be improved by using several  
22 models*) of the time evolution of the direct aerosol effect as a total and separated into six aerosol components.  
23 The total direct aerosol effect is shown to be very weak until 1920 due to a compensation of the negative  
24 sulphate RF by the positive BC RF. From 1950 to 1970 it was a strengthening of the RF of the direct aerosol  
25 effect, mainly due to a strong enhancement of the sulphate RF. After 1970 the change has been small with  
26 even a weakening of the direct aerosol RF, mainly due to a stronger BC RF as a result of increased emissions  
27 in East Asia.  
28

29 **[INSERT FIGURE 8.11 HERE]**

30 **Figure 8.11:** Time evolution of RF of the direct aerosol effect (total as well as by components). [Figure will  
31 be updated by more models]  
32

#### 33 8.4.5.3 *Aggregated Indirect Effect*

34  
35 [Placeholder for the First Order Draft: This will follow the same structure as Section 8.4.5.2; coordination  
36 with Chapter 7 needed.]  
37

38 Estimated radiative forcings include large uncertainties caused by uncertainty in the sensitivity slope of  
39 satellite-observed and model-simulated cloud parameters as a function of the aerosol number and/or aerosol  
40 index, and those of the pre-industrial condition. Some questions arise especially in differences in satellite  
41 remote sensing methods and differences in target clouds. Estimation of radiative forcing from active sensing  
42 by cloud radar and lidar is useful as an independent estimation from the traditional methods.  
43

44 High resolution (km grid) global models provide new estimates of radiative forcing through resolving the  
45 cloud system for aerosol interaction simulation. Indirect changes of the cloud field caused by atmospheric  
46 circulation change by aerosol radiative forcings in the atmosphere and at the earth's surface should be studied  
47 in the light of new definition of the adjusted radiative forcing to include the fast response of the climate  
48 system.  
49

#### 50 8.4.5.4 *Semi-Direct Effect(s)*

51  
52 [PLACEHOLDER FOR FIRST ORDER DRAFT: This will follow the same structure as Section 8.4.5.2;  
53 coordination with Chapter 7 needed.]  
54

55 [Estimation of the atmospheric BC forcing needs to be improved. Limited satellite observation for  
56 validation.]  
57

#### 8.4.5.5 Black Carbon/Dust Deposition Snow/Ice

The RF estimation due to reduced surface albedo caused by BC in snow and ice has started by Hansen and Nazarenko (2004) and others. In AR4 this mechanism was given a best estimate of  $0.1 \text{ W m}^{-2}$  and a low LOSU. Since AR4, however, several studies have re-examined this issue and find that RF may be weaker than Hansen and Nazarenko (2004) and AR4's estimation (Flanner et al., 2009; Koch et al., 2009 and Rypdal et al., 2009). Estimates of present-day global-mean radiative forcing from black carbon (BC) in snow are only  $\sim 0.04\text{--}0.20 \text{ W m}^{-2}$  (Flanner et al., 2007). The mean surface forcing caused by black carbon over springtime Eurasian and North American snow are  $3.9 \text{ W m}^{-2}$  and  $1.2 \text{ W m}^{-2}$ , averaged from 1979–2000, and contributions from mineral dust to albedo forcing in these regions are  $1.2$  and  $0.2 \text{ W m}^{-2}$  (see Figure 8.12), respectively (Flanner et al., 2009). The global and annual mean RF estimation is  $0.01 \text{ W m}^{-2}$  (between 1890 and 1995) from Koch et al. (2009) and  $0.03 \text{ W m}^{-2}$  from Rypdal et al. (2009), which is weaker than Flanner et al. (2007), and significant lower than AR4. The value of the RF metric is especially limited in this case, however, as the efficacy is very different from 1 (Flanner et al., 2009; Koch et al., 2009).

Global mean change in albedo from BC in snow effects is  $-0.12\%$ , while Arctic is  $-1.1\%$  between 1995 and 1890, and the relevant radiative forcings are  $0.01 \text{ W m}^{-2}$  and  $0.03 \text{ W m}^{-2}$  (between 1890 and 1995) (Koch et al., 2009). Deposition of BC onto Greenland is most sensitive to North American emissions. North America and Europe each contribute  $\sim 40\%$  of total BC deposition to Greenland, with  $\sim 20\%$  from East Asia (Shindell et al., 2008). Note that this study only examined the influence of North American, European, East Asian and South Asian emissions, and hence the influence of other regions such as Asian Russia was not included. BC mixed with snow results in a  $0.5\text{--}3\%$  perturbation to the snow albedo over most of the northwestern states of United State during winter (Qian et al., 2009). A large area field campaign found that the BC content of snow in northeast China is comparable to values found in Europe ( $20\text{--}800$  ppb). The steep drop off in BC content of snow with latitude may indicate that a small fraction of BC emitted in China in the winter is exported northward to the Arctic (Huang, 2010). The global mean continental ice volume reduction from dust in snow increases temperature by  $1.4^\circ\text{C}$  (Bar-Or et al., 2008), though the contribution of changes in dust-albedo forcing during recent decades to centuries is not well known.

#### [INSERT FIGURE 8.12 HERE]

**Figure 8.12:** March–May surface radiative forcing, averaged spatially and temporally only over snow, caused by (top) black carbon in snow, (middle) mineral dust in snow, and (bottom) both agents. Middle panel does show rather large mean radiative forcing on snow in Central Asia, caused by BC and mineral dust (Flanner et al., 2009)

### 8.5 Synthesis (Global Mean Temporal Evolution)

[PLACEHOLDER FOR FIRST ORDER DRAFT]

#### 8.5.1 Summary of Radiative Forcing by Species and Uncertainties

[PLACEHOLDER FOR FIRST ORDER DRAFT: Definition of components included in the RF and ARF concept and a status of the quantification of their RF, with a table similar to in AR4 (Table 2.11).]

**Table 8.2:** [PLACEHOLDER FOR FIRST ORDER DRAFT]

	Evidence	Consensus	LOSU	Basis for Estimated Range	Change in Understanding Since AR4
LLGHG	A	1	High	Uncertainty assessment of measured trends from different observed data sets and differences between radiative transfer models	No change
Tropospheric ozone					

1 RF bar chart with time evolution (Figure 8.13). Highlight different time periods, with natural and  
 2 anthropogenic contributions. Can we say anything about the trend in anthropogenic or natural RF in  
 3 particular since 1970 (or since 1979 when several datasets start, e.g., solar, stratosphere ozone,...)?  
 4

5 The RF from CO<sub>2</sub> and other LLGHG has increased continuously with a somewhat larger growth for CO<sub>2</sub>  
 6 over the last decades.  
 7

8 The aerosol RF was rather weak until 1950 and has strengthened in the later half of last century and in  
 9 particular in the period between 1950 and 1980. Until 1950 the warming effect BC compensated to some  
 10 extent the cooling effect from the direct aerosol effect and cloud albedo effect of sulphate and organic  
 11 carbon. After 1950 the cooling effect of sulphate and organics has dominated more relative to BC due to a  
 12 larger increase in the emissions.  
 13

14 For both the LLGHG and aerosols the magnitude of the RF shown in the bar chart has increased from 1940  
 15 to 2005.  
 16

17 Volcanic RF is very weak from 1970 to the present, but it is intermittently strong a few (2–3) years after  
 18 major eruptions. For this RF mechanism the chosen time period is very important. Solar RF is slightly  
 19 negative for the period from 1979 to 2010, the time with satellite measurements, but was slightly stronger  
 20 and positive for the first half of the 20th century.  
 21

22 **[INSERT FIGURE 8.13]**

23 **Figure 8.13:** RF bar chart with time evolution of RF from major components  
 24  
 25

26 **Table 8.3:** [PLACEHOLDER FOR FIRST ORDER DRAFT: Summary table similar to AR4 (Table 2.12)]

	Global Mean Radiative Forcing (W m <sup>-2</sup> )			
	<i>SAR</i>	<i>TAR</i>	<i>AR4</i>	<i>AR5</i>
Long-lived Greenhouse Gases (Comprising CO <sub>2</sub> , CH <sub>4</sub> , N <sub>2</sub> O, and halocarbons)	2.45	2.43	2.63	2.76
Tropospheric ozone				

27  
 28  
 29 Figure 8.14 shows the development in the LOSU the last 4 assessments of the various RF mechanisms. The  
 30 Figure shows a general increased LOSU but also that more RF mechanisms have been included. Preliminary  
 31 LOSU for AR5 is included. Describe causes for changes in LOSU since AR4.  
 32

33 **[INSERT FIGURE 8.14 HERE]**

34 **Figure 8.14:** LOSU of the RF mechanisms in the 4 last IPCC assessments. The thickness of the bars  
 35 represents the relative magnitude of the RF (preliminary values). [For AR5 very preliminary values are  
 36 included.]  
 37

### 38 **8.5.2 Impacts by Emissions**

39  
 40 **LLGHG:** Calculate GWP and GTP values based on new input data (lifetimes, radiative efficiency, Impulse  
 41 Response Functions for CO<sub>2</sub> and dT; IRF\_CO<sub>2</sub>, IRF\_dT) and produce a table for selected gases; see example  
 42 below.  
 43

44 Will use Impact Response Function for CO<sub>2</sub> and dT that are consistent with other chapters.  
 45 dT response: Refer to (Boucher and Reddy, 2008; Fuglestvedt et al., 2010a; Jarvis and Li, 2011; Li and  
 46 Jarvis, 2009; Shine et al., 2005b) etc.  
 47  
 48

49 **Table 8.4:** [PLACEHOLDER FOR FIRST ORDER DRAFT] Specific radiative forcings, adjustment times,  
 50 GWPs for 20, 100 and 500 years and GTP values for 20, 50 and 100 years, for selected LLGHG. (For ozone

1 depleting substances only the direct effect on climate is included here). The GTP values are specific to a  
 2 given value of climate sensitivity. [Table to be updated.]

	Specific Forcing (W m <sup>-2</sup> kg <sup>-1</sup> )	Adjustment Time (years)	GWP			GTP		
			H=20	H=100	H=500	H=20	H=50	H=100
CH <sub>4</sub>	1.82E-13	12	72	25	7.6	57	12	4
N <sub>2</sub> O	3.88E-13	114	289	298	153	303	322	265
HFC-23	1.53E-11	270	12000	14800	12200	12800	15600	16000
HFC-125	1.08E-11	29	6350	3500	1100	6050	3370	1130
HFC-134a	8.83E-12	14	3830	1430	435	3140	795	225
HFC-152a	7.67E-12	1.4	437	124	38	149	22	18
CFC-11	1.02E-11	45	6730	4750	1620	6710	5050	2440
CFC-12	1.49E-11	100	11000	10900	5200	11500	11800	9200
CFC-113	9.01E-12	85	6540	6130	2700	6770	6660	4820
HCFC-22	1.30E-11	12	5160	1810	549	4100	871	275
HCFC-123	5.15E-12	1.3	273	77	24	91	14	11
HCFC-124	9.08E-12	5.8	2070	609	185	1220	140	87
HCFC-141b	6.74E-12	9.3	2250	725	220	1640	258	106
HCFC-142b	1.12E-11	18	5490	2310	705	4840	1680	439
CCl <sub>4</sub>	4.76E-12	26	2700	1400	435	2540	1290	397
CH <sub>3</sub> Br	5.93E-13	0.7	17	5	1	5	1	1
CH <sub>3</sub> CCl <sub>3</sub>	2.53E-12	5	506	146	45	277	31	21
H-1211	1.02E-11	16	4750	1890	575	4080	1240	328
H-1301	1.21E-11	65	8480	7140	2760	8660	7760	4840
SF <sub>6</sub>	2.00E-11	3200	16300	22800	32600	17500	23400	28000
PFC-14	6.40E-12	50000	5210	7390	11200	5620	7560	9180
PFC-116	1.06E-11	10000	8630	12200	18200	9300	12500	15100

3  
4  
5 [GWP and GTP values for other LLGHGs may be given in appendix.]

6  
7 **Short-lived Climate Forcers (SLCF):**

8 Calculate GWP and GTP values based on published papers (HTAP (O<sub>3</sub>, sulphate); Bounding BC paper and  
 9 Bond et al., 2011; Myhre et al., 2011 (Atmos Environ) etc.)

10 Will use Impact Response Function for CO<sub>2</sub> and dT that are consistent with other chapters.

11  
12  
13 **Table 8.5:** [PLACEHOLDER FOR FIRST ORDER DRAFT] GWP and GTP for time horizons (H) of 20  
 14 and 100 years derived from values of forcings and lifetimes available in the literature. (Effect of BC on  
 15 surface albedo is not included here). [Values will be updated.]

	GWP		GTP	
	H = 20	H =1 00	H = 20	H =1 00
Mid-Latitude NO <sub>x</sub>	-43 to +23	-18 to +1.6	-55 to -37	-29 to -0.02
Tropical NO <sub>x</sub>	43 to 130	-28 to -10	-260 to -220	-6.6 to -5.4
Aviation NO <sub>x</sub>	92 to 338	21 to 67	396 to 121	5.8 to 7.9
Shipping NO <sub>x</sub>	-76 to -31	-36 to - 25	-190 to -130	-35 to -30
CO	6 to 9.3	2 to 3.3	3.7 to 6.1	0.29 to 0.33
VOCs	14	4.5	7.5	1.5
Black carbon aerosol	1600	460	470	64
Organic carbon aerosol	-240	-69	-71	-10
Sulphate aerosol (dir)	-140	-40	-41	-6
Shipping sulphate (dir)	-150 to -37	-43 to -11	-44 to -11	-6.1 to -1.5

---

Shipping sulphate (indirect)	-1600 to -760	-440 to -220	-450 to -220	-63 to -31
------------------------------	---------------	--------------	--------------	------------

---

We use these metrics to estimate climate impacts of various components (in a forward looking perspective). In these examples we have used emission from Unger et al. (2010). [Emission data will be updated.]

Figure 8.15 shows integrated radiative forcing (iRF) by component for global man-made emissions; for two time horizons; 20 and 100 years.

**[INSERT FIGURE 8.15 HERE]**

**Figure 8.15:** (*Sketch*) integrated RF for Global man-made emissions by component (pulse for the year 2000 emissions) for two time horizons, 20 and 100 years. [Will be an update of Figure 2.22 in AR4 but given by driver instead. We may also show individual responses as in Figure 2.22 in AR4, e.g., O<sub>3</sub>, primary mode O<sub>3</sub> and CH<sub>4</sub> for NO<sub>x</sub>. Will also include nitrate, HFCs/CFCs/PFCs, indirect effects via clouds and albedo effect of BC.]

[While Figure 8.15 used *integrated forcing* as indicator of climate impact (in line with the GWP perspective), we may (in line with the GTP perspective) move down the cause effect chain to temperature response; see Figure 8.2, Section 8.1.2.1.]

Discuss what Figure 8.16 and Figure 8.17 show (in pulse case: SLCF decay quickly due to their atmospheric adjustment times but effects are prolonged due to climate response time. In sustained case, SLCF reach approx. constant levels since emissions are replenished every year, while long-lived components accumulate.)]

[In order to illustrate uncertainty: May add bar graph with uncertainty ranges for selected horizons (10, 20, 50, 100).]

**[INSERT FIGURE 8.16 HERE]**

**Figure 8.16:** dT(t) by component from total man-made emissions for year 2000 (one year pulse). AIC: aviation-induced cirrus. The effects of aerosols on clouds (and in the case of black carbon, on surface albedo) are not included. [Will be made consistent with rest of the chapter/other chapters.]

**[INSERT FIGURE 8.17 HERE]**

**Figure 8.17:** dT(t) by component from total man-made emissions kept constant at 2000 level. AIC: aviation-induced cirrus. The effects of aerosols on clouds (and in the case of black carbon, on surface albedo) are not included. [Will be made consistent with rest of the chapter/other chapters.]

### 8.5.3 Impacts by Activity

While subsection 8.5.2 used a *component-by-component* view a *sectoral* view is adopted here.

The transport sectors have received much attention: (Balkanski et al., 2010; Berntsen and Fuglestvedt, 2008b; Corbett et al., 2010; Eyring et al., 2010a; Fuglestvedt et al., 2008; IPCC, 1999; Lee et al., 2009; Lee et al., 2010; Skeie et al., 2009; Stevenson and Derwent, 2009; Uherek et al., 2010) etc.

Also some broader studies including other sectors: (Shindell and Faluvegi, 2010; Unger et al., 2009; Unger et al., 2008; Unger et al., 2010)

We here apply a forward looking perspective on effects (in terms of integrated RF or dT) of current emissions by sectors/activity.

Unger et al. (2010) calculated RF for a set of components emitted from each sector.

- Account for interactions and non-linearities.
- But fixed mix of emissions makes it less general and useful for different emission cases and variation within the sectors.

- Relevant for policymaking that focuses on regulating the *total activity* of that sector or for understanding the contributions from the sector to climate change.

Alternatively, one may adopt a component-by-component view:

- Relevant for policy making directed towards specific components.
- But this view will not capture interactions and non-linearities within the suite of components emitted by that sector.

RF at chosen points in time (20 and 50 years) for *sustained* emissions was used by Unger et al. (2010) as the metric for comparison. This is approximately equal to using integrated RF up to the chosen times for *pulse* emissions (and is thus consistent with the iRF and GWP perspective)

A “package view” can be obtained by studying the effect of the suite of emissions per sector in a model. Alternatively, one may adopt a component-by-component view and use emission data directly with metrics,  $E_i \times M(H)_i$ , where  $i$  is component,  $H$  is time horizon and  $M$  is the chosen metric

These metrics are usually based on complex models results; i.e., extract RF and lifetimes (e.g., Shindell et al., 2009b; Collins et al., 2010; Fuglestedt et al., 2010a)

Figure 8.18 shows integrated RF per sector and component for two time horizons; 20 and 100 years. (Emission data from Unger et al. (2010))

**[INSERT FIGURE 8.18 HERE]**

**Figure 8.18:** Integrated RF for Global man-made emissions by sector (PULSE for the year 2000) for two time horizons, 20 and 100 years. May add rectangular frame to show net, or give net numbers in Figure. Will add more components and mechanisms (e.g., indirect effects on clouds). [Will be made consistent with rest of the chapter/other chapters.]

If *temperature change* is chosen as indicator, the GTP concept can be used to study how the various components develop over time. Figures 8.19 and 8.20 show the *net* temperature effect over time for 13 sectors. One year of global emissions (i.e., one year pulses) are taken from Unger et al. (2010). In addition, we have also shown effect of keeping year 2000 emissions constant (sustained emissions cases). The Figures illustrate the effects of mix of components in the emissions profiles of the various sectors; the role of cooling vs warming agents and their differing lifetimes. The effects of aerosols on clouds (and in the case of black carbon, on surface albedo) are not included. [Will be made consistent with rest of the chapter/other chapters.]

**[INSERT FIGURE 8.19 HERE]**

**Figure 8.19:** Net  $dT(t)$  by sector from total man-made emissions (one year pulse)

**[INSERT FIGURE 8.20 HERE]**

**Figure 8.20:** Net  $dT(t)$  by sector from total man-made emissions kept constant

[May add bar graph with uncertainty ranges for selected horizons (10, 20, 50, 100)?]

In order to see the contributions from the various components (instead of having separate Figures for all sectors) we can look at the contributions after 20 years. This is done below for the pulse case shown in Figure 8.21.

**[INSERT FIGURE 8.21 HERE]**

**Figure 8.21:** net  $dT(t)$  by sector after 20 years (for one year pulse emissions). CT: Contrails. AIC: aviation-induced cirrus. The effects of aerosols on clouds (and in the case of black carbon, on surface albedo) are not included. [Will be made consistent with rest of the chapter/other chapters.]

#### 8.5.4 Future Radiative Forcing

Differences between IAM RCP forcings and CCM CMIP5/ACCMIP forcings. [Coordination needed on CO<sub>2</sub> in Chapter 6 and other species in Chapter 11 and Chapter 12.]

1  
2 The primary output of IAMs are emissions. For the purpose of generating projections of radiative forcing (as  
3 is the case of the RCPs where the main target is the 2100 total radiative forcing), those emissions are  
4 converted into concentrations using a variety of simplified representation of atmospheric chemistry and  
5 overall lifetime of the species of interest. By design, these are only available and meaningful as global  
6 averages (relate to Section 8.3.4). Additional limitations to this approach include: lack or underrepresentation  
7 of chemistry-climate feedbacks (mainly impact of temperature and water vapour), assumption of constant  
8 natural emissions (biogenics, soil and wetlands).

9  
10 The net impact of climate change on tropospheric ozone is uncertain, but it is likely to vary significantly by  
11 region, altitude, and season (Murazaki and Hess; Johnson et al.; Stevenson et al., 2006; Isaksen et al., 2009;  
12 Jacob and Winner, 2009).

13  
14 Example: Tropospheric ozone from CAM simulations (lines and equivalent RF) compared with RCP RF  
15 (squares); RCP8.5 is strongly underestimating the RF because of the lack of consideration of ozone super-  
16 recovery (Lamarque et al., 2010). (see Figure 8.22)

17  
18 **[INSERT FIGURE 8.22 HERE]**

19 **Figure 8.22:** Tropospheric ozone from CAM simulations (lines and equivalent RF) compared with RCP RF  
20 (squares); RCP8.5 is strongly underestimating the RF because of the lack of consideration of ozone super-  
21 recovery (Lamarque et al., 2010).

## 22 23 **8.6 Geographic Distribution of Radiative Forcing**

24  
25 [PLACEHOLDER FOR FIRST ORDER DRAFT]

### 26 27 **8.6.1 Spatial Distribution of Current Radiative Forcing**

28  
29 [PLACEHOLDER FOR FIRST ORDER DRAFT: Input from ACCMIP + additional simulations +  
30 observations to be included.]

31  
32 The spatial pattern of the RF of the various radiative forcing mechanisms varies substantially (Ramaswamy  
33 et al., 2001). The homogeneous distributed LLGHGs have a rather homogenous spatial pattern of the RF, but  
34 are influenced by variability of the temperature (surface as well as atmospheric), humidity, and clouds. For  
35 the short-lived components like tropospheric ozone and aerosols the spatial pattern in their concentrations are  
36 highly inhomogeneous and that is the main cause for the inhomogeneous pattern in RF, but also here factors  
37 such as temperature (for ozone), humidity, clouds, and surface albedo contributes.

38  
39 The differences between the RF (according to definition in Section 8.1.1) and the surface radiative forcing  
40 are very small for some components but larger for other RF mechanisms (Andrews et al., 2010; Forster et al.,  
41 2007; Ramanathan and Carmichael, 2008). The cause for this difference is that some components absorb  
42 longwave or solar radiation in the atmosphere. Components that affect the radiation balance by pure  
43 scattering of radiation have a very small difference in the RF and the surface radiative forcing. The direct  
44 aerosol effect of sulphate and the cloud albedo effect are examples of components that affect the radiative  
45 balance by scattering of solar radiation.

46  
47 Figure 8.23 shows RF and surface radiative forcing for the total direct aerosol effect with much larger  
48 changes in the surface radiative forcing than RF mainly due to BC. [This will be extended with similar  
49 Figures for CO<sub>2</sub>, tropospheric ozone, direct aerosol effect of sulphate and BC and others.]

50  
51 Figure 8.24 shows a bar chart of the difference in the RF and the surface radiative forcing for LLGHG, BC  
52 and direct and indirect aerosol effect of scattering aerosols (Ramanathan and Carmichael, 2008). The Figure  
53 also shows that the main cause of this difference is due to the atmospheric absorption. [Figure will be  
54 updated with more components and based on a larger number of models].

55  
56 **[INSERT FIGURE 8.23 HERE]**

1 **Figure 8.23:** RF of the total direct aerosol effect (left) and surface radiative forcing of the total direct aerosol  
2 effect (right) as a mean of two AeroCom models.  
3

4 **[INSERT FIGURE 8.24 HERE]**

5 **Figure 8.24:** RF and surface radiative forcing for LLGHG, CO<sub>2</sub>, BC and direct and indirect aerosol effect of  
6 scattering aerosols, taken from (Ramanathan and Carmichael, 2008).  
7

### 8 **8.6.2 Spatial Evolution of Radiative Forcing and Response over the Industrial Era**

9

10 For the LLGHG the magnitude of the RF has changed over the industrial era, but the spatial distribution of  
11 the RF has been unchanged. This is different for the short-lived components that respond to regional changes  
12 in the emissions of components or precursors affecting the radiative balance. Figure 8.25 shows that the  
13 distribution of the direct aerosol effect of BC has changed substantially from 1950 to 2000, but with rather  
14 similar pattern from 1900 to 1950 (Skeie et al., 2011). The direct aerosol effect of BC has increased  
15 substantially over South East Asia in the latter part of the 20th century but on the other hand reduced over  
16 Europe and the eastern part of USA.  
17

18 **[INSERT FIGURE 8.25 HERE]**

19 **Figure 8.25:** Direct aerosol effect of BC for 1900, 1950, and 2000. [Preliminary results from Oslo CTM2  
20 and will be updated with results from more models.]  
21

22 Figure 8.26 shows the zonal mean RF as a time evolution from 1900 to 2000 with 1850 as a reference. For  
23 the RF of tropospheric ozone the zonal mean pattern has been rather similar and the largest change over the  
24 time period has been from 1960 to 1980. The pattern for the total direct aerosol effect has many similarities  
25 until 1980 with a slightly southward shift in the maximum of the strength in the RF. In 2000 there has been a  
26 substantial reduction in the RF in the maximum strength around 40 degree north. This reduction in the  
27 strength of RF is caused mainly by the reduction in RF of sulphate. Both for sulphate and BC there has been  
28 a southward shift in the maximum of the RF. For BC the change been 1920 and 1960 was rather small.  
29

30 **[INSERT FIGURE 8.26 HERE]**

31 **Figure 8.26:** Zonal mean radiative forcing as a time evolution from 1900 to 2000 with a reference to 1850  
32 conditions, a) tropospheric ozone, b) total direct aerosol effect, c) direct aerosol effect of sulphate, d) direct  
33 aerosol effect of BC. [These are preliminary results that will be updated with more modeling results.]  
34

### 35 **8.6.3 Spatial Evolution of Radiative Forcing and Response for the Future**

36

37 [PLACEHOLDER FOR FIRST ORDER DRAFT: Coordination with Chapter 12 needed; consider a Box or  
38 perhaps a Section 8.6.0 – presenting forcing and response spatial relationships (at least temperature and  
39 precipitation); Shindell et al., JGR, 2010; comparison of responses with observations in Chapter 10.]  
40

41  
42 **[START FAQ 8.1 HERE]**  
43

#### 44 **FAQ 8.1: How Important is Water Vapour for Climate Change?**

45

46 Water vapour is the primary greenhouse gas (GHG) in the Earth's atmosphere. The contribution of water  
47 vapour to the greenhouse effect relative to that of carbon dioxide depends on several hypotheses, but can be  
48 considered to be approximately two to three times greater. Additional water vapour is injected into the  
49 atmosphere as a result of anthropogenic activities, mostly through enhanced evaporation from irrigated  
50 crops, but also through power plant cooling, and marginally through the combustion of fossil fuel. One may  
51 therefore question why there is so much focus on carbon dioxide, and not on water vapour, as a forcing to  
52 climate change.  
53

54 Water vapour behaves differently to carbon dioxide in one fundamental way -: it can condense and  
55 precipitate. The capacity of air to contain water vapour depends on its temperature; warmer air can hold  
56 more water vapour than cold air. When air with high humidity cools, some of the vapour condenses into  
57 water droplets and precipitates. The typical residence time of water vapour in the atmosphere is one week.

1 As a consequence, any additional water vapour injected into the atmosphere is rapidly eliminated, so that it  
2 has a negligible impact on the concentration, and does not contribute significantly to the long-term  
3 greenhouse effect. This is the fundamental reason why tropospheric water vapour (i.e., typically below 10  
4 km altitude) is not considered to be an anthropogenic gas contributing significantly to radiative forcing.  
5

6 On the other hand, the amount of water vapour in the stratosphere (i.e., above 10 km altitude) has shown  
7 variations in the past decades, with significant impacts on the greenhouse effect. An increase in  
8 concentration was observed up to 2000, which could be explained in part by the increase in atmospheric  
9 methane as a result of anthropogenic emissions. In this case it is considered a radiative forcing agent.  
10 However, the full extent of the variations of stratospheric water vapour concentration, and in particular the  
11 decrease that is observed since 2000, is not well understood.  
12

13 The capacity of air to hold water vapour increases rapidly with its temperature. A typical polar air  
14 atmospheric column may contain a few kilogram of water vapour per square metre while the equivalent for a  
15 tropical air mass is up to 100 kilograms. If an initial forcing warms the air temperature, the atmosphere will  
16 increase its potential to contain water vapour. The water vapour concentration will then increase (less  
17 precipitation during the transition period) which leads to a further increase in the greenhouse effect and  
18 therefore to an additional temperature increase. This process, referred to as the water vapour feedback, is  
19 well understood and quantified. Although an increase in the atmosphere water vapour content has been  
20 observed, this change is understood as a climate feedback and cannot be interpreted as a Radiative Forcing.  
21 The water vapour feedback is included in models used to anticipate climate change.  
22

23 In the present-day Earth atmosphere, water vapour has the largest greenhouse effect. However, other  
24 greenhouse gases, and primarily carbon dioxide, are necessary to sustain the presence of water vapour in the  
25 atmosphere. Indeed, if these other GHGs were removed from the atmosphere, its temperature would drop  
26 sufficiently to induce a decrease of water vapour, leading to a runaway drop of the greenhouse effect that  
27 would plunge the Earth into a frozen state. So GHGs other than water vapour have provided the temperature  
28 structure which sustains current levels of atmospheric water vapour.  
29 Therefore, although carbon dioxide is the main control knob on climate, water vapour is a strong and fast  
30 feedback that amplifies any initial forcing by a factor of typically three. Water vapour is not a significant  
31 initial forcing, but is nevertheless a fundamental agent of climate change.  
32

33 [END FAQ 8.1 HERE]  
34  
35

36 [START FAQ 8.2 HERE]  
37

### 38 **FAQ 8.2: Do Improvements in Air Quality have an Effect on Climate Change?**

39  
40 [PLACEHOLDER FOR FIRST ORDER DRAFT]  
41

42 [END FAQ 8.1 HERE]  
43  
44

**References**

- 1 Aaheim, A., J. Fuglestedt, and O. Godal, 2006: Costs savings of a flexible multi-gas climate policy. *Energy Journal*,  
2 485-501.
- 3 Abreu, J. A., J. Beer, F. Steinhilber, S. M. a. Tobias, and N. O. Weiss, 2008: For how long will the. *Geophys. Res. Lett.*,  
4 **35**, L20109.
- 5 Aghedo, A., et al., 2011: The vertical distribution of ozone instantaneous radiative forcing from satellite and chemistry  
6 climate models. *Journal of Geophysical Research-Atmospheres*, -.
- 7 Ammann, C. M., and P. Naveau, 2003: Statistical analysis of tropical explosive volcanism occurrences over the last 6  
8 centuries. *Geophysical Research Letters*, **30**, 4.
- 9 —, 2010: A statistical volcanic forcing scenario generator for climate simulations. *Journal of Geophysical Research-*  
10 *Atmospheres*, **115**.
- 11 Anchukaitis, K. J., B. M. Buckley, E. R. Cook, B. I. Cook, R. D. D'Arrigo, and C. M. Ammann, 2010: Influence of  
12 volcanic eruptions on the climate of the Asian monsoon region. *Geophysical Research Letters*, **37**.
- 13 Andersen, M., D. Blake, F. Rowland, M. Hurley, and T. Wallington, 2009: Atmospheric Chemistry of Sulfuryl  
14 Fluoride: Reaction with OH Radicals, Cl Atoms and O-3, Atmospheric Lifetime, IR Spectrum, and Global  
15 Warming Potential. *Environmental Science & Technology*, 1067-1070.
- 16 Andrews, T., and P. M. Forster, 2008: CO2 forcing induces semi-direct effects with consequences for climate feedback  
17 interpretations. *Geophysical Research Letters*, **35**.
- 18 Andrews, T., P. Forster, O. Boucher, N. Bellouin, and A. Jones, 2010: Precipitation, radiative forcing and global  
19 temperature change. *Geophysical Research Letters*, -.
- 20 Bala, G., K. Caldeira, M. Wickett, T. J. Phillips, D. B. Lobell, C. Delire, and A. Mirin, 2007: Combined climate and  
21 carbon-cycle effects of large-scale deforestation. *Proceedings of the National Academy of Sciences of the United*  
22 *States of America*, **104**, 6550-6555.
- 23 Balkanski, Y., G. Myhre, M. Gauss, G. Radel, E. Highwood, and K. Shine, 2010: Direct radiative effect of aerosols  
24 emitted by transport: from road, shipping and aviation. *Atmospheric Chemistry and Physics*, 4477-4489.
- 25 Bar-Or, R., C. Erlick, and H. Gildor, 2008: The role of dust in glacial-interglacial cycles. *Quaternary Science Reviews*,  
26 **27**, 201-208.
- 27 Barnes, C. A., and D. P. Roy, 2008: Radiative forcing over the conterminous United States due to contemporary land  
28 cover land use albedo change. *Geophysical Research Letters*, **35**, -.
- 29 Bathiany, S., M. Claussen, V. Brovkin, T. Raddatz, and V. Gayler, 2010: Combined biogeophysical and  
30 biogeochemical effects of large-scale forest cover changes in the MPI earth system model. *Biogeosciences*, **7**,  
31 1383-1399.
- 32 Bekki, S., J. A. Pyle, W. Zhong, R. Toumi, J. D. Haigh, and D. M. Pyle, 1996: The role of microphysical and chemical  
33 processes in prolonging the climate forcing of the Toba eruption. *Geophysical Research Letters*, **23**, 2669-2672.
- 34 Berntsen, T., and J. Fuglestedt, 2008a: Global temperature responses to current emissions from the transport sectors.  
35 *Proceedings of the National Academy of Sciences of the United States of America*, **105**, 19154-19159.
- 36 —, 2008b: Global temperature responses to current emissions from the transport sectors. *Proceedings of the National*  
37 *Academy of Sciences of the United States of America*, 19154-19159.
- 38 Berntsen, T., et al., 2005: Response of climate to regional emissions of ozone precursors: sensitivities and warming  
39 potentials. *Tellus Series B-Chemical and Physical Meteorology*, 283-304.
- 40 Betts, R. A., P. D. Falloon, K. K. Goldewijk, and N. Ramankutty, 2007: Biogeophysical effects of land use on climate:  
41 Model simulations of radiative forcing and large-scale temperature change. *Agricultural and Forest*  
42 *Meteorology*, **142**, 216-233.
- 43 Bond, T. C., C. Zarzycki, F. M. G, and D. M. Koch, 2011: Quantifying immediate radiative forcing by black carbon and  
44 organic matter with the Specific Forcing Pulse. *Atmospheric chemistry and physics*, **11**, 1505-1525.
- 45 Bonfils, C., and D. Lobell, 2007: Empirical evidence for a recent slowdown in irrigation-induced cooling. *Proceedings*  
46 *of the National Academy of Sciences of the United States of America*, **104**, 13582-13587.
- 47 Boucher, O., and M. Reddy, 2008: Climate trade-off between black carbon and carbon dioxide emissions. *Energy*  
48 *Policy*, 193-200.
- 49 BOUCHER, O., P. FRIEDLINGSTEIN, B. COLLINS, and K. SHINE, 2009: The indirect global warming potential and  
50 global temperature change potential due to methane oxidation. *ENVIRONMENTAL RESEARCH LETTERS*, **4**.
- 51 Bourassa, A. E., D. A. Degenstein, and E. J. Llewellyn, 2008: Retrieval of stratospheric aerosol size information from  
52 OSIRIS limb scattered sunlight spectra. *Atmospheric Chemistry and Physics*, **8**, 6375-6380.
- 53 Bourassa, A. E., D. A. Degenstein, B. J. Elash, and E. J. Llewellyn, 2010: Evolution of the stratospheric aerosol  
54 enhancement following the eruptions of Okmok and Kasatochi: Odin-OSIRIS measurements. *Journal of*  
55 *Geophysical Research-Atmospheres*, **115**.
- 56 Bradford, D., 2001: Global change - Time, money and tradeoffs. *Nature*, 649-650.
- 57 Brueckner, G. E., L. E. Floyd, and M. E. Vanhoosier, 1993: The solar ultraviolet spectral irradiance monitor (SUSIM)  
58 experiment on board the Upper Atmosphere Research Satellite (UARS). *J. Geophys. Res.*, **98**, 10695-10711.
- 59 Campra, P., M. Garcia, Y. Canton, and A. Palacios-Orueta, 2008: Surface temperature cooling trends and negative  
60 radiative forcing due to land use change toward greenhouse farming in southeastern Spain. *Journal of*  
61 *Geophysical Research-Atmospheres*, **113**, -.
- 62

- 1 COLLINS, W., R. DERWENT, C. JOHNSON, and D. STEVENSON, 2002: The oxidation of organic compounds in  
2 the troposphere and their global warming potentials. *CLIMATIC CHANGE*, **52**, 453-479.
- 3 Collins, W. D., et al., 2006: Radiative forcing by well-mixed greenhouse gases: Estimates from climate models in the  
4 Intergovernmental Panel on Climate Change (IPCC) Fourth Assessment Report (AR4). *Journal of Geophysical  
5 Research-Atmospheres*, **111**.
- 6 Collins, W. J., S. Sitch, and O. Boucher, 2010: How vegetation impacts affect climate metrics for ozone precursors.  
7 *Journal of Geophysical Research-Atmospheres*, **115**.
- 8 Corbett, J., D. Lack, J. Winebrake, S. Harder, J. Silberman, and M. Gold, 2010: Arctic shipping emissions inventories  
9 and future scenarios. *Atmospheric Chemistry and Physics*, 9689-9704.
- 10 Davin, E. L., and N. de Noblet-Ducoudre, 2010: Climatic Impact of Global-Scale Deforestation: Radiative versus  
11 Nonradiative Processes. *Journal of Climate*, **23**, 97-112.
- 12 Davin, E. L., N. de Noblet-Ducoudre, and P. Friedlingstein, 2007: Impact of land cover change on surface climate:  
13 Relevance of the radiative forcing concept. *Geophysical Research Letters*, **34**, -.
- 14 De Cara, S., E. Galko, and P. Jayet, 2008: The Global Warming Potential Paradox: Implications for the Design of  
15 Climate Policy. *Design of Climate Policy*, 359-384.
- 16 DeAngelis, A., F. Dominguez, Y. Fan, A. Robock, M. D. Kustu, and D. Robinson, 2010: Evidence of enhanced  
17 precipitation due to irrigation over the Great Plains of the United States. *Journal of Geophysical Research-  
18 Atmospheres*, **115**.
- 19 Delaygue, G. a., and E. Bard, 2010: An Antarctic view of Beryllium-10 and solar activity. *Clim. Dynam.*, **In press**.
- 20 Deligne, N. I., S. G. Coles, and R. S. J. Sparks, 2010: Recurrence rates of large explosive volcanic eruptions. *Journal of  
21 Geophysical Research-Solid Earth*, **115**.
- 22 den Elzen, M., et al., 2005: Analysing countries' contribution to climate change: scientific and policy-related choices.  
23 *Environmental Science & Policy*, 614-636.
- 24 DERWENT, R., W. COLLINS, C. JOHNSON, and D. STEVENSON, 2001: Transient behaviour of tropospheric ozone  
25 precursors in a global 3-D CTM and their indirect greenhouse effects. *CLIMATIC CHANGE*, **49**, 463-487.
- 26 Dewitte, S., D. Crommelynck, S. a. Mekaoui, and A. Joukoff, 2004: Measurement and uncertainty of the long-term total  
27 solar irradiance trend. *Sol. Phys.*, **224**.
- 28 Doutriaux-Boucher, M., M. Webb, J. Gregory, and O. Boucher, 2009: Carbon dioxide induced stomatal closure  
29 increases radiative forcing via a rapid reduction in low cloud. *Geophysical Research Letters*, -.
- 30 Eyring, V., et al., 2010a: Transport impacts on atmosphere and climate: Shipping. *Atmospheric Environment*, **44**, 4735-  
31 4771.
- 32 —, 2010b: Multi-model assessment of stratospheric ozone return dates and ozone recovery in CCMVal-2 models.  
33 *Atmospheric Chemistry and Physics*, **10**, 9451-9472.
- 34 FAO, 2010: *Global Forest Resources Assessment 2010*.
- 35 Feng, X., and F. S. Zhao, 2009: Effect of changes of the HITRAN database on transmittance calculations in the near-  
36 infrared region. *J. Quant. Spectrosc. Radiat. Transfer*, **110**, 247-255.
- 37 Feng, X., F. S. Zhao, and W. H. Gao, 2007: Effect of the improvement of the HITRAN database on the radiative  
38 transfer calculation. *J. Quant. Spectrosc. Radiat. Transfer*, **108**, 308-318.
- 39 Findell, K. L., E. Shevliakova, P. C. D. Milly, and R. J. Stouffer, 2007: Modeled impact of anthropogenic land cover  
40 change on climate. *Journal of Climate*, **20**, 3621-3634.
- 41 FISHER, D., et al., 1990: MODEL-CALCULATIONS OF THE RELATIVE EFFECTS OF CFCS AND THEIR  
42 REPLACEMENTS ON STRATOSPHERIC OZONE. *Nature*, 508-512.
- 43 Flanner, M. G., C. S. Zender, J. T. Randerson, and P. J. Rasch, 2007: Present-day climate forcing and response from  
44 black carbon in snow. *Journal of Geophysical Research-Atmospheres*, **112**.
- 45 Flanner, M. G., C. S. Zender, P. G. Hess, N. M. Mahowald, T. H. Painter, V. Ramanathan, and P. J. Rasch, 2009:  
46 Springtime warming and reduced snow cover from carbonaceous particles. *Atmospheric Chemistry and Physics*,  
47 **9**, 2481-2497.
- 48 Fomin, B., and M. d. P. Correa, 2005: A k-distribution technique for radiative transfer simulation in inhomogeneous  
49 atmosphere: 2. FKDM, fast k-distribution model for the shortwave. *J. Geophys. Res.*, **110**, D02106.
- 50 Fomin, B. A., 2004: A k-distribution technique for radiative transfer simulation in inhomogeneous atmosphere: 1.  
51 FKDM, fast k-distribution model for the longwave. *J. Geophys. Res.*, **109**.
- 52 Fomin, B. A., and V. A. Falaleeva, 2009: Recent progress in spectroscopy and its effect on line-by-line calculations for  
53 the validation of radiation codes for climate models. *Atmos. Oceanic Opt.*, **22**, 626-629.
- 54 Forster, P., et al., 2007: Changes in Atmospheric Constituents and in Radiative Forcing. *Climate Change 2007: The  
55 Physical Science Basis. Contribution of Working Group I to the Fourth Assessment Report of the  
56 Intergovernmental Panel on Climate Change*, Cambridge University Press.
- 57 Foukal, P., C. Fröhlich, <span style="">, H. a. Spruit, and T. M. M. Wigley, 2006: Variations in solar luminosity and  
58 their effect on the Earth's climate. *Nature*, **443**, 161-166.
- 59 Frame, T. H. A. a., and L. J. Gray, 2010: The 11-year solar cycle in ERA-40 data: An Update to 2008. *J. Clim.*, **23**,  
60 2213-2222.
- 61 Fröhlich, C., 2006: Solar irradiance variability since 1978: revision of the PMOD composite during solar cycle 21.  
62 *Space Sci. Rev.*, **125**, 53-65.
- 63 —, 2009: Evidence of a long-term trend in total solar irradiance. *Astron. Astrophys.*, **501**, L27-L30.

- 1 Fuglestad, J., T. Berntsen, O. Godal, and T. Skodvin, 2000: Climate implications of GWP-based reductions in  
2 greenhouse gas emissions. *Geophysical Research Letters*, 409-412.
- 3 Fuglestad, J., T. Berntsen, G. Myhre, K. Rypdal, and R. Skeie, 2008: Climate forcing from the transport sectors.  
4 *Proceedings of the National Academy of Sciences of the United States of America*, 454-458.
- 5 Fuglestad, J., T. Berntsen, O. Godal, R. Sausen, K. Shine, and T. Skodvin, 2003: Metrics of climate change:  
6 Assessing radiative forcing and emission indices. *Climatic Change*, 267-331.
- 7 Fuglestad, J., et al., 2010a: Transport impacts on atmosphere and climate: Metrics. *Atmospheric Environment*, 4648-  
8 4677.
- 9 Fuglestad, J. S., et al., 2010b: Transport impacts on atmosphere and climate: Metrics. *Atmospheric Environment*, **44**,  
10 4648-4677.
- 11 Gao, C., A. Robock, and C. Ammann, 2008: Volcanic forcing of climate over the past 1500 years: An improved ice  
12 core-based index for climate models. *Journal of Geophysical Research-Atmospheres*, **113**.
- 13 —, 2009: Correction to "Volcanic forcing of climate over the past 1500 years: An improved ice core-based index for  
14 climate models (vol 113, D23111, 2008)". *Journal of Geophysical Research-Atmospheres*, **114**.
- 15 Gao, C., L. Oman, A. Robock, and G. L. Stenchikov, 2007: Atmospheric volcanic loading derived from bipolar ice  
16 cores: Accounting for the spatial distribution of volcanic deposition. *Journal of Geophysical Research-  
17 Atmospheres*, **112**.
- 18 Gao, C., et al., 2006: The 1452 or 1453 AD Kuwae eruption signal derived from multiple ice core records: Greatest  
19 volcanic sulfate event of the past 700 years. *Journal of Geophysical Research-Atmospheres*, **111**.
- 20 Gillett, N., and H. Matthews, 2010: Accounting for carbon cycle feedbacks in a comparison of the global warming  
21 effects of greenhouse gases. *Environmental Research Letters*, **5**, -.
- 22 Godal, O., 2003: The IPCC's assessment of multidisciplinary issues: The case of greenhouse gas indices - An editorial  
23 essay. *Climatic Change*, 243-249.
- 24 Gohar, L. K., G. Myhre, and K. P. Shine, 2004: Updated radiative forcing estimates of four halocarbons. *J Geophys  
25 Res*, **109(D01)**.
- 26 Goosse, H., et al., 2006: The origin of the European "Medieval Warm Period". *Climate of the Past*, **2**, 99-113.
- 27 Gray, L. J., S. T. a. Rumbold, and K. P. Shine, 2009: Stratospheric temperature and radiative forcing response to 11-  
28 years solar cycle changes in irradiance and ozone. *J. Atm. Sci.*, **66**, 2402-2416.
- 29 Gray, L. J., et al., 2010: Solar influences on climate, **48**, RG4001.
- 30 Grewe, V., and A. Stenke, 2008: AirClim: an efficient tool for climate evaluation of aircraft technology. *Atmospheric  
31 Chemistry and Physics*, 4621-4639.
- 32 Gusev, A. A., 2008: Temporal structure of the global sequence of volcanic eruptions: Order clustering and intermittent  
33 discharge rate. *Physics of the Earth and Planetary Interiors*, **166**, 203-218.
- 34 Haigh, J. D., 1994: The role of stratospheric ozone in modulating the solar radiative forcing of climate. *Nature*, **370**,  
35 544-546.
- 36 —, 1999: A GMC study of climate change in response to the 11-year solar cycle. *Q.J.R. Meteorol. Soc.*, **125**, 871-  
37 892.
- 38 Haigh, J. D., A. R. Winning, R. a. Toumi, and J. W. Harder, 2010: An influence of solar spectral variations on radiative  
39 forcing of climate. *Nature*, **467**, 696-699.
- 40 Hansen, J., et al., 2005: Efficacy of climate forcings. *Journal of Geophysical Research-Atmospheres*, **110**.
- 41 Harder, J. W., J. M. Fontenla, P. Pilewskie, E. C. Richard, and T. N. Woods, 2009: Trends in solar spectral irradiance  
42 variability in the visible and infrared. *Geophys. Res. Lett.*, **36**, L07801.
- 43 Hasekamp, O. P., and A. Butz, 2008: Efficient calculation of intensity and polarization spectra in vertically  
44 inhomogeneous scattering and absorbing atmospheres. *J. Geophys. Res.*, **113**, D20309.
- 45 Haywood, J. M., et al., 2010: Observations of the eruption of the Sarychev volcano and simulations using the  
46 HadGEM2 climate model. *Journal of Geophysical Research-Atmospheres*, **115**.
- 47 Hofmann, D., J. Barnes, M. O'Neill, M. Trudeau, and R. Neely, 2009: Increase in background stratospheric aerosol  
48 observed with lidar at Mauna Loa Observatory and Boulder, Colorado. *Geophysical Research Letters*, **36**.
- 49 Hogan, R. J., 2010: The Full-Spectrum Correlated-k Method for Longwave Atmospheric Radiative Transfer Using an  
50 Effective Planck Function. *J. Atmos. Sci.*, **67**, 2086-2100.
- 51 Höhne, N., et al., 2010: Contributions of individual countries' emissions to climate change and their uncertainty.  
52 *Climatic Change*, 1-33.
- 53 Horiuchi, K., T. Uchida, Y. Sakamoto, A. Ohta, H. Matsuzaki, Y. Shibata, and, and H. Motoyama, 2008: Ice record of  
54 <sup>10</sup>Be over the past millennium from Dome Fuji, Antarctica: A new proxy record of past solar activity and a  
55 powerful tool for stratigraphic dating. *Quaternary Geochronology*, **3**, 253-261.
- 56 Houghton, J. T., G. J. Jenkins, and J. J. Ephraums, 1990: *Climatic Change. The IPCC Scientific Assessment*, 364 pp pp.
- 57 Huang, J., Q. Fu, W. Zhang, X. Wang, R. Zhang, H. Ye, and S.G. Warren, 2010: Dust and Black Carbon in Seasonal  
58 Snow across Northern China. *Bull. Amer. Meteor. Soc.*
- 59 IPCC, 1999: IPCC Special Report on Aviation and the Global Atmosphere. Prepared by Working Group I and III of the  
60 Intergovernmental Panel on Climate Change in collaboration with the Scientific Assessment Panel to the  
61 Montreal Protocol on Substances that deplete the Ozone Layer.
- 62 Isaksen, I., et al., 2009: Atmospheric composition change: Climate-Chemistry interactions. *Atmospheric Environment*,  
63 5138-5192.

- 1 Jacquinet-Husson, N., and Coauthors, 2008: The GEISA spectroscopic database: Current and future archive for Earth  
2 and planetary atmosphere studies. *J. Quant. Spectrosc. Radiat. Transfer*, **109**, 1043-1059.
- 3 Jarvis, A., and S. Li, 2011: The contribution of timescales to the temperature response of climate models. *Climate*  
4 *Dynamics*, 523-531.
- 5 Jin, Y., and D. P. Roy, 2005: Fire-induced albedo change and its radiative forcing at the surface in northern Australia.  
6 *Geophysical Research Letters*, **32**, -.
- 7 Johansson, D., U. Persson, and C. Azar, 2006: The cost of using global warming potentials: Analysing the trade off  
8 between CO<sub>2</sub>, CH<sub>4</sub> and N<sub>2</sub>O. *Climatic Change*, 291-309.
- 9 Johansson, D. J. A., 2008: Economics vs. Physical-based Metrics for Relative Greenhouse Gas Valuations. *Working*  
10 *Papers in Economics No. 363*, No. 363, University of Gothenburg.
- 11 ———, 2010: Economics- and Physical-Based Metrics for Comparing Greenhouse Gases. *Climatic Change*, **submitted**.
- 12 Joiner, J., M. Schoeberl, A. Vasilkov, L. Oreopoulos, S. Platnick, N. Livesey, and P. Levelt, 2009: Accurate satellite-  
13 derived estimates of the tropospheric ozone impact on the global radiation budget. *Atmospheric Chemistry and*  
14 *Physics*, 4447-4465.
- 15 Joshi, M. M., and G. S. Jones, 2009: The climatic effects of the direct injection of water vapour into the stratosphere by  
16 large volcanic eruptions. *Atmospheric Chemistry and Physics*, **9**, 6109-6118.
- 17 KANDLIKAR, M., 1995: THE RELATIVE ROLE OF TRACE GAS EMISSIONS IN GREENHOUSE ABATEMENT  
18 POLICIES. *Energy Policy*, 879-883.
- 19 Kratz, D. P., 2008: The sensitivity of radiative transfer calculations to the changes in the HITRAN database from 1982  
20 to 2004. *J. Quant. Spectrosc. Radiat. Transfer*, **109**, 1060-1080.
- 21 Kravitz, B., and A. Robock, 2011: The climate effects of high latitude volcanic eruptions: The role of the time of year.  
22 *J. Geophys. Res.*, **116**.
- 23 Kravitz, B., A. Robock, and A. Bourassa, 2010: Negligible climatic effects from the 2008 Okmok and Kasatochi  
24 volcanic eruptions. *Journal of Geophysical Research-Atmospheres*, **115**.
- 25 Krivova, N. A., and S. K. Solanki, 2007: Reconstruction of solar total irradiance since 1700 from the surface magnetic  
26 flux.. *Astron. Astrophys.*, **467**, 335-346.
- 27 Krivova, N. A., L. E. A. a. Vieira, and S. K. Solanki, 2011: Reconstruction of solar spectral irradiance since the  
28 maunder minimum. *J. Geophys. Res.*
- 29 Kueppers, L. M., M. A. Snyder, and L. C. Sloan, 2007: Irrigation cooling effect: Regional climate forcing by land-use  
30 change. *Geophysical Research Letters*, **34**, -.
- 31 Kvalevag, M. M., G. Myhre, G. Bonan, and S. Levis, 2010: Anthropogenic land cover changes in a GCM with surface  
32 albedo changes based on MODIS data. *International Journal of Climatology*, **30**, 2105-2117.
- 33 Lamarque, J., et al., 2010: Historical (1850-2000) gridded anthropogenic and biomass burning emissions of reactive  
34 gases and aerosols: methodology and application. *Atmospheric Chemistry and Physics*, 7017-7039.
- 35 Lee, D., et al., 2009: Aviation and global climate change in the 21st century. *Atmospheric Environment*, 3520-3537.
- 36 ———, 2010: Transport impacts on atmosphere and climate: Aviation. *Atmospheric Environment*, 4678-4734.
- 37 Li, J., C. L. Curry, Z. Sun, and F. Zhang, 2010: Overlap of Solar and Infrared Spectra and the Shortwave Radiative  
38 Effect of Methane. *J. Atmos. Sci.*, **67**, 2372-2389.
- 39 Li, S., and A. Jarvis, 2009: Long run surface temperature dynamics of an A-OGCM: the HadCM3 4xCO<sub>2</sub> forcing  
40 experiment revisited. *Climate Dynamics*, 817-825.
- 41 Liang, X. Z., et al., 2005: Development of land surface albedo parameterization based on Moderate Resolution Imaging  
42 Spectroradiometer (MODIS) data. *Journal of Geophysical Research-Atmospheres*, **110**, -.
- 43 Llewellyn, E., et al., 2004: The OSIRIS instrument on the Odin spacecraft. *Canadian Journal of Physics*, **82**, 411-422.
- 44 Lockwood, M., A. P. Rouillard, and, and I. D. Finch, 2009: The rise and fall of open solar flux during the current grand  
45 solar maximum. *Astrophys. J.*, **700**, 937-944.
- 46 Lockwood, M. a., and C. Fröhlich, 2007: Recent oppositely directed trends in solar climate forcings and the global  
47 mean surface air temperature. *Proc. R. Soc. A*, **463**, 2447-2460.
- 48 Lohila, A., et al., 2010: Forestation of boreal peatlands: Impacts of changing albedo and greenhouse gas fluxes on  
49 radiative forcing. *Journal of Geophysical Research-Biogeosciences*, **115**, -.
- 50 Manne, A., and R. Richels, 2001: An alternative approach to establishing trade-offs among greenhouse gases. *Nature*,  
51 675-677.
- 52 Manning, M., and A. Reisinger, 2011: Broader perspectives for comparing different greenhouse gases.  
53 *PHILOSOPHICAL TRANSACTIONS OF THE ROYALSOCIETY A*, **in press**.
- 54 McCarthy, M. P., M. J. Best, and R. A. Betts, 2010: Climate change in cities due to global warming and urban effects.  
55 *Geophysical Research Letters*, **37**, -.
- 56 McComas, D. J., R. W. Ebert, H. A. Elliott, B. E. Goldstein, J. T. Gosling, N. A. Schwadron, and, and R. M. Skoug,  
57 2008: Weaker solar wind from the polar coronal holes and the whole Sun. *Geophys. Res. Lett.*, **35**, L18103.
- 58 Meehl, G. H., et al., 2007: Global climate projections., 747-846 pp.
- 59 Meinshausen, M., S. C. B. Raper, and T. M. L. Wigley, 2011a: Emulating coupled atmosphere-ocean and carbon cycle  
60 models with a simpler model, MAGICC6 – Part 1: Model description and calibration. *Atmos. Chem. Phys.*, **11**,  
61 1417-1456.
- 62 Meinshausen, M., T. M. L. Wigley, and S. C. B. Raper, 2011b: Emulating atmosphere-ocean and carbon cycle models  
63 with a simpler model, MAGICC6 – Part 2: Applications. *Atmos. Chem. Phys.*, **11**, 1457-1471.

- 1 Meinshausen, M., et al., 2009: Greenhouse-gas emission targets for limiting global warming to 2 degrees C. *Nature*,  
2 1158-U1196.
- 3 Meure, C., et al., 2006: Law Dome CO<sub>2</sub>, CH<sub>4</sub> and N<sub>2</sub>O ice core records extended to 2000 years BP. *Geophysical*  
4 *Research Letters*, -.
- 5 Mickley, L., D. Jacob, and D. Rind, 2001: Uncertainty in preindustrial abundance of tropospheric ozone: Implications  
6 for radiative forcing calculations. *Journal of Geophysical Research-Atmospheres*, 3389-3399.
- 7 Moncet, J.-L., G. Uymin, A. E. Lipton, and H. E. Snell, 2008: Infrared Radiance Modeling by Optimal Spectral  
8 Sampling. *J. Atmos. Sci.*, **65**, 3917–3934.
- 9 Muhle, J., et al., 2009: Sulfuryl fluoride in the global atmosphere (vol 114, D05306, 2009). *Journal of Geophysical*  
10 *Research-Atmospheres*, -.
- 11 Muscheler, R., F. Joos, J. Beer, S. Mueller, M. Vonmoos, and, and I. Snowball, 2007: Solar activity during the last 1000  
12 yr inferred from radionuclide records. *Quaternary Sci. Rev.*, **26**, 82-97.
- 13 Myhre, G., M. M. Kvalevag, and C. B. Schaaf, 2005a: Radiative forcing due to anthropogenic vegetation change based  
14 on MODIS surface albedo data. *Geophysical Research Letters*, **32**, -.
- 15 Myhre, G., Y. Govaerts, J. M. Haywood, T. K. Berntsen, and A. Lattanzio, 2005b: Radiative effect of surface albedo  
16 change from biomass burning. *Geophysical Research Letters*, **32**, -.
- 17 Myhre, G., J. Nilsen, L. Gulstad, K. Shine, B. Rognerud, and I. Isaksen, 2007: Radiative forcing due to stratospheric  
18 water vapour from CH<sub>4</sub> oxidation. *Geophysical Research Letters*, -.
- 19 Naik, V., D. Mauzerall, L. Horowitz, M. D. Schwarzkopf, V. Ramaswamy, and M. Oppenheimer, 2005: Net radiative  
20 forcing due to changes in regional emissions of tropospheric ozone precursors. *Journal of Geophysical*  
21 *Research-Atmospheres*, **110**.
- 22 Nair, U. S., D. K. Ray, J. Wang, S. A. Christopher, T. J. Lyons, R. M. Welch, and R. A. Pielke, 2007: Observational  
23 estimates of radiative forcing due to land use change in southwest Australia. *Journal of Geophysical Research-*  
24 *Atmospheres*, **112**, -.
- 25 O'Neill, B., 2000: The jury is still out on global warming potentials. *Climatic Change*, 427-443.
- 26 —, 2003: Economics, natural science, and the costs of global warming potentials - An editorial comment. *Climatic*  
27 *Change*, 251-260.
- 28 Olivie, D., and N. Stuber, 2010: Emulating AOGCM results using simple climate models. *Climate Dynamics*, 1257-  
29 1287.
- 30 Peters, G. P., B. Aamaas, M. Lund, C. Solli, and J. Fuglestvedt, 2011: Alternative 'Global Warming' Metrics in Life  
31 Cycle Assessment: A case study with existing transportation data. *submitted*.
- 32 Pinto, J. P., R. P. Turco, and O. B. Toon, 1989: Self-limiting physical and chemical effects in volcanic-eruption clouds.  
33 *Journal of Geophysical Research-Atmospheres*, **94**, 11165-11174.
- 34 Pitman, A. J., et al., 2009: Uncertainties in climate responses to past land cover change: First results from the LUCID  
35 intercomparison study. *Geophysical Research Letters*, **36**, -.
- 36 Plattner, G.-K., T. Stocker, P. Midgley, and M. Tignor, 2009: IPCC Expert Meeting on the Science of Alternative  
37 Metrics: Meeting Report.
- 38 Pongratz, J., C. Reick, T. Raddatz, and M. Claussen, 2008: A reconstruction of global agricultural areas and land cover  
39 for the last millennium. *Global Biogeochemical Cycles*, **22**, -.
- 40 Pongratz, J., C. H. Reick, T. Raddatz, and M. Claussen, 2010: Biogeophysical versus biogeochemical climate response  
41 to historical anthropogenic land cover change. *Geophysical Research Letters*, **37**, -.
- 42 Pongratz, J., T. Raddatz, C. H. Reick, M. Esch, and M. Claussen, 2009: Radiative forcing from anthropogenic land  
43 cover change since AD 800. *Geophysical Research Letters*, **36**, -.
- 44 Prather, M., et al., 2009: Tracking uncertainties in the causal chain from human activities to climate. *Geophysical*  
45 *Research Letters*, -.
- 46 Puma, M. J., and B. I. Cook, 2010: Effects of irrigation on global climate during the 20th century. *Journal of*  
47 *Geophysical Research-Atmospheres*, **115**, -.
- 48 Qian, Y., W. I. Gustafson, L. R. Leung, and S. J. Ghan, 2009: Effects of soot-induced snow albedo change on snowpack  
49 and hydrological cycle in western United States based on Weather Research and Forecasting chemistry and  
50 regional climate simulations. *Journal of Geophysical Research-Atmospheres*, **114**.
- 51 Ramanathan, V., and G. Carmichael, 2008: Global and regional climate changes due to black carbon. *Nature*  
52 *Geoscience*, **1**, 221-227.
- 53 Ramaswamy, V., et al., 2001: Radiative Forcing of Climate Change. *Climate Change 2001: The Scientific Basis.*  
54 *Contribution of Working Group I to the Third Assessment Report of the Intergovernmental Panel on Climate*  
55 *Change*, Cambridge University Press.
- 56 Randel, W., and F. Wu, 2007: A stratospheric ozone profile data set for 1979-2005: Variability, trends, and  
57 comparisons with column ozone data. *Journal of Geophysical Research-Atmospheres*, -.
- 58 Rechid, D., T. Raddatz, and D. Jacob, 2009: Parameterization of snow-free land surface albedo as a function of  
59 vegetation phenology based on MODIS data and applied in climate modelling. *Theoretical and Applied*  
60 *Climatology*, **95**, 245-255.
- 61 Reddy, M., and O. Boucher, 2007: Climate impact of black carbon emitted from energy consumption in the world's  
62 regions. *Geophysical Research Letters*, -.

- 1 REILLY, J., 1992: CLIMATE-CHANGE DAMAGE AND THE TRACE-GAS-INDEX ISSUE. *Economic Issues in*  
2 *Global Climate Change*, 72-88.
- 3 Reisinger, A., M. Meinshausen, and M. Manning, 2011: Future changes in Global Warming Potentials under  
4 Representative  
5 Concentration Pathways. *submitted*.
- 6 Reisinger, A., M. Meinshausen, M. Manning, and G. Bodeker, 2010: Uncertainties of global warming metrics: CO<sub>2</sub> and  
7 CH<sub>4</sub>. *Geophysical Research Letters*, **37**, 6 pp.
- 8 Rigozo, N. R., E. Echer, L. E. A. a. Vieira, and D. J. R. Nordemann, 2001: Reconstruction of Wolf sunspot number on  
9 the basis of spectral characteristics and estimates of associated radio flux and solar wind parameters for the last  
10 millennium. *Solar Phys.*, **203**, 179-191.
- 11 Rigozo, N. R., D. J. R. Nordemann, <span style="">, E. Echer, M. P. S. a. Echer, and H. E. Silva, 2010: Prediction of  
12 solar minimum and maximum epochs on the basis of spectral characteristics for the next millennium. *Planetary*  
13 *and Space Sci.*, **58**, 1971-1976.
- 14 Robock, A., 2000: Volcanic eruptions and climate. *Reviews of Geophysics*, **38**, 191-219.  
15 —, 2010: New START, Eyjafjallajökull, and Nuclear Winter. *Eos*, **91**, 444-445.
- 16 Robock, A., C. M. Ammann, L. Oman, D. Shindell, S. Levis, and G. Stenchikov, 2009: Did the Toba volcanic eruption  
17 of similar to 74 ka BP produce widespread glaciation? *Journal of Geophysical Research-Atmospheres*, **114**.
- 18 Rotenberg, E., and D. Yakir, 2010: Contribution of Semi-Arid Forests to the Climate System. *Science*, **327**, 451-454.
- 19 Rothman, L. S., 2010: The evolution and impact of the HITRAN molecular spectroscopic database. *J. Quant.*  
20 *Spectrosc. Radiat. Transfer*, **111**, 1565-1567.
- 21 Rothman, L. S., and Coauthors, 2009: The HITRAN 2008 molecular spectroscopic database. *J. Quant. Spectrosc.*  
22 *Radiat. Transfer*, **110**, 533-572.
- 23 Rottman, G., 2006: Measurement of total and spectral solar irradiance. *Space. Sci. Rev.*, **125**, 39-51.
- 24 Rottman, G., T. N. a. Woods, and T. P. Sparn, 1993: Solar stellar irradiance comparison experiment 1: 1. instrument  
25 design and operation. *J. Geophys. Res.*, **98**, 10667-10677.
- 26 Russell, C. T., J. G. a. s. s. Luhmann, and L. K. Jian, 2010: How unprecedented a solar minimum? *Rev. Geophys.*, **48**,  
27 RG2004.
- 28 Rypdal, K., N. Rive, T. Berntsen, Z. Klimont, T. Mideksa, G. Myhre, and R. Skeie, 2009: Costs and global impacts of  
29 black carbon abatement strategies. *Tellus Series B-Chemical and Physical Meteorology*, 625-641.
- 30 Salzer, M. W., and M. K. Hughes, 2007: Bristlecone pine tree rings and volcanic eruptions over the last 5000 yr.  
31 *Quaternary Research*, **67**, 57-68.
- 32 Sausen, R., and U. Schumann, 2000: Estimates of the climate response to aircraft CO<sub>2</sub> and NO<sub>x</sub> emissions scenarios.  
33 *Climatic Change*, 27-58.
- 34 Sausen, R., et al., 2005: Aviation radiative forcing in 2000: An update on IPCC (1999). *Meteorologische Zeitschrift*,  
35 555-561.
- 36 Schmidt, G. A., et al., 2011: Climate forcing reconstructions for use in PMIP simulations of the last millennium (v1.0).  
37 *Geosci. Model Dev.*, **4**, 33-45.
- 38 Self, S., and S. Blake, 2008: Consequences of explosive supereruptions. *Elements*, **4**, 41-46.
- 39 Shi, G. Y., and H. Zhang, 2007: The relationship between absorption coefficient and temperature and their effect on the  
40 atmospheric cooling rate. *J. Quant. Spectrosc. Radiat. Transfer*, **105**, 459-466.
- 41 Shi, G. Y., X. N., W. B., D. T., and Z. J. Q., 2009: An improved treatment of overlapping absorption bands based on the  
42 correlated k distribution model for thermal infrared radiative transfer calculations. *J. Quant. Spectrosc. Radiat.*  
43 *Transfer*, **110**, 435-451.
- 44 Shindell, D., and G. Faluvegi, 2009: Climate response to regional radiative forcing during the twentieth century. *Nature*  
45 *Geoscience*, **2**, 294-300.
- 46 —, 2010: The net climate impact of coal-fired power plant emissions. *Atmospheric Chemistry and Physics*, **10**, 3247-  
47 3260.
- 48 Shindell, D., G. Faluvegi, A. Lacis, J. Hansen, R. Ruedy, and E. Aguilar, 2006a: Role of tropospheric ozone increases  
49 in 20th-century climate change. *Journal of Geophysical Research-Atmospheres*, -.
- 50 Shindell, D., G. Faluvegi, D. Koch, G. Schmidt, N. Unger, and S. Bauer, 2009a: Improved Attribution of Climate  
51 Forcing to Emissions. *Science*, 716-718.
- 52 Shindell, D., et al., 2006b: Simulations of preindustrial, present-day, and 2100 conditions in the NASA GISS  
53 composition and climate model G-PUCCINI. *Atmospheric Chemistry and Physics*, 4427-4459.
- 54 Shindell, D. T., G. Faluvegi, J. E. a. s. s. Hansen, and S. Sun, 2006c: Solar and anthropogenic forcing of tropical  
55 hydrology. *Geophys. Res. Lett.*, **33**, L24706.
- 56 Shindell, D. T., G. Faluvegi, D. M. Koch, G. A. Schmidt, N. Unger, and S. E. Bauer, 2009b: Improved Attribution of  
57 Climate Forcing to Emissions. *Science*, **326**, 716-718.
- 58 Shindell, D. T., et al., 2008: A multi-model assessment of pollution transport to the Arctic. *Atmospheric Chemistry and*  
59 *Physics*, **8**, 5353-5372.
- 60 Shine, K., 2009: The global warming potential-the need for an interdisciplinary retrieval. *Climatic Change*, 467-472.
- 61 Shine, K., T. Berntsen, J. Fuglestedt, and R. Sausen, 2005a: Scientific issues in the design of metrics for inclusion of  
62 oxides of nitrogen in global climate agreements. *Proceedings of the National Academy of Sciences of the United*  
63 *States of America*, 15768-15773.

- 1 Shine, K., J. Fuglestedt, K. Hailemariam, and N. Stuber, 2005b: Alternatives to the global warming potential for  
2 comparing climate impacts of emissions of greenhouse gases. *Climatic Change*, 281-302.
- 3 Shine, K., T. Berntsen, J. Fuglestedt, R. Skeie, and N. Stuber, 2007: Comparing the climate effect of emissions of  
4 short- and long-lived climate agents. *Philosophical Transactions of the Royal Society a-Mathematical Physical  
5 and Engineering Sciences*, 1903-1914.
- 6 Sihra, K., M. D. Hurley, K. P. Shine, and T. J. Wallington, 2001: Updated radiative forcing estimates of 65 halocarbons  
7 and nonmethane hydrocarbons. *J Geophys Res*, **106(D17)**, 20493 – 20506.
- 8 Sitch, S., P. Cox, W. Collins, and C. Huntingford, 2007: Indirect radiative forcing of climate change through ozone  
9 effects on the land-carbon sink. *Nature*, 791-U794.
- 10 Skeie, R. B., J. Fuglestedt, T. Berntsen, M. T. Lund, G. Myhre, and K. Rypdal, 2009: Global temperature change from  
11 the transport sectors: Historical development and future scenarios. *Atmospheric Environment*, **43**, 6260-6270.
- 12 Skeie, R. B., T. Berntsen, G. Myhre, C. A. Pedersen, J. Ström, S. Gerland, and J. A. Ogren, 2011: Black carbon in the  
13 atmosphere and snow, from pre-industrial times until present. *Atmos. Chem. Phys. Discuss.* , **11**, 7469-7534.
- 14 Skodvin, T., and J. Fuglestedt, 1997: A comprehensive approach to climate change: Political and scientific  
15 considerations. *Ambio*, 351-358.
- 16 Smith, E. J., and A. Balogh, 2008: Decrease in heliospheric magnetic flux in this solar minimum: recent Ulysses  
17 magnetic field observations. *Geophys. Res. Lett.*, **35**, L22103.
- 18 Smith, S., and T. Wigley, 2000a: Global warming potentials: 2. Accuracy. *Climatic Change*, 459-469.
- 19 Smith, S., and M. Wigley, 2000b: Global warming potentials: 1. Climatic implications of emissions reductions.  
20 *Climatic Change*, 445-457.
- 21 Solomon, S., G. Plattner, R. Knutti, and P. Friedlingstein, 2009: Irreversible climate change due to carbon dioxide  
22 emissions. *Proceedings of the National Academy of Sciences of the United States of America*, 1704-1709.
- 23 Solomon, S., J. Daniel, T. Sanford, D. Murphy, G. Plattner, R. Knutti, and P. Friedlingstein, 2010a: Persistence of  
24 climate changes due to a range of greenhouse gases. *Proceedings of the National Academy of Sciences of the  
25 United States of America*, 18354-18359.
- 26 Solomon, S., K. Rosenlof, R. Portmann, J. Daniel, S. Davis, T. Sanford, and G. Plattner, 2010b: Contributions of  
27 Stratospheric Water Vapor to Decadal Changes in the Rate of Global Warming. *Science*, 1219-1223.
- 28 Soukharev, B. E. a., and L. L. Hood, 2006: Solar cycle variation of stratospheric ozone: Multiple regression analysis of  
29 long-term satellite data sets and comparisons with models. *J. Geophys. Res.*, **111**, D20314.
- 30 Steinhilber, F., J. Beer, and C. Fröhlich, 2009: Total solar irradiance during the Holocene. *Geophys. Res. Lett.*, **36**,  
31 L19704.
- 32 Stevenson, D., and R. Derwent, 2009: Does the location of aircraft nitrogen oxide emissions affect their climate impact?  
33 *Geophysical Research Letters*, -.
- 34 STEVENSON, D., R. DOHERTY, M. SANDERSON, W. COLLINS, C. JOHNSON, and R. DERWENT, 2004:  
35 Radiative forcing from aircraft NO<sub>x</sub> emissions: Mechanisms and seasonal dependence. *JOURNAL OF  
36 GEOPHYSICAL RESEARCH-ATMOSPHERES*, **109**, -.
- 37 Stothers, R. B., 2007: Three centuries of observation of stratospheric transparency. *Climatic Change*, **83**, 515-521.
- 38 Stuiver, M., et al., 1998: INTCAL 98 radiocarbon age calibration, 24, 000-0 BP. *Radiocarbon*, **40**, 1041-1083.
- 39 Tanaka, K., G. Peters, and J. S. Fuglestedt, 2010: Multicomponent climate policy: why do emission metrics matter?  
40 *Carbon Management*, **1**, 191-197.
- 41 Tanaka, K., B. O'Neill, D. Rokityanskiy, M. Obersteiner, and R. Tol, 2009: Evaluating Global Warming Potentials with  
42 historical temperature. *Climatic Change*, 443-466.
- 43 Tarasova, T. A., and B. A. Fomin, 2007: The Use of New Parameterizations for Gaseous Absorption in the CLIRAD-  
44 SW Solar Radiation Code for Models. *J. Atmos. Oceanic Technol.*, **24**, 1157–1162.
- 45 Timmreck, C., et al., 2010: Aerosol size confines climate response to volcanic super-eruptions. *Geophys. Res. Lett.*, **37**.
- 46 Tobias, S. M., N. O. Weiss, and J. Beer, 2004: Long-term prediction of solar activity. *Astron. Geophys.*, **45**, 2.06.
- 47 Tol, R. S. J., T. K. Berntsen, B. C. O'Neill, J. S. Fuglestedt, and K. P. Shine, 2009: A UNIFYING FRAMEWORK  
48 FOR METRICS FOR AGGREGATING THE CLIMATE EFFECT OF DIFFERENT EMISSIONS. *submitted*.
- 49 Trenberth, K. E., and A. Dai, 2007: Effects of Mount Pinatubo volcanic eruption on the hydrological cycle as an analog  
50 of geoengineering. *Geophysical Research Letters*, **34**.
- 51 Uherek, E., et al., 2010: Transport impacts on atmosphere and climate: Land transport. *Atmospheric Environment*,  
52 4772-4816.
- 53 Unger, N., D. Shindell, and J. Wang, 2009: Climate forcing by the on-road transportation and power generation sectors.  
54 *Atmospheric Environment*, 3077-3085.
- 55 Unger, N., D. T. Shindell, D. M. Koch, and D. G. Streets, 2008: Air pollution radiative forcing from specific emissions  
56 sectors at 2030. *Journal of Geophysical Research-Atmospheres*, **113**.
- 57 Unger, N., T. C. Bond, J. S. Wang, D. M. Koch, S. Menon, D. T. Shindell, and S. Bauer, 2010: Attribution of climate  
58 forcing to economic sectors. *Proceedings of the National Academy of Sciences of the United States of America*,  
59 **107**, 3382-3387.
- 60 Usoskin, I. G., K. a. s. s. Mursula, and K. Alanko, 2003: Millennium-scale sunspot number reconstruction: Evidence for  
61 an unusually active Sun since the 1940s. *Phys. Rev. Lett.*, **91**, 211101 (211101-211104).
- 62 van Vuuren, D., J. Weyant, and F. de la Chesnaye, 2006: Multi-gas scenarios to stabilize radiative forcing. *Energy  
63 Economics*, 102-120.

- 1 Velasco-Herrera, V. M., 2011: Prediction for the Next Solar Secular Minimum. *Solar. Phys.*
- 2 Vieira, L. E. A., S. K. Solanki, N. A. Krivova, and, and I. Usoskin, 2010: Evolution of the solar irradiance on time scales
- 3 of years to millennia. *Astron. Astrophys.*, **Submitted**.
- 4 Vonmoos, M., and R. Muscheler, 2006: Large variations in Holocene solar activity: Constraints from <sup>10</sup>Be in the
- 5 Greenland Ice Core Project ice core. *J. Geophys. Res.*, **111**, A10105.
- 6 Wang, Y.-M., L. J. L. and, and N. R. Sheeley Jr., 2005: Modeling the Sun's magnetic field and irradiance since 1713.
- 7 *Astrophys. J.*, **625**, 522-538.
- 8 Weiss, R., J. Muhle, P. Salameh, and C. Harth, 2008: Nitrogen trifluoride in the global atmosphere. *Geophysical*
- 9 *Research Letters*, -.
- 10 Wenzler, T., S. Solanki, N. Krivova, and C. Frohlich, 2006: Reconstruction of solar irradiance variations in cycles 21-
- 11 23 based on surface magnetic fields. *Astronomy & Astrophysics*, 583-595.
- 12 West, J. J., A. M. Fiore, V. Naik, L. W. Horowitz, M. D. Schwarzkopf, and D. L. Mauzerall, 2007: Ozone air quality
- 13 and radiative forcing consequences of changes in ozone precursor emissions. *Geophysical Research Letters*, **34**.
- 14 Wigley, T., and S. Raper, 2001: Interpretation of high projections for global-mean warming. *Science*, 451-454.
- 15 Willson, R. C., and, and A. V. Mordinov, 2003: Secular total irradiance trend during solar cycles 21-23. *Geophys. Res.*
- 16 *Let.*, **30**, 1199-1202.
- 17 Worden, H., K. Bo W man, J. Worden, A. Eldering, and R. Beer, 2008: Satellite measurements of the clear-sky
- 18 greenhouse effect from tropospheric ozone. *Nature Geoscience*, 305-308.
- 19 Zhang, H., and G. Y. Shi, 2005b: A new approach to solve correlated k-distribution function. *J. Quant. Spectrosc.*
- 20 *Radiat. Transfer*, **96**, 311-324.
- 21 Zhang, H., G. Y. Shi, and Y. Liu, 2005: A Comparison Between the Two Line-by-Line Integration Algorithms. *Chinese*
- 22 *Journal of Atmospheric Sciences*, **29**, 581-593.
- 23 ———, 2008: The effects of line-wing cutoff in LBL integration on radiation calculations. *Acta Meteor. Sinica*, **22**, 248-
- 24 255.
- 25 Zhang, H., J. X. Wu, and P. Lu, 2011: A study of the radiative forcing and global warming potentials of
- 26 hydrofluorocarbons. *J. Quant. Spectrosc. Radiat. Transfer*, **112**, 220-229.
- 27 Zhang, H., G. Y. Shi, T. Nakajima, and T. Suzuki, 2006a: The effects of the choice of k-interval number on radiative
- 28 calculations. *J. Quant. Spectrosc. Radiat. Transfer*, **98**, 31-43.
- 29 Zhang, H., T. Nakajima, G. Y. Shi, T. Suzuki, and R. Imasu, 2003: An optimal approach to overlapping bands with
- 30 correlated k distribution method and its application to radiative calculations. *J Geophys Res*, **108(D20)**.
- 31 Zhang, H., T. Suzuki, T. Nakajima, G. Y. Shi, X. Y. Zhang, and Y. Liu, 2006b: The effects of band division on
- 32 radiative calculations. *Optical Engineering*, **45(1)**, 016002.
- 33
- 34

---

## Chapter 8: Anthropogenic and Natural Radiative Forcing

**Coordinating Lead Authors:** Gunnar Myhre (Norway), Drew Shindell (USA)

**Lead Authors:** Francois-Marie Breon (France), William Collins (UK), Jan Fuglestad (Norway), Jianping Huang (China), Dorothy Koch (USA), Jean-Francois Lamarque (USA), David Lee (UK), Blanca Mendoza (Mexico), Teruyuki Nakajima (Japan), Alan Robock (USA), Leon Rotstayn (Australia), Graeme Stephens (USA), Hua Zhang (China)

**Contributing Authors:** Joanna Haigh (UK), Brian O'Neill (USA)

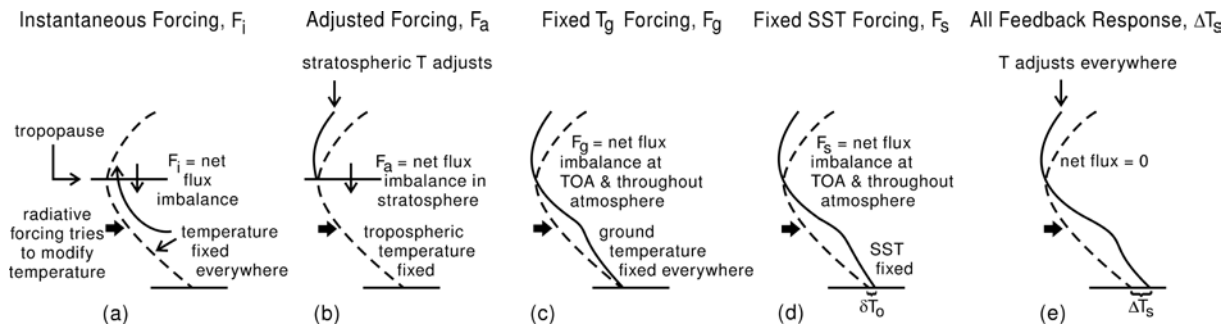
**Review Editors:** Daniel Jacob (USA), A.R. Ravishankara (USA), Keith Shine (UK)

**Date of Draft:** 15 April 2011

**Notes:** TSU Compiled Version

---

1



2

3

4

5

6

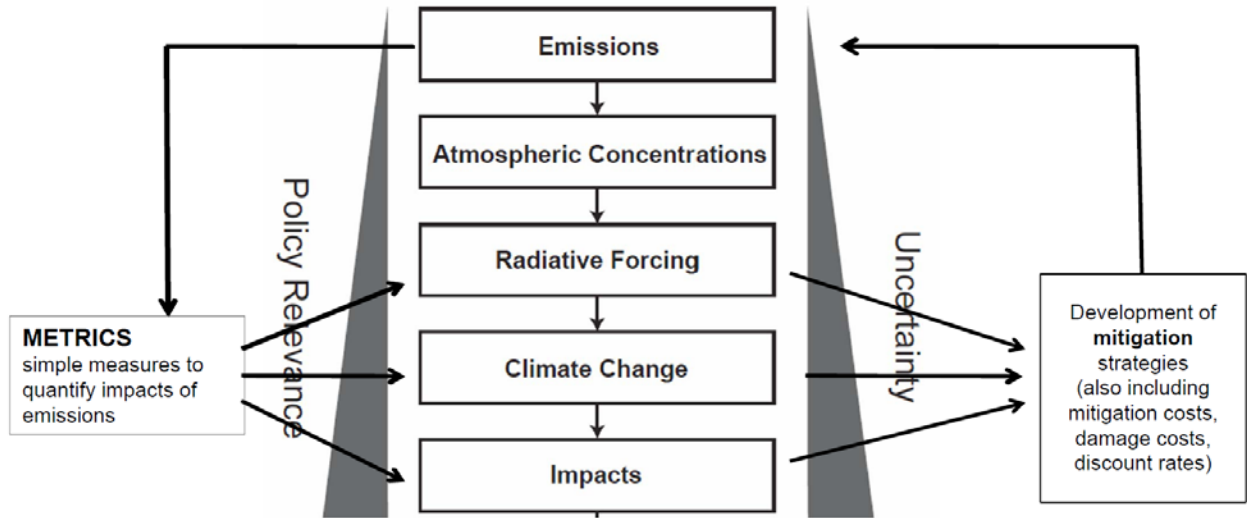
7

8

9

**Figure 8.1:** Cartoon comparing (a)  $F_i$ , instantaneous forcing, (b)  $F_a$ , adjusted forcing, which allows stratospheric temperature to adjust, (c)  $F_g$ , fixed  $T_g$  forcing, which allows atmospheric temperature to adjust, (d)  $F_s$ , fixed SST forcing, which allows atmospheric temperature and land temperature to adjust, and (e)  $\Delta T_s$ , global surface air temperature calculated by the climate model in response to the climate forcing agent. From Hansen et al. (2005)

1



2

3

4

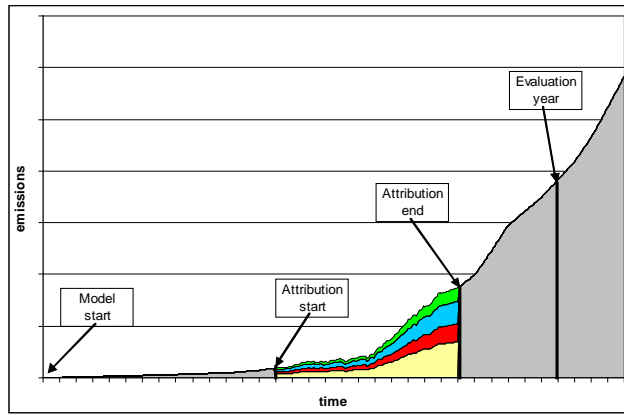
5

6

7

**Figure 8.2:** Cause effect chain from emissions to climate change and impacts showing how metrics can be used to estimate responses to emissions. (Adapted from Fuglestvedt et al. (2003) and Plattner et al. (2009)). [The Figure will be improved.]

1



2

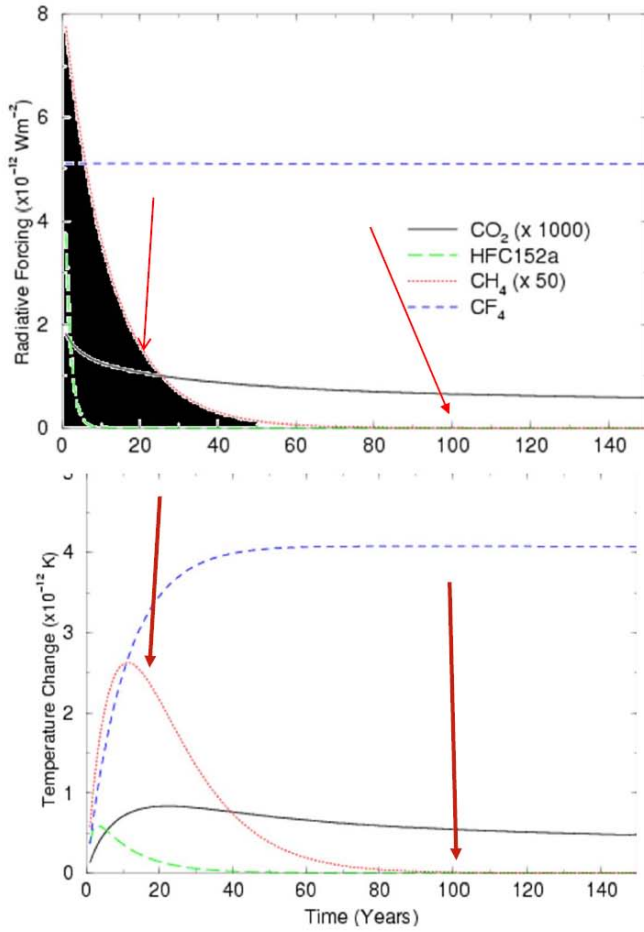
3

4

5

**Box 8.1, Figure 1:** Timeframes involved in calculations of impacts of emissions.

1



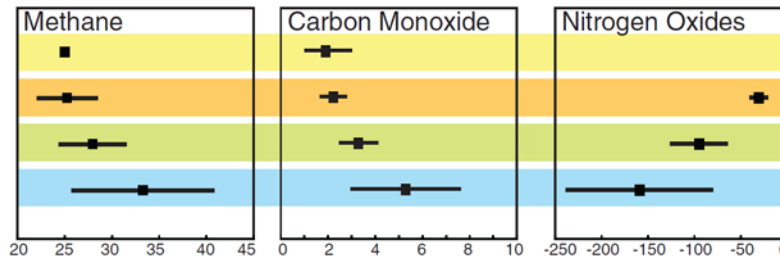
$$GWP(H)_i = \frac{\int_0^H RF_i(t) dt}{\int_0^H RF_{CO_2}(t) dt} = \frac{AGWP_i}{AGWP_{CO_2}}$$

$$GTP_p^x(t) = \frac{AGTP_p^x(t)}{AGTP_p^c(t)}$$

2  
3  
4  
5  
6  
7

**Figure 8.3:** The GWP is calculated by integrating the RF due to pulses over chosen time horizons (a), while the GTP is based on the temperature response for selected years after emission (b). [The Figure will be improved.]

1



2

3

4

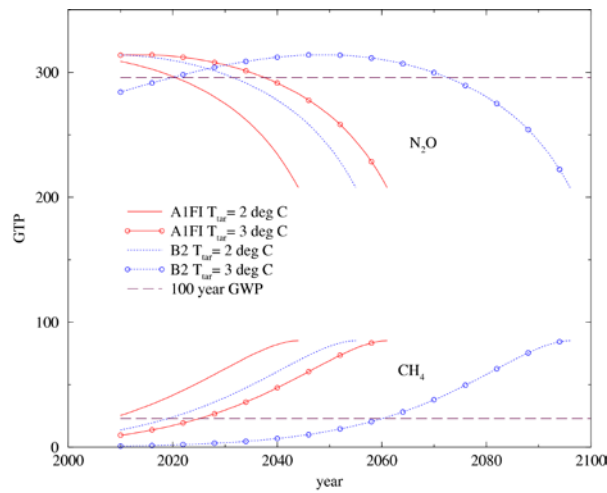
5

6

7

**Figure 8.4:** Metric values (or ranges) to give overview for NO<sub>x</sub>, CO, VOC, BC, OC, sulphate from the literature could be used here; e.g., something similar to this Figure from Shindell et al. (2009) for various studies and for GWP100 and GTP50.

1



2

3

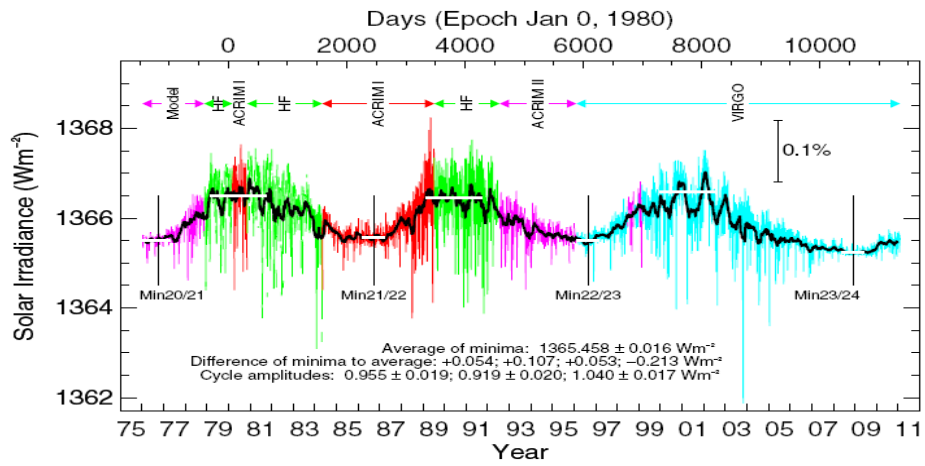
4

5

6

**Figure 8.5:** Global temperature change potential (GTP(t)) for methane and nitrous oxide for each year from 2010 to the time at which the temperature change target ( $T_{tar}$ ) is reached. The 100-year GWP is also shown for the two gases. (From Shine et al., 2007).

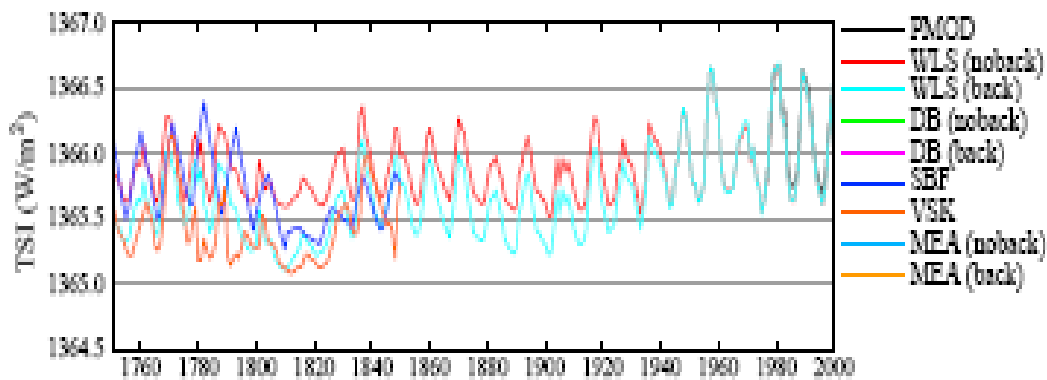
1



2  
3  
4  
5  
6

**Figure 8.6:** The Physikalisch-Meteorologisches Observatorium Davos (PMOD) composite of Total Solar Irradiance (<http://www.pmodwrc.ch/pmod.php?topic=tsi/composite/SolarConstant>).

1



2

3

4

5

6

7

8

9

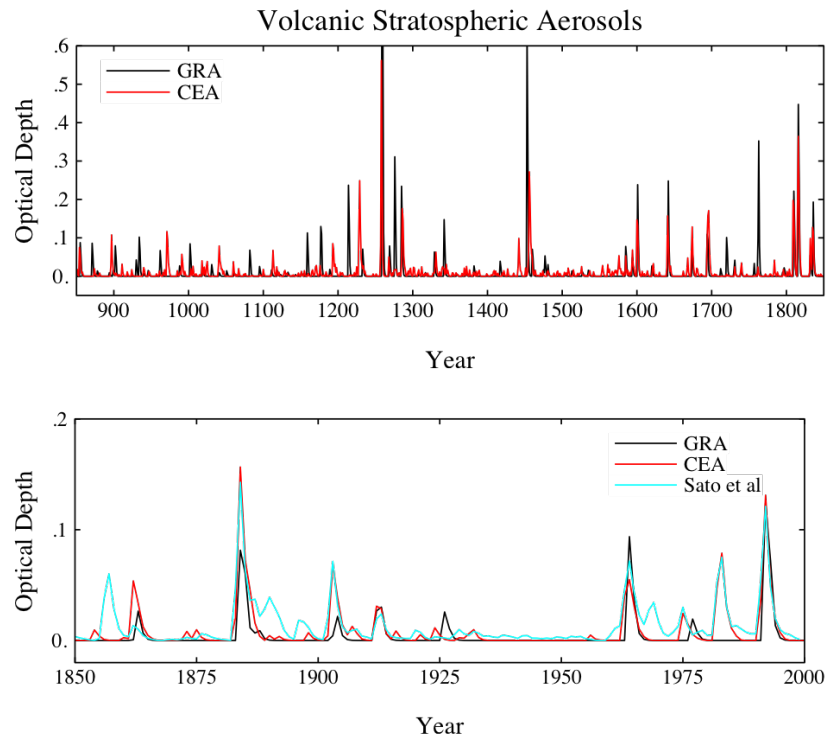
10

11

12

**Figure 8.7:** Some reconstructions of past Total Solar Irradiance time series. PMOD composite time series. WLS, physically-based model for the open flux with (back) and without (noback) independent change in the background level of irradiance (Wang et al., 2005). Taking past geomagnetic field variations into account, the solar activity record can be obtained from the isotope records: MEA (Muscheler et al., 2007) and DB (Delaygue and Bard, 2010) using a linear relation derived from WLS modern-toMm differences (back and noback cases). SBF, model using  $^{10}\text{Be}$  data and observationally derived relationships between TSI and open solar magnetic field (Steinhilber et al., 2009; Fröhlich, 2009). VSK, physical modeling of surface magnetic flux and its relationship with the isotopes (Vieira et al., 2010).

1



2

3

4

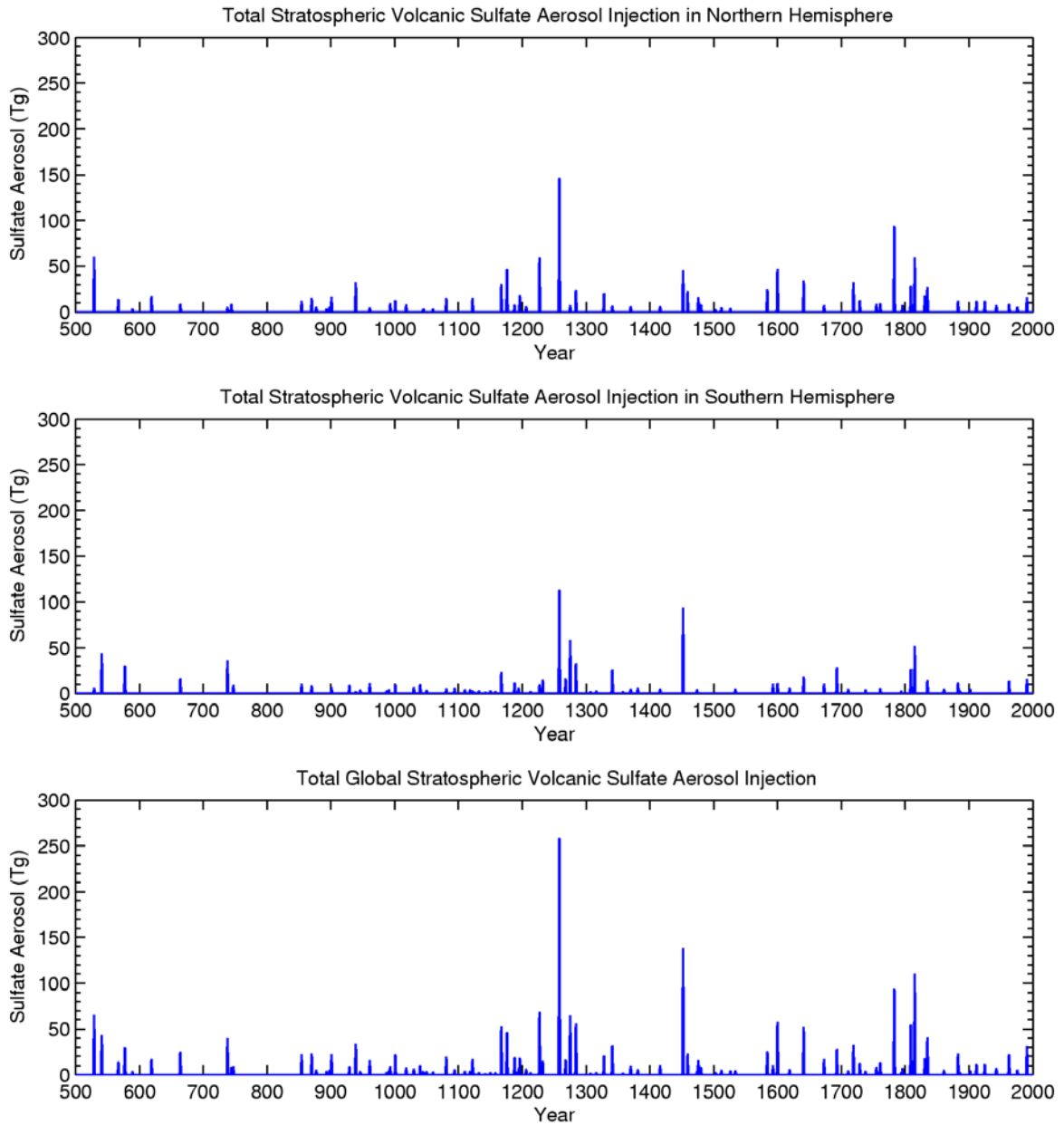
5

6

7

**Figure 8.8:** Two volcanic reconstructions of aerosol optical depth (at 550  $\mu\text{m}$ ) as developed for the Paleoclimate Model Intercomparison Project (top), with a comparison to the modern estimates of Sato et al. (1993) (bottom) (note the different vertical scales in the two panels). Figure from Schmidt et al., 2011.

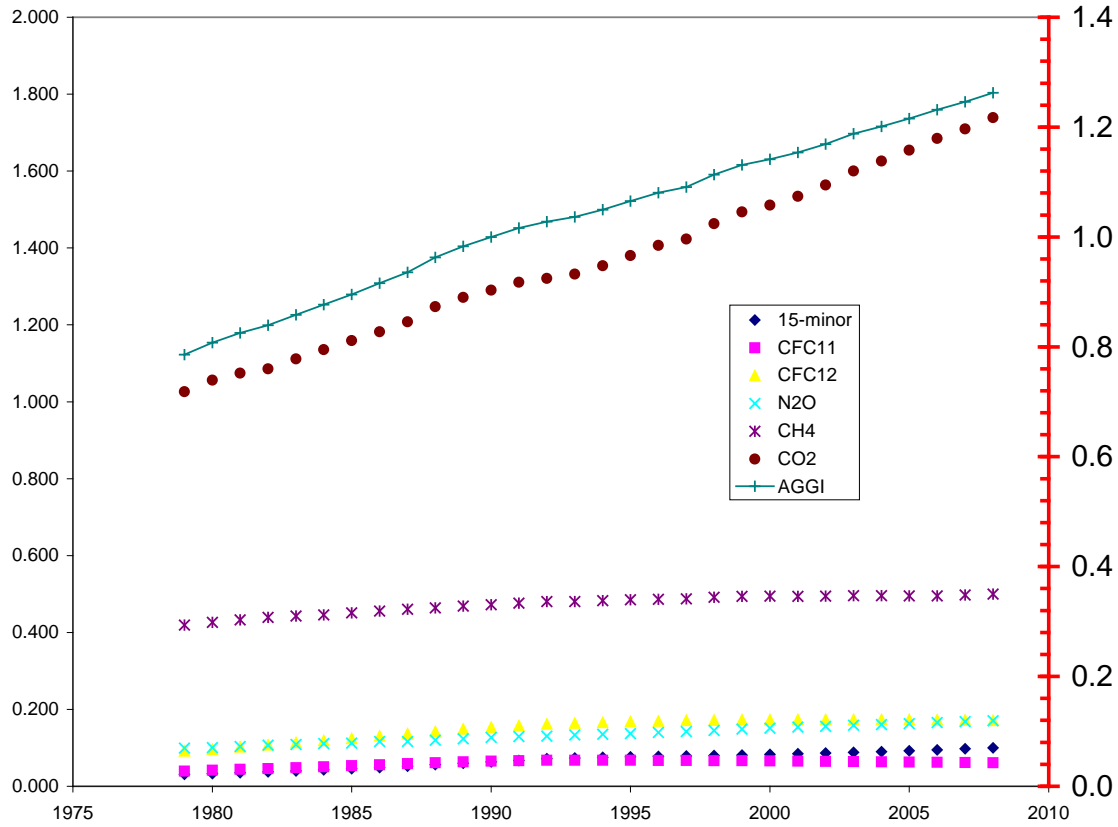
1



2  
3  
4  
5  
6

**Figure 8.9:** Annual stratospheric volcanic sulfate aerosol injection for the past 1500 years in the (top) NH, (middle) SH, and (bottom) global. Figure from Gao et al. (2008).

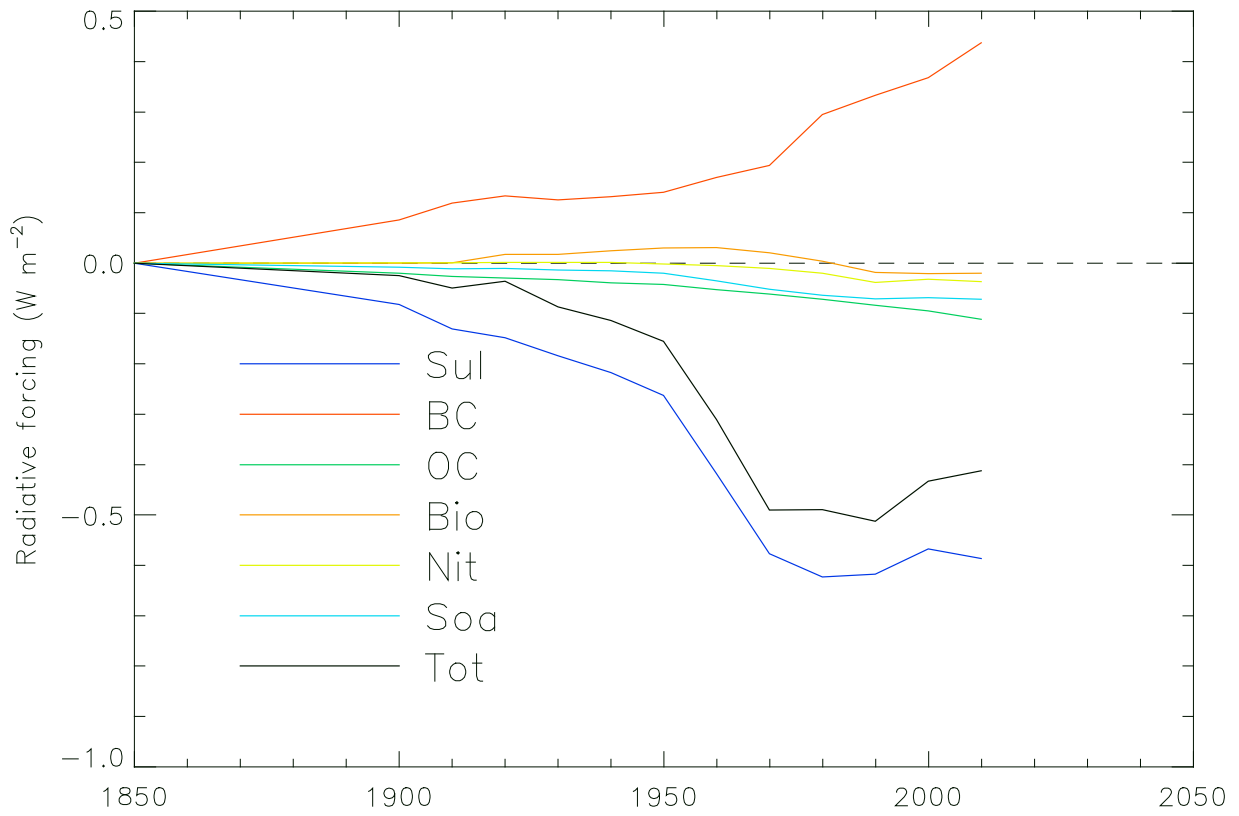
1



2  
3  
4  
5  
6

**Figure 8.10:** Radiative forcing from long-lived greenhouse gases. This will be extended backwards and forwards in time. Speciation of the 15 minor gases will be added.

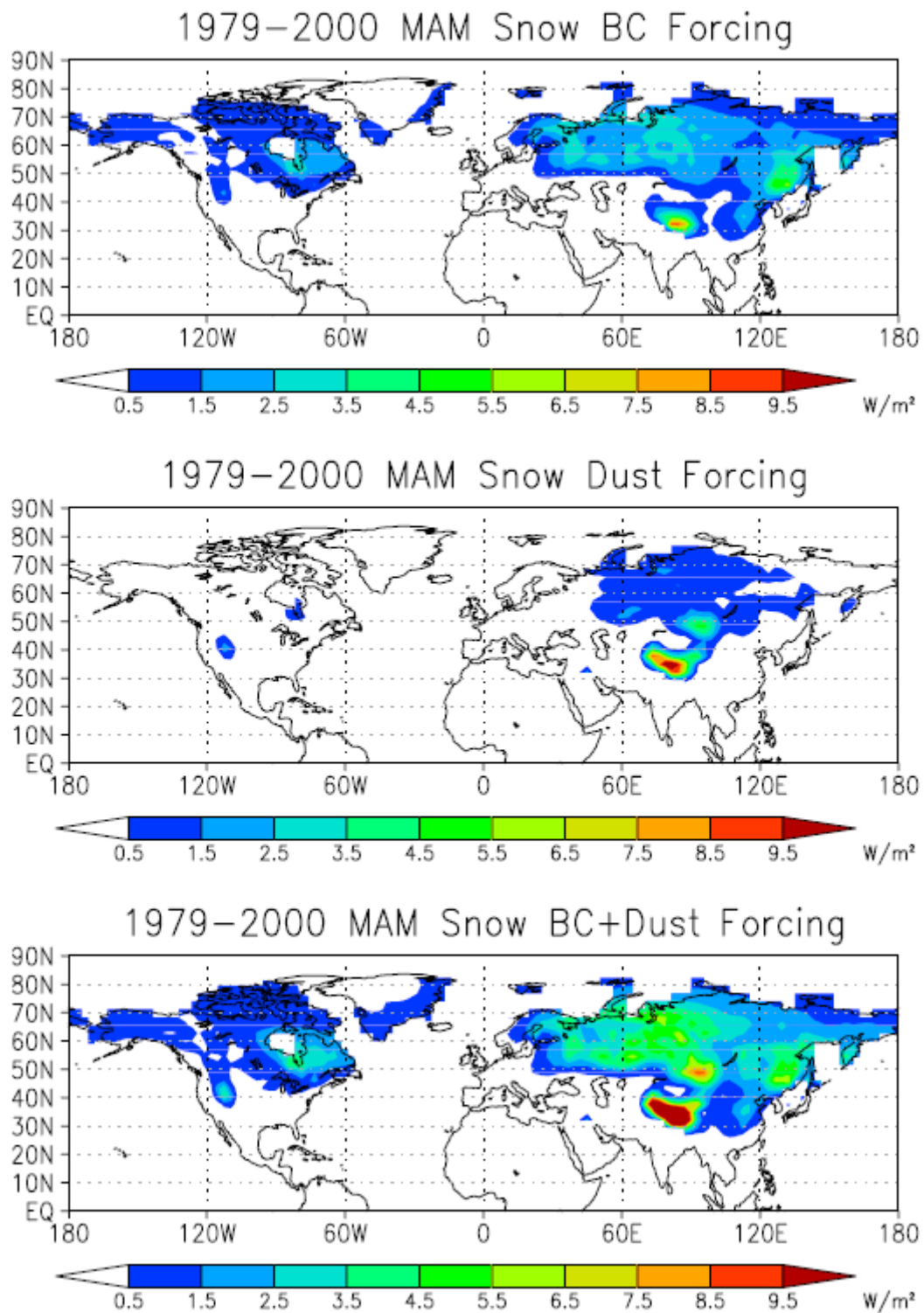
1



2  
3  
4  
5  
6

**Figure 8.11:** Time evolution of RF of the direct aerosol effect (total as well as by components). [Figure will be updated by more models.]

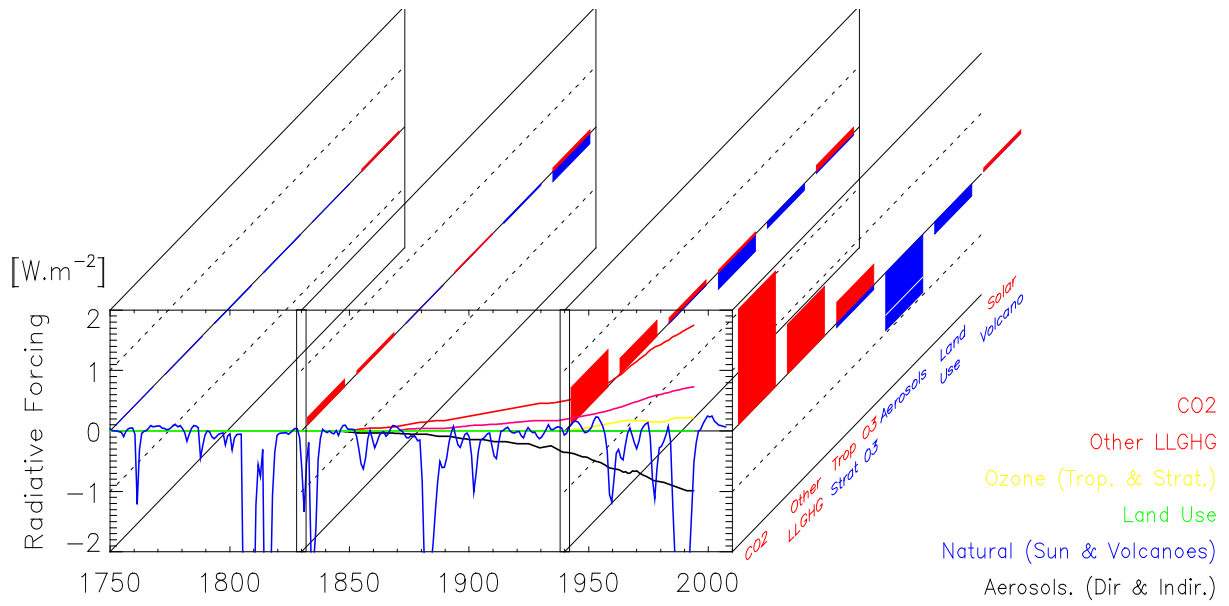
1



2  
3  
4  
5  
6  
7  
8

**Figure 8.12:** March–May surface radiative forcing, averaged spatially and temporally only over snow, caused by (top) black carbon in snow, (middle) mineral dust in snow, and (bottom) both agents. Middle panel does show rather large mean radiative forcing on snow in Central Asia, caused by BC and mineral dust (Flanner et al., 2009)

1



2

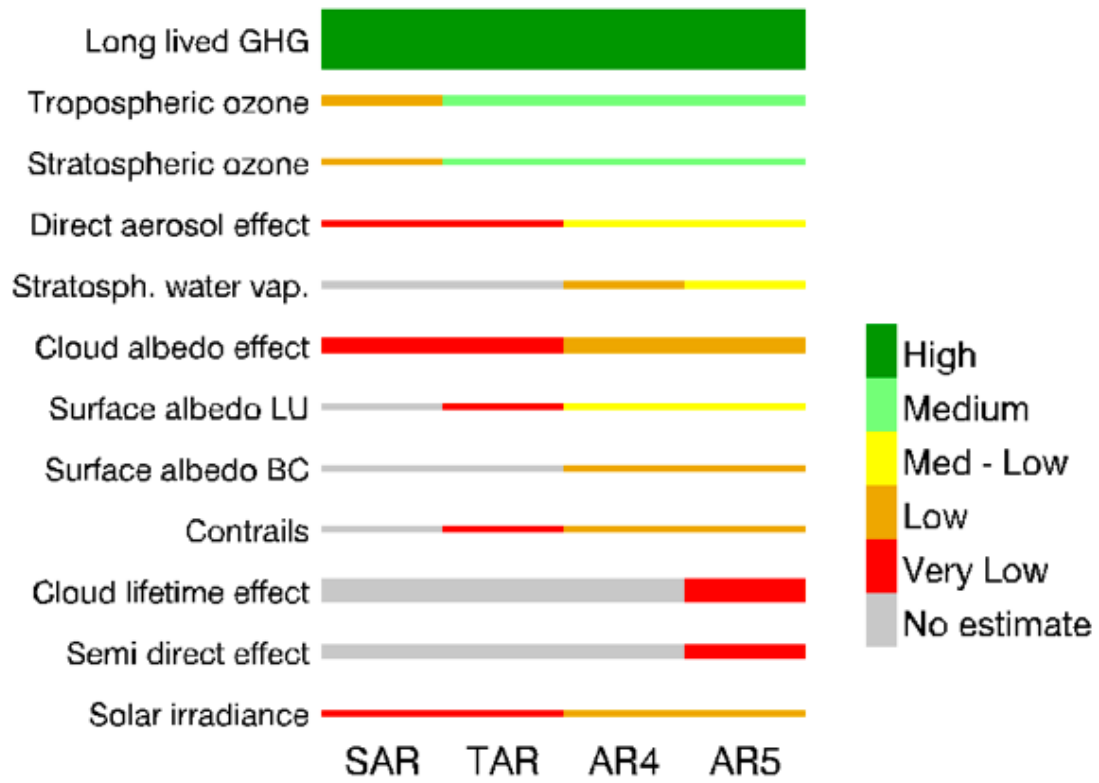
3

4

5

**Figure 8.13:** RF bar chart with time evolution of RF from major components.

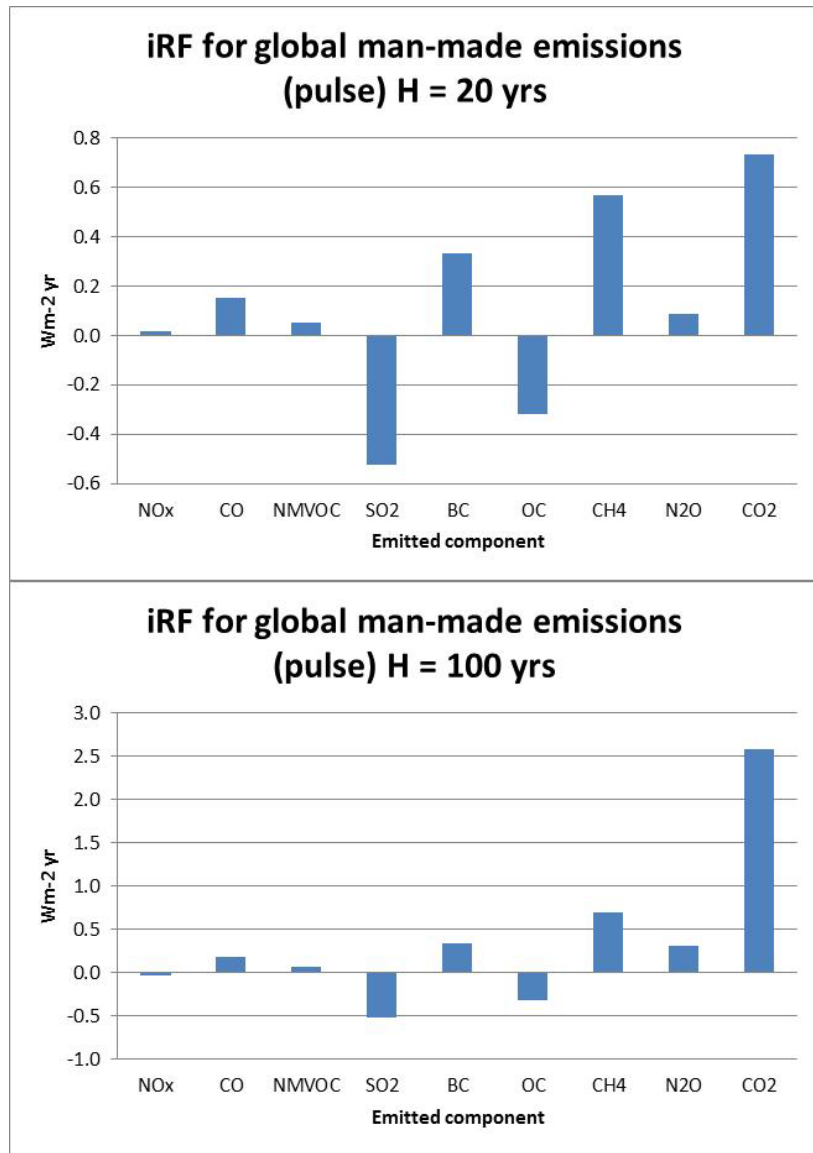
1



2  
3  
4  
5  
6  
7

**Figure 8.14:** LOSU of the RF mechanisms in the 4 last IPCC assessments. The thickness of the bars represents the relative magnitude of the RF (preliminary values). [For AR5 very preliminary values are included.]

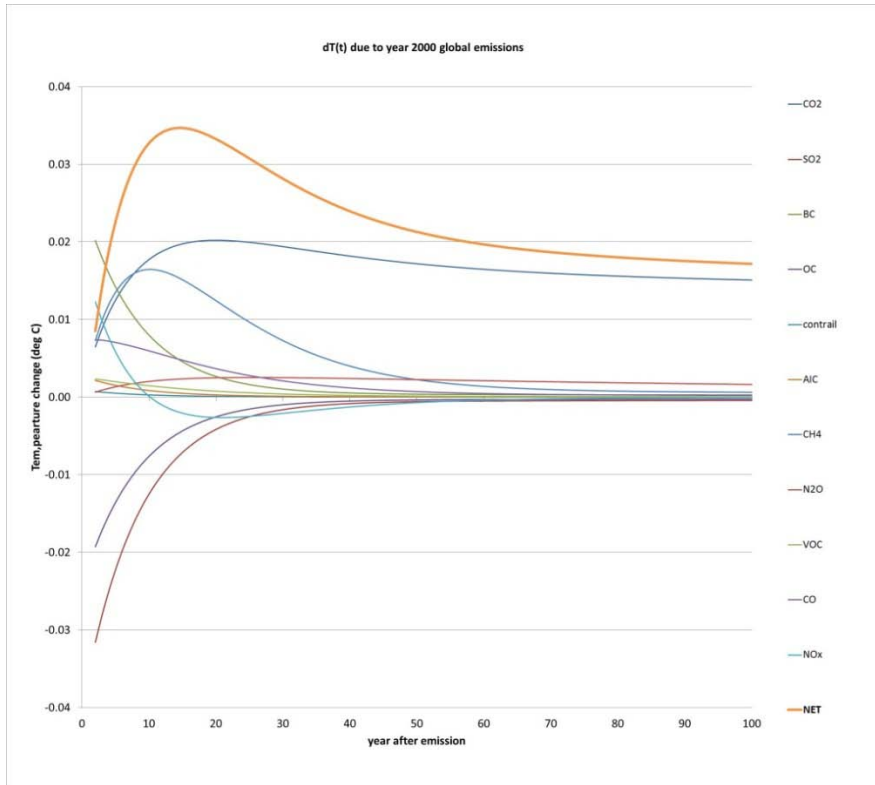
1



2  
3  
4  
5  
6  
7  
8  
9

**Figure 8.15:** [Sketch] Integrated RF for global man-made emissions by component (pulse for the year 2000 emissions) for two time horizons, 20 and 100 years. [Will be an update of Figure 2.22 in AR4 but given by driver instead. We may also show individual responses as in Figure 2.22 in AR4, e.g., O<sub>3</sub>, primary mode O<sub>3</sub> and CH<sub>4</sub> for NO<sub>x</sub>. Will also include nitrate, HFCs/CFCs/PFCs, indirect effects via clouds and albedo effect of BC.]

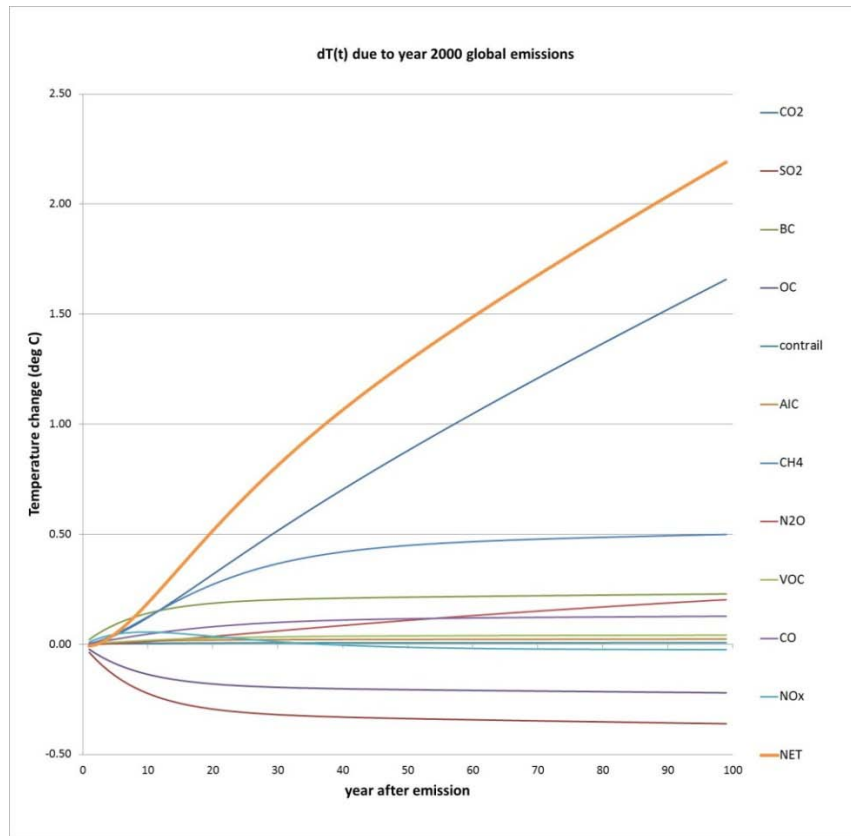
1



2  
3  
4  
5  
6  
7

**Figure 8.16:** dT(t) by component from total man-made emissions for year 2000 (one year pulse). AIC: aviation-induced cirrus. The effects of aerosols on clouds (and in the case of black carbon, on surface albedo) are not included. [Will be made consistent with rest of the chapter/other chapters.]

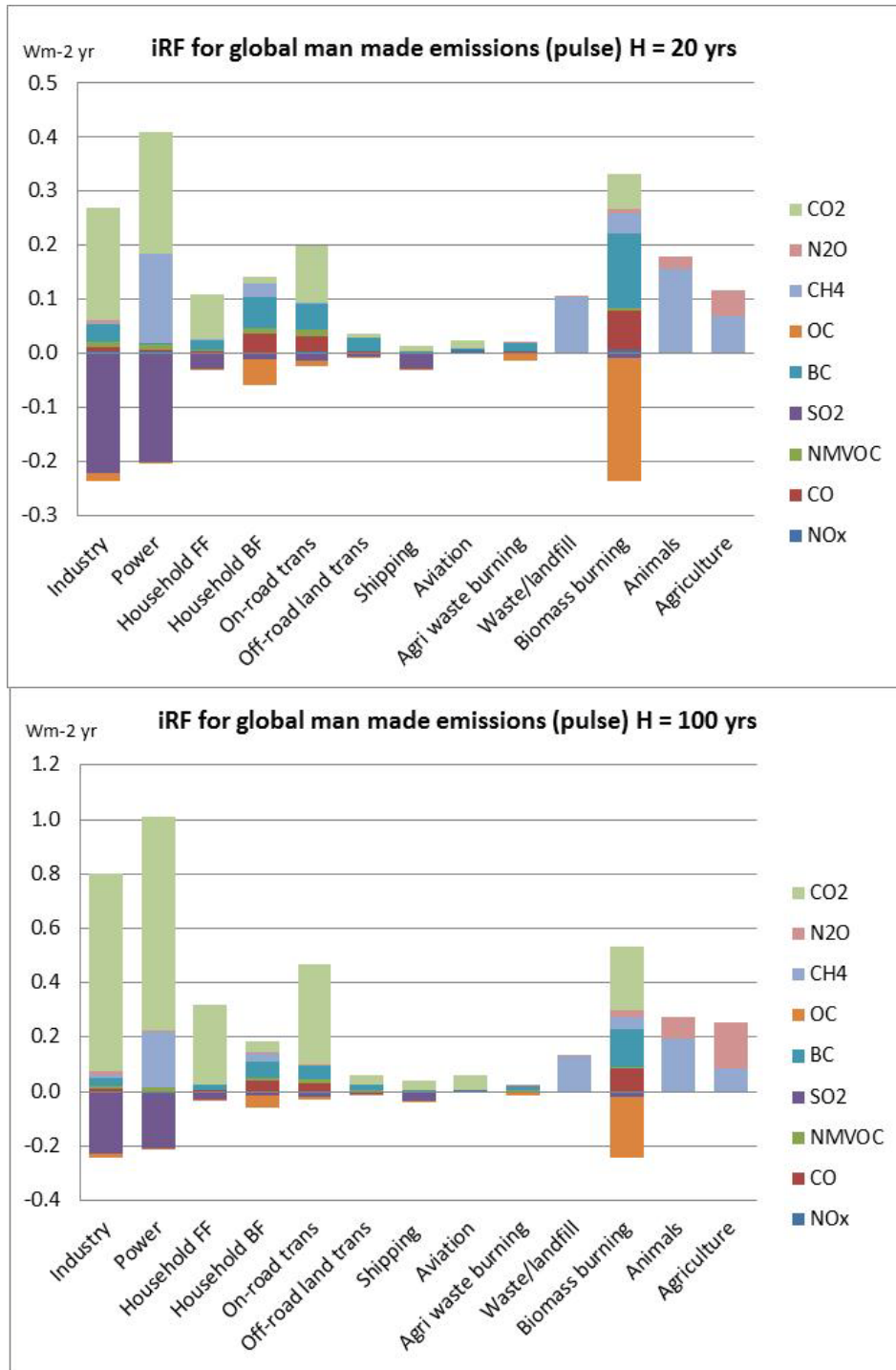
1



2  
3  
4  
5  
6  
7

**Figure 8.17:** dT(t) by component from total man-made emissions kept constant at 2000 level. AIC: aviation-induced cirrus. The effects of aerosols on clouds (and in the case of black carbon, on surface albedo) are not included. [Will be made consistent with rest of the chapter/other chapters.]

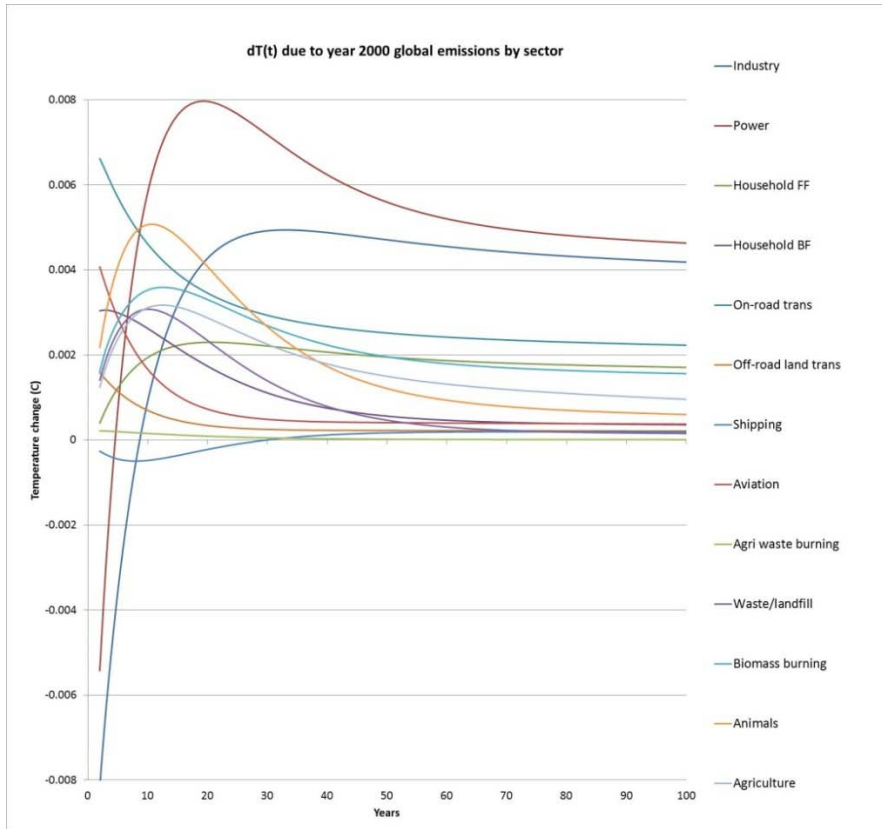
1



2  
3  
4  
5  
6  
7  
8

**Figure 8.18:** Integrated RF for Global man-made emissions by sector (PULSE for the year 2000) for two time horizons, 20 and 100 years. May add rectangular frame to show net, or give net numbers in Figure. Will add more components and mechanisms (e.g., indirect effects on clouds). [Will be made consistent with rest of the chapter/other chapters.]

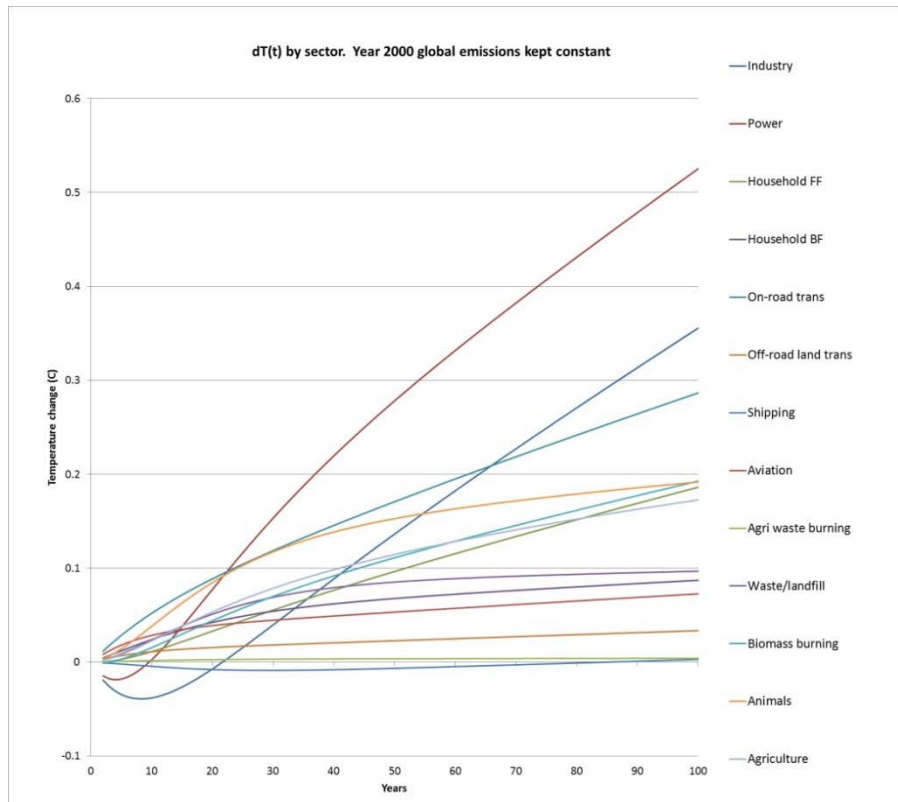
1



2  
3  
4  
5

**Figure 8.19:** Net  $dT(t)$  by sector from total man-made emissions (one year pulse)

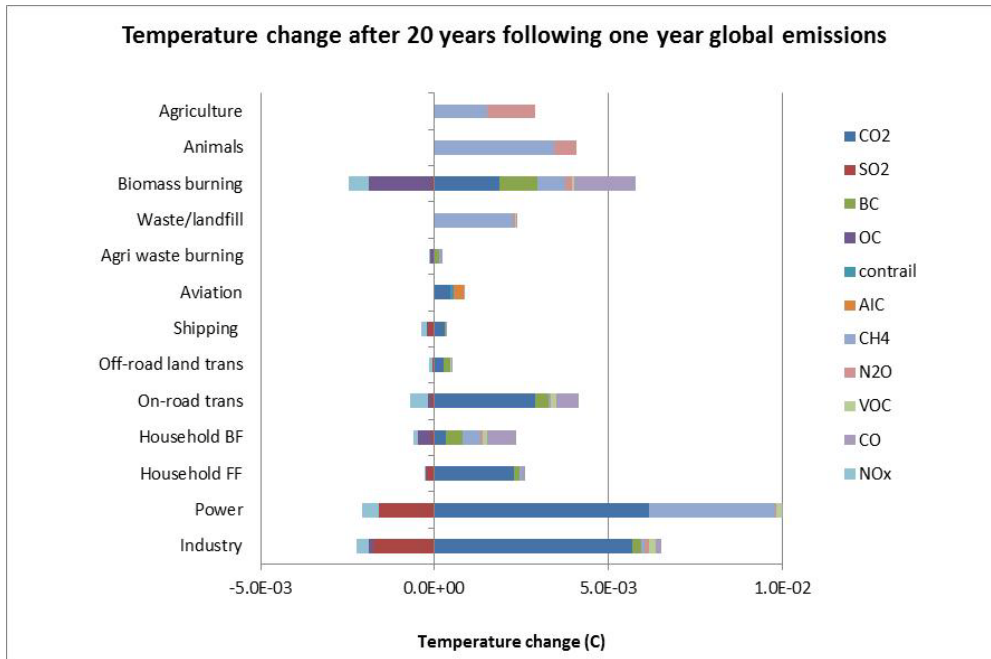
1



2  
3  
4  
5

**Figure 8.20:** Net dT(t) by sector from total man-made emissions kept constant

1



2

3

4

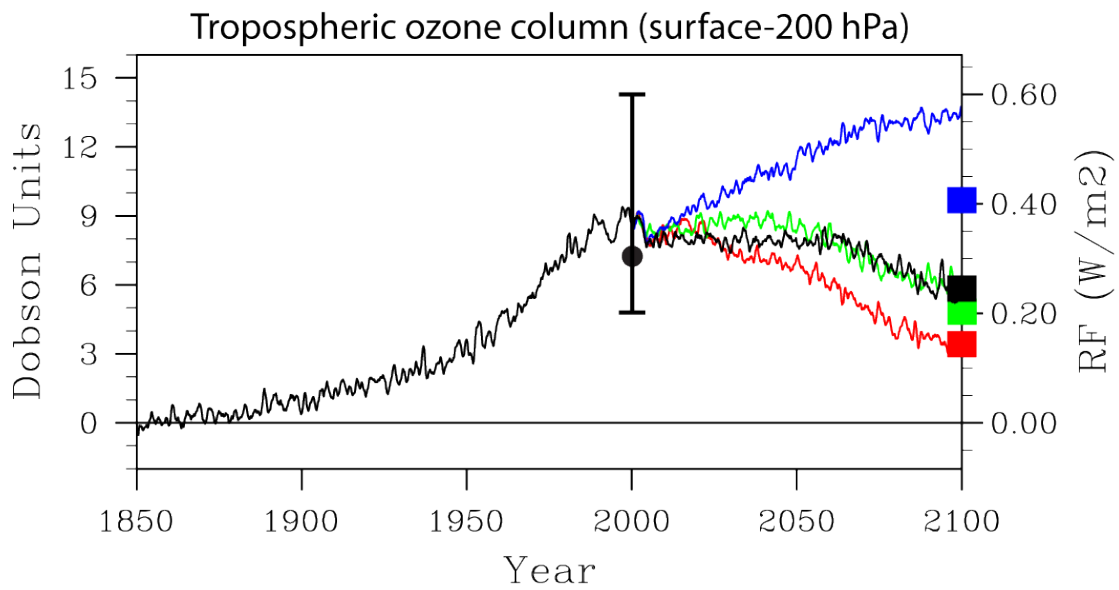
5

6

7

**Figure 8.21:** Net  $dT(t)$  by sector from total man-made emissions kept constant. CT: Contrails. AIC: aviation-induced cirrus. The effects of aerosols on clouds (and in the case of black carbon, on surface albedo) are not included. [Will be made consistent with rest of the chapter/other chapters.]

1



2

3

4

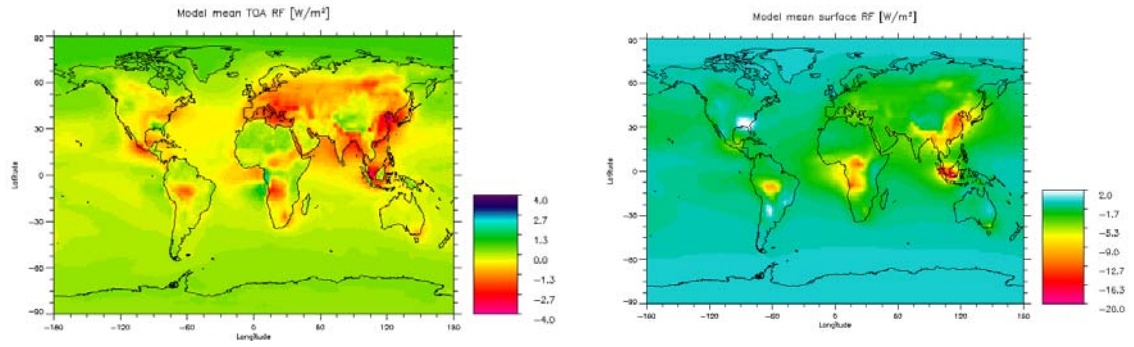
5

6

7

**Figure 8.22:** Tropospheric ozone from CAM simulations (lines and equivalent RF) compared with RCP RF (squares); RCP8.5 is strongly underestimating the RF because of the lack of consideration of ozone super-recovery (Lamarque et al, 2010).

1



2

3

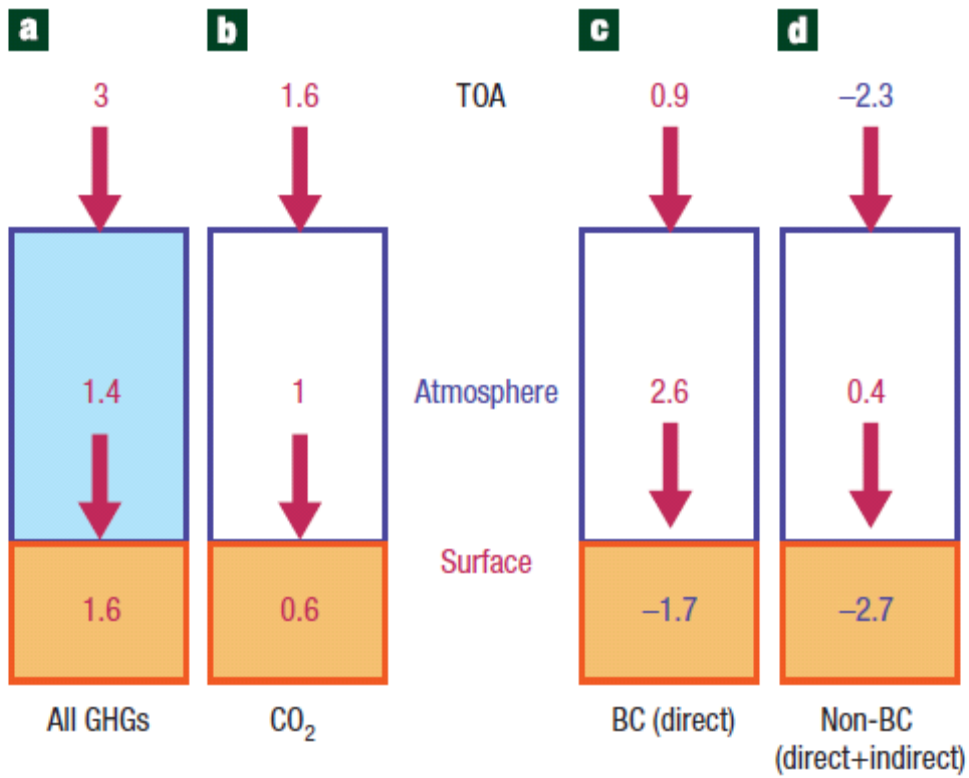
4

**Figure 8.23:** RF of the total direct aerosol effect (left) and surface radiative forcing of the total direct aerosol effect (right) as a mean of two AeroCom models.

5

6

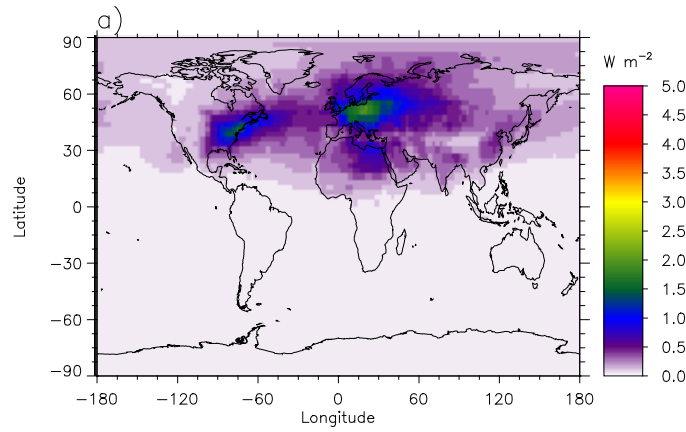
1



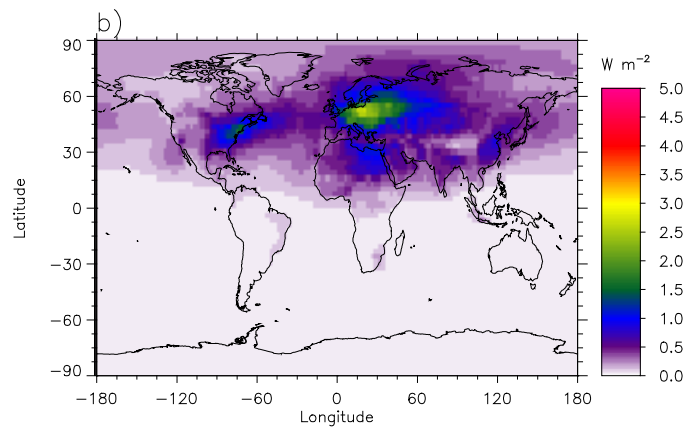
2  
3  
4  
5  
6

**Figure 8.24:** RF and surface radiative forcing for LLGHG, CO<sub>2</sub>, BC and direct and indirect aerosol effect of scattering aerosols, taken from (Ramanathan and Carmichael, 2008).

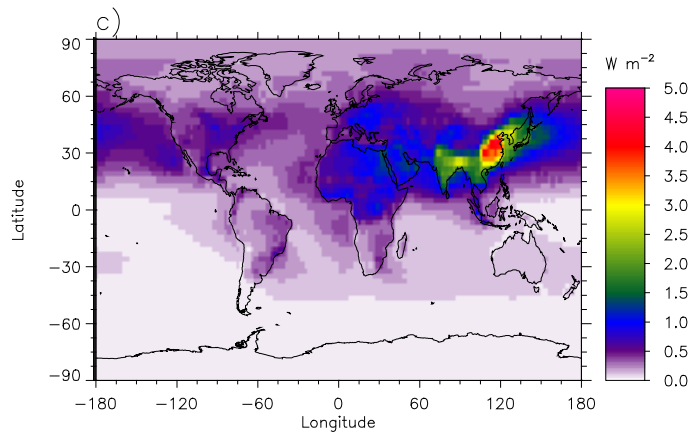
1



2



3



4

5

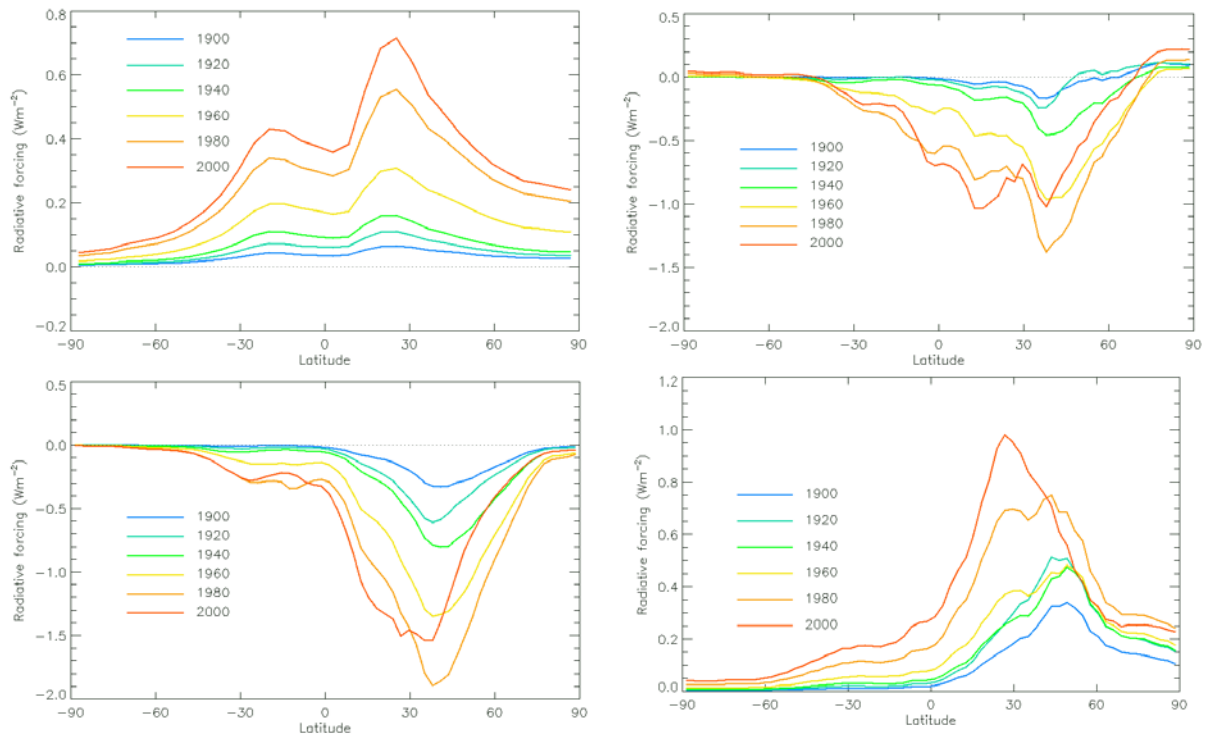
6

7

8

**Figure 8.25:** Direct aerosol effect of BC for 1900, 1950, and 2000. [Preliminary results from Oslo CTM2 and will be updated with results from more models.]

1



2

3

4

5

6

**Figure 8.26:** Zonal mean radiative forcing as a time evolution from 1900 to 2000 with a reference to 1850 conditions, a) tropospheric ozone, b) total direct aerosol effect, c) direct aerosol effect of sulphate, d) direct aerosol effect of BC. [These are preliminary results that will be updated with more modeling results.]